RE-ORDER NO. 77-123

SQT

MAYA development corporation

11675 SORRENTO VALLEY RD • SAN DIEGO, CALIFORNIA 92121 • PHONE 714/481 0688

77-1-1

STUDY OF

EFFECTS OF SPACE POWER SATELLITES ON

LIFE SUPPORT FUNCTIONS OF THE EARTH'S MAGNETOSPHERE

FINAL REPORT

Marvin Douglas
Robert LaQuey
Sherman DeForest
Charles Lindsey
Howard Warshaw

JPL - 954663

This work was performed for the Jet Propulsion Laboratory, California Institute of Technology sponsored by the National Aeronautics and Space Administration under Contract NAS 7-100.

May 5, 1977

(NASA-CR-156948) STUDY OF EFFECTS OF SPACE POWER SATELLITES ON LIFE SUPPORT FUNCTIONS OF THE EARTH'S MAGNETOSPHERE Final Report (Maya Development Corp., San Diego, Calif.) 152 p HC A08/MF A01 CSCL 04A G3/46

N78-29674

Unclas 29050

REPRODUCED BY
NATIONAL TECHNICAL INFORMATION SERVICE
US DEPARTMENT OF COMMERCE
SPRINGFIELD VA 22161

162

ABSTRACT

A proposed Satellite Solar Power System (SSPS) may have a number of deleterious effects on the life support functions of the earth's magnetosphere. A preliminary study has been carried out in order to define the scope of detailed analysis and perform preliminary analysis which will be necessary to assess the impact of the SSPS on these life support functions. The following subjects have been investigated: 1) Thruster effluent effects on the magnetosphere 2) Biological consequences of SSPS reflected light 3) Impact on Earth Bound Astronomy 4) Catastrophic Failure and Debri 5) Satellite Induced Processes 6) Microwave Power Transmission A number of important impacts have been identified and recommendations for further detailed studies are provided.

TABLE OF CONTENTS

Page

SECTION 1 - SUMMARY AND RECOMMENDATIONS 1-1

SECTION 2 - TECHNICAL DISCUSSION 2-1
2.1 Thruster Effluent Effects on the Magnetosphere . . . 2-1
A Mission Information 2-2
B Plume Characteristics 2-6
C Neutral Effluent and the Exosphere 2-14
D The Magnetosphere. 2-19
E The Magnetosphere and the Environment 2-38
F Plasma Effluent Convection and Interaction . . . 2-43
Bibliography 2-50
Appendix A - Orbits of Neutral Effluent 2-52
2.2 Biological Consequences of SPS Reflected Light . . 2-55
A Photoperiodicity 2-55
B Celestial Orientation and Navigation 2-58
C Nocturnal Behaviors Affected by Moonlight . . . 2-59
Bibliography 2-63
2.3 Impact of SSPS on Earth-Bound Astronomy 2-66
A Visual Brightness of the SSPS 2-67
B Night Sky Illumination 2-69
C Suppression Techniques 2-71
D Thermal Emission at Infrared Wavelengths 2-72
E Radio Astronomy 2-75
Bibliography 2-79
2.4 Catastrophic Failure and Debri 2-80
A Particulate Properties 2-80
B Catastrophic Failure - Collision 2-84
C Propellant Tank Rupture 2-86
D Solid Particulates 2-91
Bibliography 2-100
2.5 Satellite Induced Processes 2-101
A Particle Drag Force and Wake 2-102
B Induction Drag and Alfvén Wake 2-113
C Additional Topics 2-118

TABLE OF CONTENTS, CONTINUED

Bibliography 2-119
2.6 Microwave Power Transmission 2-120
A Parametric Instability 2-122
Appendix B - Basic Equations 2-128
B Phase Distortion and the Microwave Transmission System 2-134
Bibliography 2-139

LIST OF FIGURES

Figure		Page
2.1.1	Effluent Deposition Profile	2-7
2.1.2	Photoionization Cross Sections	2-9
2.1.3	Flux Shell Volume in Dipole Field	2-11
2.1.4	Plasma Density Profile	2-13
2.1.5	Neutral Particle Densities In The Upper Atmosphere	2-16
2.1.6	Magnetosphere Cutaway	2-21
2.1.7	Magnetosphere Section Through Noon-midnight Plane	2-22
2.1.8	Solar Wind Dynamo Circuit	2-28
2.1.9	Large Scale Plasmasheet Convection	2-29
2.1.10	Field Aligned Currents	2-31
2.1.11	Magnetosphere Electric Equipotentials	2-32
2.1.12	Forbidden Region	2-34
2.1.13	Electric Equipotentials In North Polar Cap Region	2-36
2.1.14	Atmospheric Vorticity and Geomagnetic Activity	2-42
2.1.15	Critical Energy For Wave-Particle Instability	2-47
A.1	Neutral Effluent Trajectories	2-53
2.3.1	Diffuse Sky Light	2-70
2.4.1	Debri Particle Orbit Contributions	2-93
2.5.1	Density Perturbation Near Fast Moving Body	2-103
2.5.2	Far Zone Wake	2-107

LIST OF FIGURES, CONTINUED

Figure		Page
2.5.3	Near Zone Density Perturbation	2-109
2.5.4	Far Zone On-Axis Density Perturbation	2-109
2.5.5	Angular Behavior of Far Zone Electric Field	2-111
2.5.7	Equipotentials Around Slow Moving Satellite	2-112
2.5.8	Moving Satellite and Alfven Wake	2-114
2.5.9	Induction Current Distribution	2-116
2.6.1	Self Phasing Array	2-121
2.6.2	Microwave Beam Incident upon the magnetospheric plasma	2-125
2.6.3	Total Electron Content	2-136
2.6.4	One Element of the Selfphasing Array	2-137

LIST OF TABLES

Table		Page
2.1.1	Magnetospheric Parameters	2-24
2.2.1	Biological Effects of SSPS Light Reflection .	2-62
2.3.1	SPS Infrared Fluxes	2-74
2.5.1	Drag Forces and Magnetospheric Parameters . .	2-105
2.6.1	Critical Scale Lengths for Quenching of Parametric Instabilities in the Magnetosphere	2-127

1. SUMMARY AND RECOMMENDATIONS

1 1 BACKGROUND

Serious proposals are currently under consideration to deploy an array of very large (100 km^2) spacecraft to collect solar energy, convert it to microwaves, and transmit them to earth to be converted into electricity for terrestrial use. Each such spacecraft would produce approximately 10^{10} watts As many as 200 solar power satellites (SPS's) would be placed in geosynchronous orbit.

The study upon which this report is based had the goal of surveying the total system and isolating areas of potential hazard to the biological support properties of the magnetosphere, as well as hazards to space activity within the magnetosphere. This report represents the first attempt to prepare such a study independently from the proposing agencies. Only initial inquiries were made into the various identified areas to determine whether or not further study was warranted. At this time we can safely say that within the mission parameters that are now being considered several hazards have been identified. On the other hand, certain potential hazards have been eliminated from further study based on general considerations. Proper action might be able to ameliorate adverse effects, but in all cases further study is recommended. The approach has been to consider first the function that is being performed (e.g. putting large masses into orbit) then to consider the particular proposals (e.g. use of argon ion propulsion devices).

The SSPS is a large complex system with several possible types of environmental impacts. As is well known simply raising the necessary mass to low earth orbit will introduce large amounts of pollution to the amosphere and much noise to Florida. The further raising of each SPS to

geosynchronous orbit will result in the introduction of more mass into the magnetosphere than is naturally there.

In addition the microwaves might interact with the ionosphere in a variety of deleterious modes.

However all possible impacts which directly affect terrestrial, atmospheric, and ionospheric activities without the mediating influence of the magnetosphere are beyond the scope of this study. For the most part we will consider the effects of the deployment and possible construction or assembly of the SPS at low earth orbit on the natural plasma. We continue to study the SPS as it is raised to operating orbit, placed in operation and eventually dies. Certain classes of catastrophic failure are considered along the way.

An exception to this area of study is the consideration given in Section 2.2 and 2.3 to the possible terrestrial effects of light and other electromagnetic radiation reflected from or produced by the SSPS. Attempts are made to assess possible impacts on all lifeforms in the biosphere due to the sudden appearance of very bright new "stars" at the equator, and impacts on ground based astronomy.

1.2 METHOD

As was mentioned above, this is an initial study. Many potential problem areas have been explored to attempt to identify those most needing additional attention. The general approach has been to consider the effects of assembling and raising an SPS from low earth orbit to geosynchronous, assuming normal operation. Then we consider the effect of normal operation of one SPS. Then generalizations are made to the whole SSPS, still assuming normal operation. To the extent possible we try to make statements

which are configuration independent. Then we consider various abnormal modes (such as catastrophic failure of the station-keeping mechanism). Non-plasma contaminants are also considered. However we do not directly address such problems as disruption of satellite communications or compromising of the geosynchronous orbit for purposes other than the generation of power. While these are important and worthy subjects, they are beyond the scope of this study.

1.3 SUMMARIES, CONCLUSIONS AND RECOMMENDATIONS

According to the preceeding discussion we have divided the report into six sections. In the following a brief description and summary of each section is provided, along with the statement of important results. Following each we provide a list of recommendations for further study, with a priority level attached· (1) = highest, (3) = lowest.

2.1 Thruster effluent effects on the magnetosphere

The operation of ion or chemical thrusters for raising the SPS to geosynchronous orbit and keeping it on station during operation will release large amounts of effluent gases into the magnetosphere. We have made a preliminary survey of possible alteration of the physics of the magnetosphere by the effluents The material may be released as both neutral atoms and ionized plasma The neutrals may in some circumstances return quickly to the lower atmosphere, or they may drift in orbit until they are photoionized and become part of the ambient plasma inventory. Crude estimates show that the amount of material deposited by the orbit raising of one SPS is equal to that already present. Thus loss mechanisms and convection rates come immediately to the forefront. An estimate of stationkeeping effluent deposition has indicated the possibility that the steady state density perturbation near geosynchronous orbit may be small

Alteration of the low energy plasma density can affect the operation of "wave particle instability" mechanisms. These regulate the populations of high energy radiation belt particles and are implicated in such environmentally important natural phenomena as magnetospheric substorms, the aurora, radio noise and perturbation of the earth's magnetic field. There exist both well-known environmental consequences as well as the potential for weather modification.

The overall conclusions are that the magnetosphere is complicated, and still poorly understood after twenty years of in situ observation. We cannot safely predict the absence of major changes in its composition and the plasma dynamics that control it if the SSPS is deployed. This could have effects on the life-support functions of the natural environment, but with few exceptions we are unable yet to predict with any degree of

confidence the effects of these manmade changes on the biosphere.

By its very nature any adverse change in the magnetosphere produced by man will be truly global in extent. Consider the public outcry generated by the threat posed to the ozone layer by supersonic aircraft and by the use of fluorodated hydrocarbons. The net decrease so far is less than the normal variation, yet this has been considered to be very important. With the SSPS the pollutants could completely dominate the natural plasma. This domination might very well have a much more severe effect than partial depletion of the ozone layer.

For the above reasons we strongly urge continued study of magnetospheric-ionospheric-atmospheric coupling in both the natural state and in possible altered states. We feel that the most important near term goal is the quantitative determination of the modification of the magnetospheric low energy average plasma density, and its affect on magnetospheric dynamics. Also important is a preliminary survey of phenomena to be expected from the localized deposition of high density plasma in the region near the thrusters. It should be kept in mind that definitive answers will not be easily found because the magnetosphere is still poorly understood.

RECOMMENDATIONS

1. Calculate plasma distributions resulting from photoionization, and directly deposited plasma, taking convection and transport mechanisms into account. Choose a specific SSPS mission program and one or two thruster alternatives.-- (1)
2. Use effluent profiles to assess effect on aurora, radiation belts, magnetic substorms and radio noise. Calculate material fluxes returning to upper atmosphere. -- (1)

3. Literature review of following subjects: a) magnetospheric, plasmaspheric and polar wind convections; b) processes affected by effluent type plasma, c) transient process triggered by localized plasma deposition. -- (2)

2.2 Biological effects of SSPS reflected light

Extra light in the night sky produced by SPS's may affect photoperiodicity of plants and animals, celestial orientation, and several animal behaviors correlated with night illumination. Effects on photoperiodic synchronization of daily and seasonal cycles are considered the most important due to the wide-spread use by both plants and animals of low-intensity light levels as reference points in their daily cycles, and the resulting economic implications for agriculture. Some of these effects, especially those on plants and small animals, can be relatively easily estimated through controlled simulations with artificial lights. Measuring photoperiodic effects on larger species will be difficult.

Some confusion in orientation and migration may result in animals which use the night sky as a compass. This effect is thought to be minor because many species have been shown to have other orientation mechanisms at their disposal. Many of these effects can be easily studied with simulations in a planetarium.

There may be some effects on nocturnal predation and other behaviors related to night illumination. Salmon fry for instance have been shown to be more vulnerable on moonlit nights. Insect sexual and other activity is sometimes light-dependent. These particular effects may be small for the light levels likely to be produced by SSPS's, but more information is needed. Gathering this information for large nocturnal predators will be difficult.

The priority ratings and time estimates for further study of each of the discussed biological effects are presented below.

RECOMMENDATIONS

1. Photoperiodicity
   a. Daily (1)
   b. Seasonal (1)
2. Celestial orientation (3)
3. Nocturnal behavior affected by moonlight
   a. Predator-prey balance (2)
   b. Pest activity and reproduction (2)
   c. Other light-dependent nocturnal activity (3)

Base and Time-estimate for Further Studies

1. Photoperiodicity
   a. Daily -- easy for plants and small animals, 2-6 months; difficult for larger animals, 3-12 months.
   b. Seasonal -- moderate for plants and small animals, 1-2 years, difficult for larger animals, 1-2 years.
2. Celestial orientation -- easy, 2-6 months.
3. Nocturnal behaviors affected by moonlight -- easy to difficult depending on species (smaller, more localized species generally easier), 2-12 months.

2.3 Impact of SSPS on earth-bound astronomy

A single SPS may have a light collecting area of order 140 km^2 for converting solar energy to microwaves. The total flux over this area is almost 200 gigawatts. The microwave beam would carry a power of order 10-20

gigawatts to the collecting array at the earth's surface, whose area would be of order 100 km^2. A portion of the power intercepted by the satellite would be scattered or reflected by its surface (probably about 10% of the incident flux) which could easily make it the brightest celestial object in the night sky, discounting the moon. Most of the collected power would be re-radiated diffusely in the far infrared region of the spectrum, making the SPS very bright at far infrared wavelengths as well. In this study we have considered the potential impact of these satellites on ground-based astronomical observations. We discuss four main considerations: (A) The intensity of visible sunlight scattered or reflected by the SPS; (B) diffuse night sky illumination by this scattered light, (C) the intensity of diffuse thermal radiation emitted by the SPS at far infrared wavelengths; and (D) interference with radio observations.

On the basis of this study it is anticipated that the dependence of the western hemisphere on a large number of orbiting solar power generators for electrical power will present two main potential problems concerning ground-based astronomy which need to be studied at some length.

(1) Diffuse illumination of the night sky at visible wavelengths sufficient to compete with faint diffuse extraterrestrial sources, and

(2) possible interference at microwave frequencies due to side-band noise and harmonics of the transmission frequency emitted by the microwave transmitter, as well as unavoidable interference at the fundamental transmission frequency due to side-lobes of the transmitting antenna.

This study is by no means exhaustive; the subject of orbiting solar power generators should be explored more carefully and at greater length

for further considerations regarding astronomy.

RECOMMENDATIONS

We recommend a more detailed study of the following more specialized areas of technology for their concern with aspects of problems we have discussed here.

1. Possible methods of reducing the diffuse reflectivity of all exposed surfaces on the SPS to well below 1% (1)
2. Effects of the space environment on reflecting surfaces, and degradation of optically smooth (specularly reflecting) surfaces (2)
3. Microwave side band noise and harmonics emitted by transmitters being considered for use on the SPS (1)
4. Possible effects on the ionosphere of transmitting a considerable amount of microwave power through it, and the implications of those effects to radio astronomers (1)

2.4 Catastrophic failure and debris

We have considered perturbation of the magnetospheric environment due to the dispersal of debris. This could result from satellite failure, and will certainly result from predictable degradation mechanisms such as meteoroid impact and sputtering. In considering catastrophic modes of failure the SPS must be examined for sources of uncontrollable momentum. We have considered propellant tank rupture as one source and believe it should be considered further. We have also pointed out the possible importance of waste particulate matter in SPS operations. Since meteoroid erosion is an important source of particulates we feel that careful calculation of this should be undertaken. This is also clearly important

for the reason that SPS power collection requires the use of optical surfaces that will undergo erosion. Preliminary evaluation has yielded two tentative conclusions: (1) Not enough material will be eroded to obscure sunlight or other electromagnetic radiation, and (2) the density of eroded material in the vicinity of geosynchronous orbit could approach that of the natural meteoroids, but the velocities of the material should be on the average substantially less than that of the primary meteoroids. Therefore we feel that small particulates and other ejected waste material could be important when many SPS' are operating in close conjunction with one another We do feel that problems of this nature are amenable to technical solution.

RECOMMENDATIONS

1. Studies of details of SPS geosynchronous orbits to determine collision avoidance techniques and also to determine the probability of collision as a function of uncontrollable momentum applied in a catastrophic incident. (1)
2. Study of cryogenic propellant storage systems to determine failure probability, momentum impulse, and propellant dispersal due to failure. Examine possibility of solid cryogenic storage. (3)
3. Study of meteoroid impact, sputting and other known processes both as surface degrading processes and as sources of waste particulate matter. Attempt to construct a particulate "source function." (1)
4. Study of orbits of SPS waste particulate matter to determine quantitatively densities that will build up. (1)
5. Consider scenarios for the disposition of SPS' after their useful life is over. (3)

2.5 Satellite Induced Processes

The physical motion of a satellite through the magnetospheric and atmospheric charged and neutral particle environment alters the medium particle distributions. Associated with the altered charged particle distribution are electric and magnetic disturbances. That is, the satellite produces a "wake". The intensity of these wakes depends on the size of the satellite and thus should be evaluated carefully for solar power satellites We have made a very preliminary assessment of wake to be expected from SPS operations and have not uncovered any serious electromagnetic noise problem. This should be studied further, however.

Associated with the satellite motion and wake production are satellite drag forces. These forces are generated by the impact of neutral atoms and charged particles on the satellite front surface, the deflection of charged particles, and by the current induced in an electrically conducting satellite by its motion through a magnetized plasma Given the large surface area to mass ratio of SPS' these could be very important in low earth orbit operations. We believe that since drag forces and wake production are intimately related physical phenomena it would be most efficient to consider them together in the next level of study. The following recommendations may be summarized simply by stating that the general examination begun in section 2.5 should be continued in more detail.

RECOMMENDATIONS

1. Calculation of Drag Forces and Torques on a chosen "model SPS" in low orbit configuration. Careful examination of induction drag in geosynchronous orbit. (1)
2. Calculation of wake structure from very large satellites. Evaluate EM noise from wake and compare with "magnetosphere noise spectrum." (2)

3. Review literature on instability of and dissipation of satellite wakes. (2)

4. Examine proposals for "induction propulsion" to assess applicability to SSPS (3)

2.6 Microwave Power Transmission

The microwave power transmission system used by an SPS will interact with the magnetospheric plasma. MAYA has identified two potential impacts associated with these interactions. First non-linear interactions, known as parametric instabilities, occur when a sufficiently intense electromagnetic wave propagates through a plasma. MAYA has performed an extensive bibliographic review of the literature of parametric instability. To date no serious impact upon either the magnetosphere or the microwave power transmission system has been shown to result from parametric instability. In addition, we have expended substantial effort, outside of the scope of this contract, on ionospheric interactions with the microwave beam, and while the case is much less clear-cut and deserves more study, no insurmountable problems have appeared.

A second impact which may be more problematic demands more study. In the operation of the self-phasing antenna system, it is assumed that the propagation medium is reciprocal and that its properties do not change significantly during a round trip transit time for a microwave signal. This round trip transit time is 0.3 seconds for an SPS at GSO. The total electron content and hence the plasma contribution to the index of refraction may exhibit significant change in 0.3 seconds. These changes may result from magnetic storms, solar x rays or micropulsations in the PC 1 band. Since the proper functioning of the self-phasing antenna system is essential to the success of an SSPS this problem is of the very highest priority.

RECOMMENDATIONS

1. Perform further assessment of non-linear plasma interactions which may result from microwave transmission through the magnetosphere, especially scattering off of modes which are naturally amplified by the magnetosphere such as whistlers.(3)
2. Develop a computer simulation model in order to determine the dynamic response of the self-phasing antenna system to fluctuations in the intervening plasma. Highest possible priority.(1+)

2. TECHNICAL DISCUSSION

2.1 THRUSTER EFFLUENT EFFECTS ON THE MAGNETOSPHERE

INTRODUCTION

We have made a preliminary survey of possible alteration of the physics of the magnetosphere by the effluent of thrusters that will raise solar power satellites from low earth orbit to geosynchronous orbit, and keep them in position during normal operation. Alteration of certain magnetospheric densities could potentially have environmental consequences, both on the earth and in space. In this short study it has not been possible to reach any final answers. Thus we shall recommend further explicit calculations to determine with some confidence alterations of charged particle densities and possible consequences.

In the following we provide background to the problem and indicate important considerations for further work. In Sections A, B we describe the mission requirements, describe some of the thruster alternatives, and discuss some implications of these alternatives. In Section C we consider the special properties of neutral particles that would be emitted, in relation to the neutral particle dynamics of the upper atmosphere. It is argued that this is important to the magnetosphere mainly because of the potential for neutral particles to change into charged plasma. Another important factor is the re-entry of the effluent particles into the ionospheric and denser upper atmospheric regions, where collisions and chemical transformations, such as alteration of the ozone layer, are important. We have not specifically considered this region because it is being studied by other groups in relation to operations at low earth orbit and below. We feel that in this regard one output of future magnetospheric study should be prediction of the distribution of effluent particles

returning from the magnetosphere to this lower level. It will probably turn out reasonable to assign the heights where magnetospheric study leaves off and ionospheric and atmospheric study begins to be those levels, called critical levels, above which collisions are a small perturbation and below which they contribute importantly to particle dynamics. In Section D we provide a short qualitative description of the physical functioning of the magnetosphere. Section E contains discussion of some known and suspected environmental implications of magnetospheric functioning In Section F we briefly describe how it is that certain magnetospheric mechanisms bearing on environmental effects tend to be regulated by the type of plasma that will result from SSPS operations. A program for further study is discussed.

A. MISSION INFORMATION

To begin to assess the effect of propellant deposition on the magnetosphere (MS) it is necessary to obtain some rough idea of the amount and properties of effluent deposited. We shall see that it is possible that the amount of material deposited in the MS by only one SPS will exceed that normally present. In this sense the effluent is not strictly a pollutant but could change drastically its normal functioning For this reason loss and convection rates are important. It should also be pointed out that the propellants under consideration and their byproducts (H, O, H_2, O_2, H_2O, Argon) will not constitute a chemical pollutant as they reenter the atmosphere in that they are its normal constituents.

The magnitude of any environmental problems created in the magnetosphere by the SSPS transportation system may well be related to the specific system chosen. This is true because the alternative systems differ greatly in the amount and type of effluent deposited. Estimates presented here are

based primarily on the Johnson Space Flight Center (JSC) SSPS study[1] of propulsion alternatives. There are basically two types of missions required in the construction and operation of SSPS in the MS. These are the orbit raising of the partially assembled solar power satellite (SPS) from low earth orbit (LEO), circular and of altitude ~500 Km, to geosynchronous orbit (GSO) at altitude 35,800 Km, and the transport of personnel and priority cargo on the personnel orbital transfer vehicle (POTV) from LEO to GSO. The orbit raising mission considered will be of the low thrust type, due to the structural requirement of low acceleration forces on the structure, to be carried out either by chemical or ion thrusters. The amount of mass deposited for a given momentum imparted to the SPS is inversely proportional to the exit velocity v_{ex} of the propellant. For the MPD arcject thruster this velocity is ~20 Km/sec, for a chemical thruster typically 2-4 Km/sec, and ~40-80 Km/sec for ion engines. Thus in a given radius interval the chemical thruster deposits 5-10 times the effluent as the MPD thruster. The POTV missions are to be carried out with high thrust chemical rockets. We have found by using the JSC program projections that the amount of effluent deposited from POTV missions per SSPS is only some 20% of that minimum deposited by the MPD thruster orbit raising. It is thus most likely negligible for the purpose of crude estimates.

In the following we describe the low thrust orbit raising mission. It is potentially important that for the low thrust mission the thrust $\vec{F}$, is approximately tangential to a slowly expanding circular orbit. The magnitude of $\vec{F}$ is given by $F = \dot{M}v_{ex}$ where $\dot{M}$ is the exhaust mass flow rate. The equations describing a circular orbit may be found by balancing centrifugal force against gravitational force

$$\frac{Mv^2}{r} = \frac{KM}{r^2} \qquad (1)$$

where M, v and r are the SPS mass, speed, and geocentric distance and $K \equiv GM_{earth} = 3.99 \times 10^{20}$ dyne cm^2 gm^{-1} (we shall typically work in cgs units and where appropriate express results in mks). From (1) the SPS speed angular momentum and total energy are found to be

$$v = \sqrt{\frac{K}{r}} \tag{2a}$$

$$L = M\sqrt{Kr} \tag{2b}$$

$$E = -\frac{1}{2}\frac{KM}{r} \tag{2c}$$

We assume that the force $\vec{F}$ makes an angle θ with the velocity $\vec{v}$ which is perpendicular to the radius vector. In time Δt the SPS total energy changes by

$$\Delta E = \vec{F}\cdot d\vec{r} = F\, v\Delta t \cos\theta + F\,\Delta r \sin\theta = \frac{1}{2}\frac{KM}{r^2}\Delta r, \tag{3}$$

the second equation being obtained by differentiating (2c). The change in angular momentum is

$$\Delta L = \frac{M\sqrt{K}\,\Delta r}{2\sqrt{r}} = rF\cos\theta\,\Delta t \tag{4}$$

Substituting (4) in (3) to eliminate Δt we find

$$\sin\theta = 0, \tag{5}$$

or

$$\theta = 0. \tag{6}$$

Circular spiral-type orbits are maintained by tangential thrusting; normal thrust introduces additional ellipticity.

To calculate the rate of ascent we set $\theta = 0$. Putting $\cos\theta = 1$ in (4) enables us to calculate r(t) as the solution to

$$\frac{dr}{dt} = \frac{2a}{\sqrt{K}} r^{3/2} \tag{7}$$

whose solution may be expressed inversely as

$$t(r) = \frac{\sqrt{K}}{a}\left(\frac{1}{\sqrt{r_1}} - \frac{1}{\sqrt{r}}\right) \tag{8}$$

where $r_1 = r\ (t=0) = r_{LEO} \sim 6.9 \times 10^8$ cm. Using $r_2 = r_{GEO} = 4\ 22 \times 10^9$ cm we find the time trip T ~160 days. This time is proporational to M and inversely proportional to the thrust F.

Using the orbit equations we may calculate the amount of effluent ejected as a function of r. This is of course only preliminary to establishing what subsequently happens to the effluent. We define m(r) dr to be the mass of effluent deposited during time dt. It is given by

$$m(r)dr = \dot{M}dt = \dot{M}\,\frac{dt(r)}{dr}\,dr\ ,$$

or

$$m(r) = \dot{M}\,\frac{dt(r)}{dr}\ . \tag{9}$$

From (8) we find

$$m(r) = \dot{M}\,\frac{\sqrt{K}}{2a}\,\frac{1}{r^{3/2}} = \frac{\sqrt{K}}{2}\,\frac{M}{v_{ex}}\,\frac{1}{r^{3/2}} \tag{10}$$

Note that m(r) depends only on the SPS mass and Vex, and not on the trip time (this assumes that the mass expended is small compared to M, for the above mission the propellant mass is about .1M). Using $M = 47 \times 10^6$ Kg we find finally,

$$m(r) = \beta(2.35\times10^{14})/r^{3/2} \text{ gm/cm.} \qquad (11)$$

β is an adjustable parameter we have inserted to take approximate account of the various thruster alternatives;

$\beta = 1$ for the MPD thruster, $\beta \sim .5$ for ion thrusters, $\beta = 5\text{-}10$ for the chemical mission, and r is expressed in cm. (For chemical thruster orbit raising the equation would in fact be modified to take into account the large mass of propellant). $m(r)$ and $\int_{LEO}^{r} m(r)dr$ are plotted in Figure 2 1.1.

Using JSC estimates that station-keeping would require a total velocity increment to an SPS of 50 meters per second per year we calculate that the mass per year that is ejected at GSO is $1.2 \times 10^8\beta$ gm/year. The total mass required to raise the SPS is

$$\Delta M = \int_{r_1}^{r_2} m(r)\, dr = 4.7 \times 10^{14}\beta \left(\frac{1}{\sqrt{r_1}} \quad \frac{1}{\sqrt{r_2}} \right) = 1.07 \times 10^{10}\beta \text{gm.}$$

Over a thirty year period the station keeping propellant would amount to about 35% of the orbit raising propellant. A more useful comparison might be to note that stationkeeping requires $3.3 \times 10^5\beta$ gm per day, whereas we calculate that orbit raising in the vicinity of GEO requires $6.75 \times 10^7\beta$ gm per day. Thus it is probably the case that any untoward effects that result from stationkeeping of 100 SPS at GEO would show up in an analysis of the simple orbit raising mission for one SPS, however the long-term nature of stationkeeping could modify this.

B. PLUME CHARACTERISTICS

The next major factor to be considered is the properties of the thruster exhaust plume. Some important distinctions can be based on certain general properties of the thruster alternatives. Of course it may be ultimately necessary to understand the detailed plume properties of the thruster

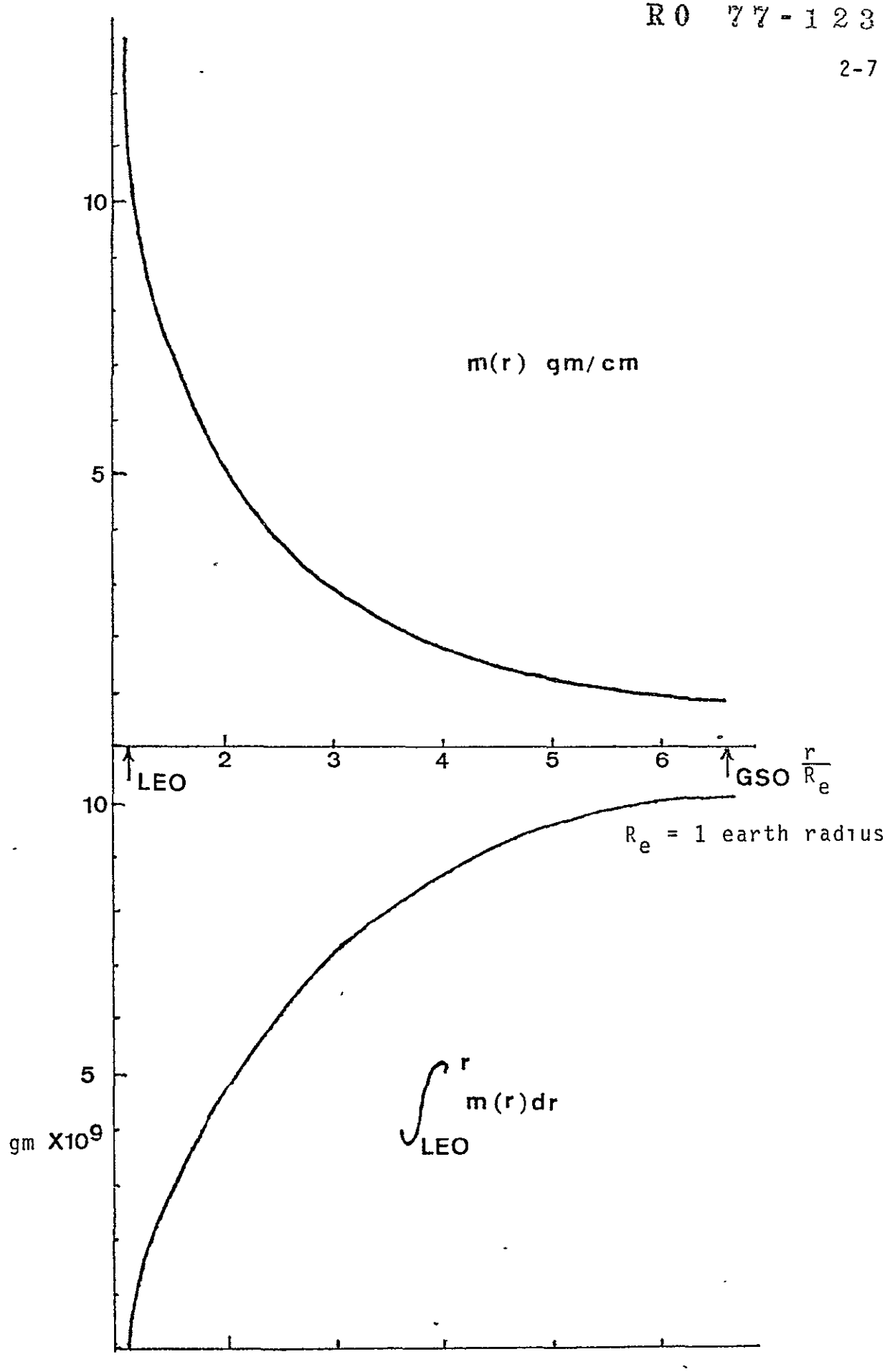

Figure 2.1.1 Effluent Deposition Profile

operating in space, and it may be that information will be found reliably only by resorting to space experiments.

The most important gross effluent characteristics seem to be the charge of the particles and their speed. If fully ionized plasma is emitted its individual particles will move in tight spirals on the earth's magnetic field lines on which they were emitted, spreading in latitude up and down that field line and then drifting off the field line in a direction determined by the ambient electric field. If neutrals are emitted they will move on ballistic trajectories at the higher altitudes. These two statements depend on the fact that the MS is so rarified that collisions may be neglected. The neutrals run the risk of being photoionized by solar ultraviolet radiation, at which time they become part of the ionized plasma inventory. We shall argue later that it is ionized effluent that has the potential for causing environmental disruption.

In Figure 2.1.2 we show rough plots of photoionization cross-sections for the various possible neutral exhaust products. Since Ar has the largest cross-section we use it to estimate the lifetime τ_1. Using a value for the solar spectral radiance in the ultraviolet of 20 ergs|cm^2-sec-micron[2,4] as an average value somewhere between solar minimum and solar maximum, we estimate the photon energy flux between 800Å and 300Å to be ~1.2 erg cm^{-2}sec^{-1}. The photon energies lie between 6.6 x 10^{-11}erg and 2.5 x 10^{-11}erg, giving a photon flux of 2 x 10^{10}|cm^2-sec to 5 x 10^{10}|cm^2-sec. Using for the cross-section 30 x 10^{-18}cm^2, Ref. 3, we find the lifetime τ_i = 1.7 x 10^{6}sec -6.7 x 10^{5}sec or τ_1 ~8 - 20 days. τ_i is somewhat longer for H_2O, the principal constituent of the chemical thruster exhaust. These numbers are important for two reasons. In the first place, τ_i might be long enough for a large fraction of the slow neutrals from a chemical thruster to

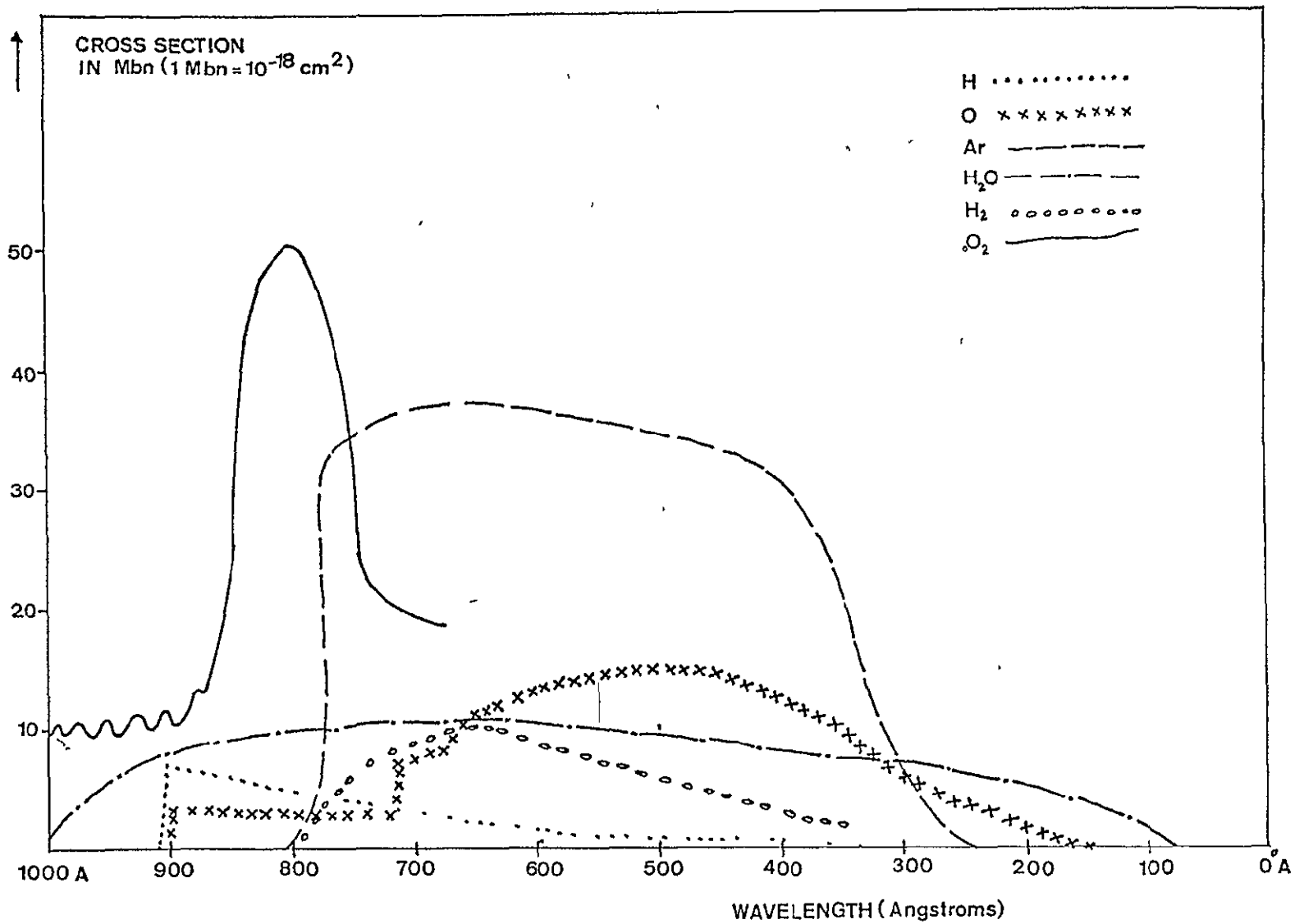

Figure 2.1.2. Photoionization Cross Sections (Ref. 2)

be absorbed in the denser lower atmosphere. In the second place, tests of the MPD thruster have indicated that the fast ions and electrons, which constitute ~90% of the effluent, in the beam recombine almost completely in a time of about .25 msec.[27] With v_{ex} ~20 Km/sec we find that the net actual velocity of the neutral Ar is greater than earth escape velocity at its point of emission by a factor ranging from 1.2 at LEO to 3.9 at GSO Since the plume is directed tangentially to the orbit this raises the possibility that most of the neutral Ar can escape completely before being turned into charged plasma. The neutrals will be discussed further in the section on the exosphere.

It is interesting to compare the density of deposited material with the ambient density in the MS. We shall see that only one orbit raising could deposit an amount of material in the MS equal to that normally present. This should not be taken too seriously since normally material is circulated on a rapid time scale. To make the comparison it is necessary to make some assumption as to the form of the effluent. It is simplest to assume that the total amount is deposited as ionized plasma in the earth's magnetic field, taken to be that of a dipole. This might apply to the bombardment ion thruster whose plume does not quickly recombine or to that fraction of effluent from an MPD thruster that does not recombine.

We assume that all the plasma deposited between r and r + dr in the equatorial plane spreads uniformly up and down the field lines and uniformly in longitude, filling the flux shell, Figure 2.1.3. We note that if the ions have a small cone angle velocity distribution they will tend to remain near the equator since they will be reflected by the increasing B field. If there were no atmosphere or ionosphere most of the particles would bounce back and forth in latitude, without hitting the

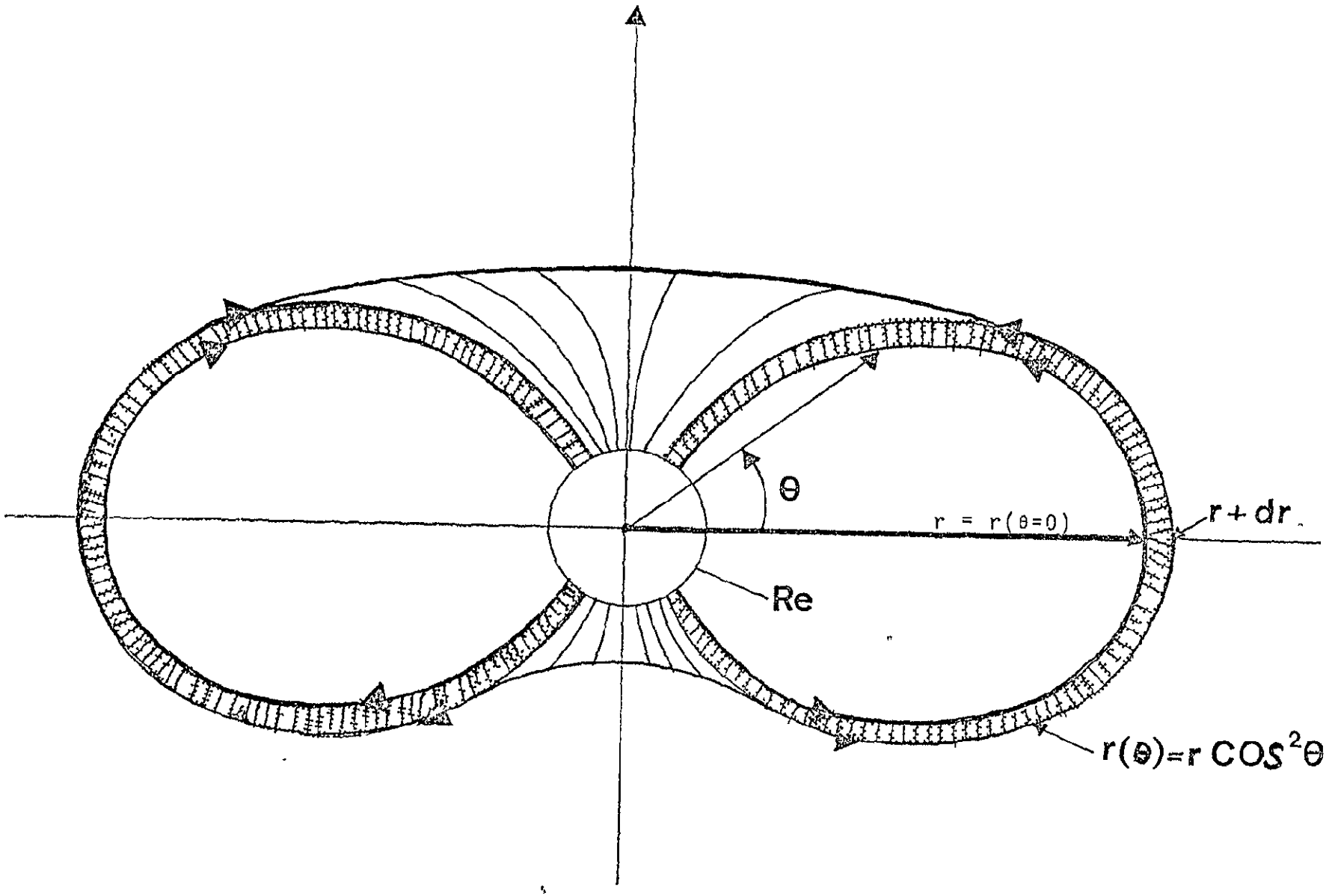

Figure 2.1.3 Flux Shell Volume In Dipole Field.

earth, as they would be reflected by the converging B field. The flux shell volume (using R_e as the limit of the volume) is

$$V'(r)\,dr = 4\pi R_e^2\, N(x) \tag{12}$$

where $x \equiv r/R_e$, $V'(r)\,dr$ is the volume contained between the flux shells intersecting r and r + dr at $\theta = 0$,

$$N(x) = 2\left[x^2\left\{\frac{3}{7}q^{7/2} - \frac{6}{5}q^{5/2} + q^{3/2}\right\} + x\left\{\frac{1}{2}q^{5/2} - q^{3/2} + \frac{1}{2}q^{1/2}\right\}\right] \tag{13}$$

and $q = (1 - \frac{1}{x})$.

The mass density is given by (putting $\beta = 1$ in (11))

$$\rho(r) = \frac{m(r)}{V'(r)} = \frac{2.8 \times 10^{-18}}{x^{3/2}\, N(x)}\ \mathrm{gm/cm^3} \tag{14}$$

which, assuming singly ionized Ar, translates to

$$n(x) = \frac{\rho(x)}{M_{Ar}} = \frac{4.73 \times 10^4}{x^{3/2}\, N(x)}\ \frac{\text{ions, electrons}}{\mathrm{cm^3}} \tag{15}$$

n(x) is plotted in Figure 2.1.4 along with a crude plot of the total ambient electron number density.[4,5] We see that for the most of the range from LEO to GSO it exceeds the ambient density, in some places by more than an order of magnitude.

Finally we summarize the thermal properties of the effluent. The Ar ions have velocity 2×10^6 cm/sec, determined by the acceleration forces in the thruster. The electrons are observed to have temperatures in the range of 1-5 eV, corresponding to velocity 6×10^7 cm/sec - 1.3×10^8 cm/sec. The neutral Ar temperature seems to be commonly about 500°K, corresponding to velocity 5×10^4 cm/sec. This means their actual velocities will lie in

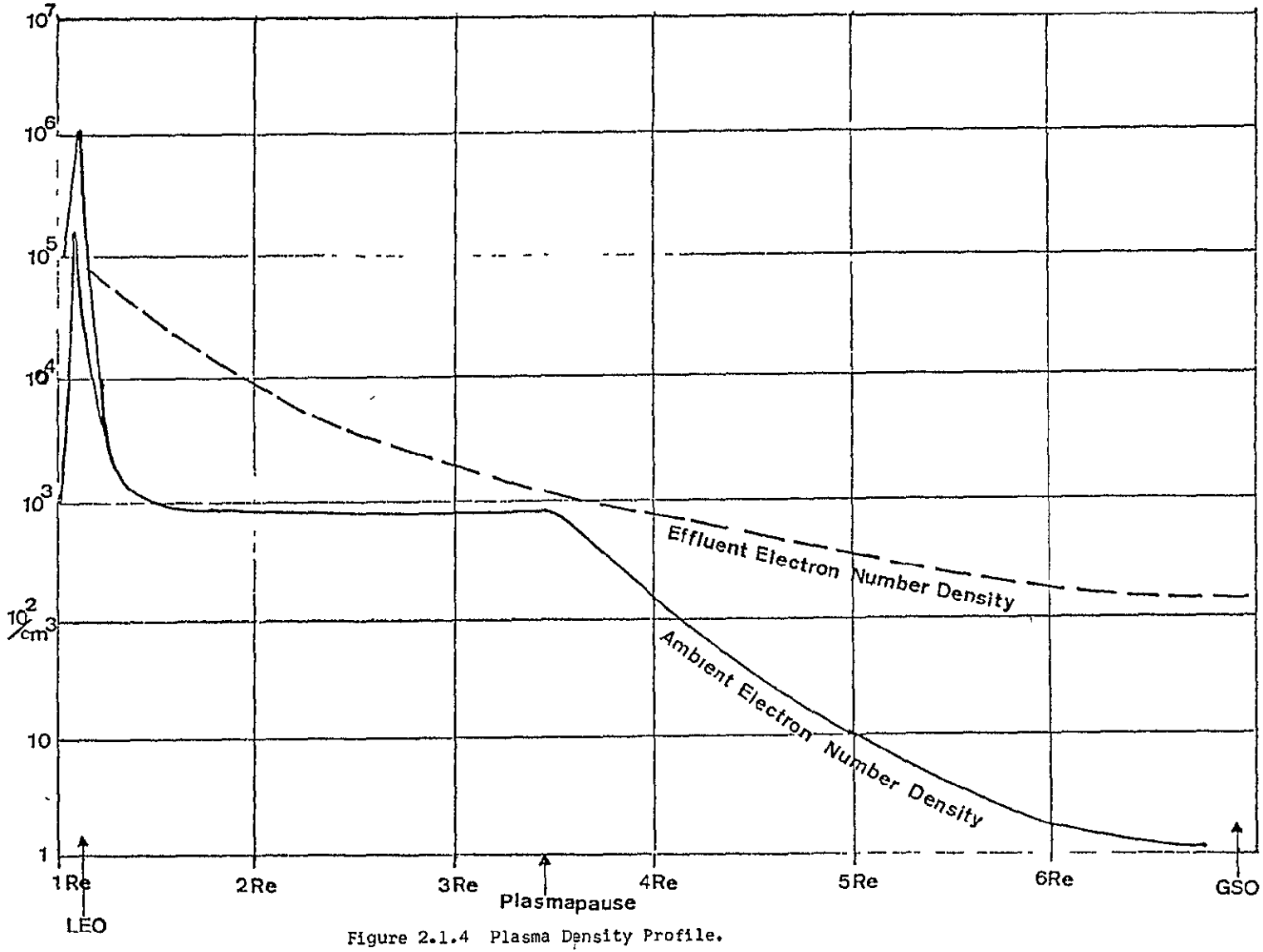

Figure 2.1.4 Plasma Density Profile.

a range close to the SPS velocity which ranges from 7.6×10^5 cm/sec at LEO to 3×10^5 cm/sec at GSO. They will probably then form a ring around the earth, see Appendix A and Figure A.1, until they collide with ambient particles or are photoionized. A major factor that can be deduced from the electron and ion speeds and the known magnetospheric electric and magnetic fields is that the electric EXB drift velocity is much greater than the ∇B drift velocity. This may allow a fairly simple determination of the plasma motion perpendicular to B in regions where collisions are unimportant, which is the case above about 1000-2000 Km altitude. In the plasmasphere region, that is out to about 3-4 R_e, EXB motion is just co-rotation with the earth, and the effluent plasma depletion takes place along field lines, the plasma being essentially absorbed by the much denser atmosphere and ionosphere at low altitudes. An unimpeded ion takes on the order of 10-20 minutes to hit the earth whereas a typical SPS rotation period might be 150 minutes or longer. This could mean that plasma deposited will equilibriate with the low altitude atmosphere along field lines before the SPS makes a complete revolution to deposit more on the same field line. It is probably difficult but should be possible to calculate this process. This is important because it could be determined whether or not the ambient low energy plasma density tends to increase or remain the same on the average as the satellites are raised. The importance of low energy plasma densities will be pointed out in the discussion of magnetospheric processes.

C. NEUTRAL EFFLUENT AND THE EXOSPHERE

In contrast to the charged plasma emitted the neutral atoms and molecules assume ballistic trajectories until they suffer a collision, or a reaction which changes their form. The most important reaction is

photoionization by solar photons. We feel that the neutrals as such at high altitude could not have any environmental consequences since it is the charged particle populations that govern magnetospheric processes. At atmospheric densities neutrals of course do have important functions, for example the attenuation of UV solar radiation. It will be important to see if the neutrals such as H_2O, returning to the atmosphere could change the relative molecular abundances and energy balance enough to upset these functions.

To discuss the fate of neutral effluent it is useful to review the properties of the natural neutral atmosphere at high altitudes[6,7]. The density of a species i decreases exponentially according to

$$n_i(h) = n_i(h_o)e^{-m_i g(h-h_o)/kT} \qquad (1)$$

where m is the mass and T is the temperature. Figure 2.1.5 is a plot of species densities.[5] If one species dominates over a range of h the total number density here will fall exponentially. It is usually reasonable to represent the total number density also as an exponential

$$n(h) = n(h_o)e^{-(h-h_o)/H},$$

where H is a slowly varying scale height, which depends on temperature and other factors such as the variability of gravity with height.

Since the number density decreases with altitude the mean free path for collision will increase, until at some altitude it exceeds the scale height H. A particle traveling upward from this point will travel much farther than a particle traveling downward. Most upward going particles will turn around and return without having a collision. This outermost region where collisions are negligible is called the exosphere. The base of the exosphere is an altitude from which collisions send up particles

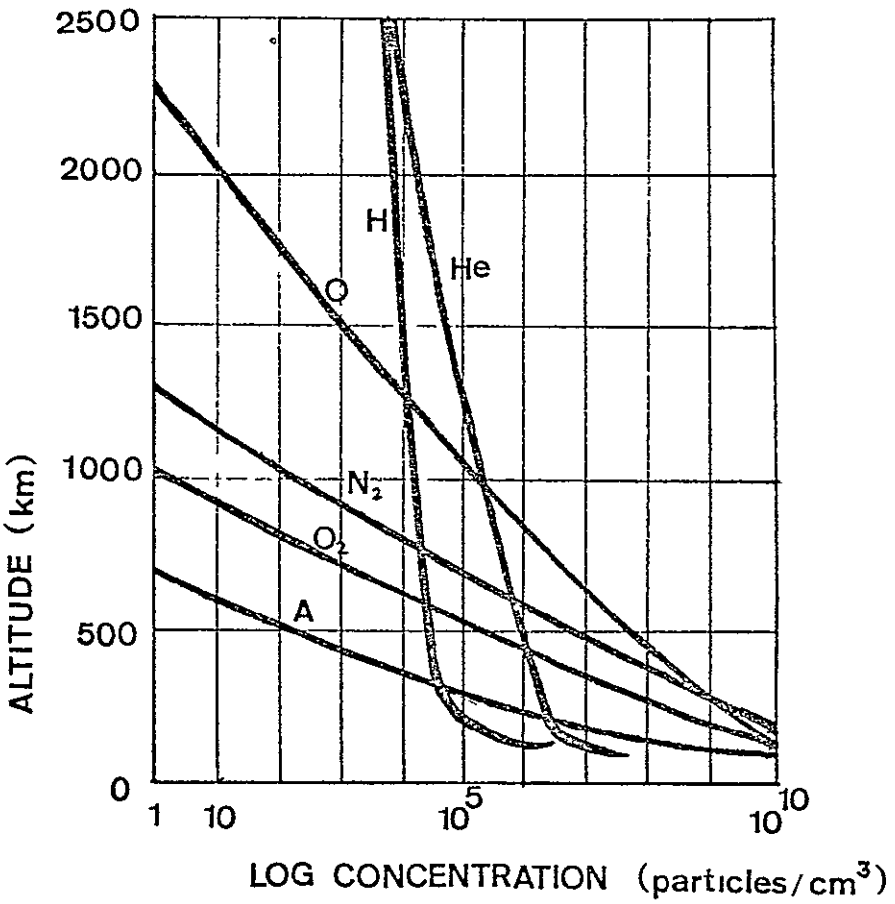

Figure 2.1.5. Neutral Particle Densities In The Upper Atmosphere.

and down into which they fall after a few minutes of free flight.

In discussing the exosphere it is usual to introduce the concept of critical height h_c This is an altitude determined by the condition that a fraction 1/e of fast particles moving upward at h_c at high speed will experience no collision as they proceed to infinitely great height. h_c must depend on H, whose value is assumed known. The probability that the particle collides in the range dh is $4\pi a^2 n(h)\ dh$, where a ~1.5 x 10^{-8} cm is a typical particle radius, and $n(h) = n(h_c)\ e^{-(h-h_c)/H}$. The number of the fast particles that suffer a collision in dh is thus

$$dN(h) = -N(h)\ 4\pi a^2\ n(h_c) e^{-(h-h_c)/H} dh \tag{2}$$

leading to the condition

$$-\log \frac{N(\infty)}{N(h_c)} = \log e = 1 = \int_{h_c}^{\infty} 4\pi a^2 n(h_c)\ e^{-(h-h_c)/H}\ dh \tag{3}$$

or

$$n(h_c) = \frac{1}{4\pi a^2\ H} \quad . \tag{4}$$

This density at h_c must be consistent with the scale height at h_c. The density plots indicate h_c ~600km at which the density of the predominant species, O, is about 2 x $10^7/cm^3$, and H ~100Km. It is interesting to note that (4) implies that h_c is the altitude at which the mean free path for a horizontally travelling particle equals the scale height, and this happens to coincide with LEO. The distribution of particles at very high altitudes must be the same as at lower altitudes because of Liouville's theorem. This says that the density in phase space is the same along particle trajectories. The Maxwellian form established by collisions at low altitude must hold at high altitude where there are no collisions. The

lighter particles, He and H, whose energy kT gives them a large velocity should predominate at high altitudes according to (1) and this is observed. Also the temperature T of the exospheric particles should equal approximately that at low altitudes and this too is observed.

The nature of the exospheric critical level might be important in future more detailed analyses of neutral effluent effects. We show in Appendix A, Figure A.1 that neutral effluent from the chemical orbit raising mission might fall in such a manner that if unimpeded it would simply hit the earth. It is tempting to say that if this is the case the particles are immediately absorbed. However we note that if a particle collides elastically at the critical level it would be just as likely to bounce back out again if it and the target particle had roughly equal speeds. An H_2O molecule dropped from GSO would be travelling at about 10Km/sec. At 1300°K an oxygen atom with which it is most likely to collide, would be travelling at about 1 Km/sec. This would mean that the collision products would tend to be directed downward. For this effluent the absorption picture could be correct. It would take a more detailed analysis to determine if reflection from the critical level would build up the density of the exosphere. It is doubtful even so that this would do much for the following reason. Photoionization of H at the ambient exospheric density of say $100/cm^3$ produces plasma ions at the rate of about $10^{-4}/cm^3$-sec. On the other hand, taking a conservative corotation drift speed of 3×10^5 cm/sec and plasma number density $1/cm^3$ we see that 3×10^5 particles stream through a 1 cm^3 volume in 1 sec. Thus photoionization of the exosphere would appear to be a negligible source.

The energy content of these falling neutrals should be considered. Their number is about 1% the number of UV solar photons hitting the

atmosphere, and at 10 Km/sec their energy is approximately 19 eV. This does not necessarily mean, however, that they can ionize atmospheric atoms because there exists a threshold "activation energy" [26] below which ionization is very improbable. This question would have to be considered in detail if chemical thrusters were used for orbit raising.

As shown in Appendix A and Figure A.1, very slow neutrals would tend to form a sheet consisting of concentric rings deposited as the SPS spirals outward. In this case, their density might build up to the point where they would constitute an important localized plasma source. This could probably be determined by a straightforward numerical computation given detailed knowledge of MPD thruster characteristics.

The major potential consequence of the slow neutrals emitted from chemical thrusters would be their deposition of energy and contaminants in the upper atmosphere. However this would not be localized as in the case of heavy lift launch vehicle emissions. It should not be difficult to perform reliable trajectory calculations using anticipated thruster characteristics to determine if any possible perturbation on the upper atmosphere could result. It is already believed[1] that heavy lift launch vehicle (HLLV) operations will not significantly perturb the upper atmosphere, although this viewpoint is not universally held.

D. THE MAGNETOSPHERE

To facilitate the discussion of the consequences of large amounts of extra cold plasma in the MS we provide here a short discussion of its geometry and functioning. [8,9,10,11] No major conclusions are presented in this section, thus it may be bypassed by the reader familiar with magnetospheric phenomenology. It should be kept in mind that even in some of its gross features the MS is not fully understood and the interpretation of many of the observed phenomena is controversial. In

particular, we shall focus on phenomena relating to plasma loss and flow in order to discuss the fate of additional deposited plasma.

The MS consists of charged particle populations interacting with magnetic field B, Figures 2.1.6,7. The B field lines outline its gross geometry and divide it more or less into various functional regions which are distinguished by the types of particle populations present. The B field of the earth itself is essentially that of a dipole placed at its center, tilted with respect to the earth-sun line, the currents generating this dipole flowing in the earth's core. Impinging on this dipole field, which acts as an obstacle, is the "solar wind", a cold, dilute, supersonic ($T_{electron} \sim 20\text{-}100eV, n \sim 5/cm^3$, $v_s \sim 400$ Km sec^{-1}) plasma emanating from the sun. The balance of solar wind directed pressure against the B field pressure $B^2/8\pi$ yields the observed boundary form, an elongated teardrop, pointing away from the sun at all times, outside of which $B \simeq 0$. This boundary is known as the magnetopause and in an ideal fluid description no plasma will cross it. This analysis indicates that the magnetopause in the sunward direction lies at about 10 earth radii, R_e, geocentric distance and this is observed. It also would indicate that the MS would close at a point about 15 Re in the direction away from the sun (anti-sunward) but it is in fact found that the tail extends for hundreds of earth radii. This is attributed to "vicous drag" forces exerted by the solar wind across the magnetopause, which stretch out the field lines.

In addition to the dipole field the MS is immersed in the "interplanetary magnetic field"(IMF) a weak approximately uniform field whose direction depends on the rotational position of the sun from whence it emanates. Many workers in the field feel that the IMF plays an important role in the functioning of the MS. For example it combines with the dipole

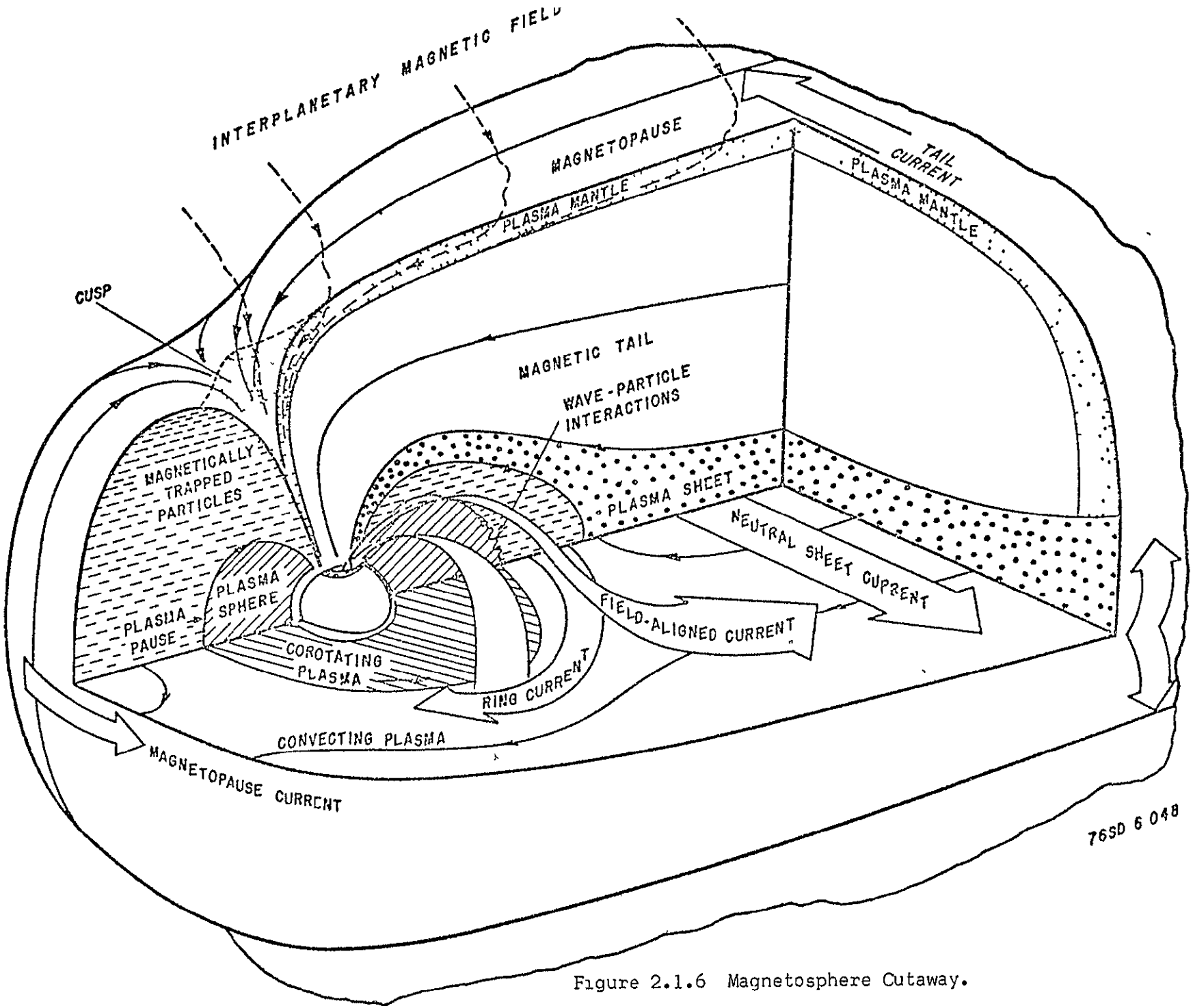

Figure 2.1.6 Magnetosphere Cutaway.

ORIGINAL PAGE IS
OF POOR QUALITY

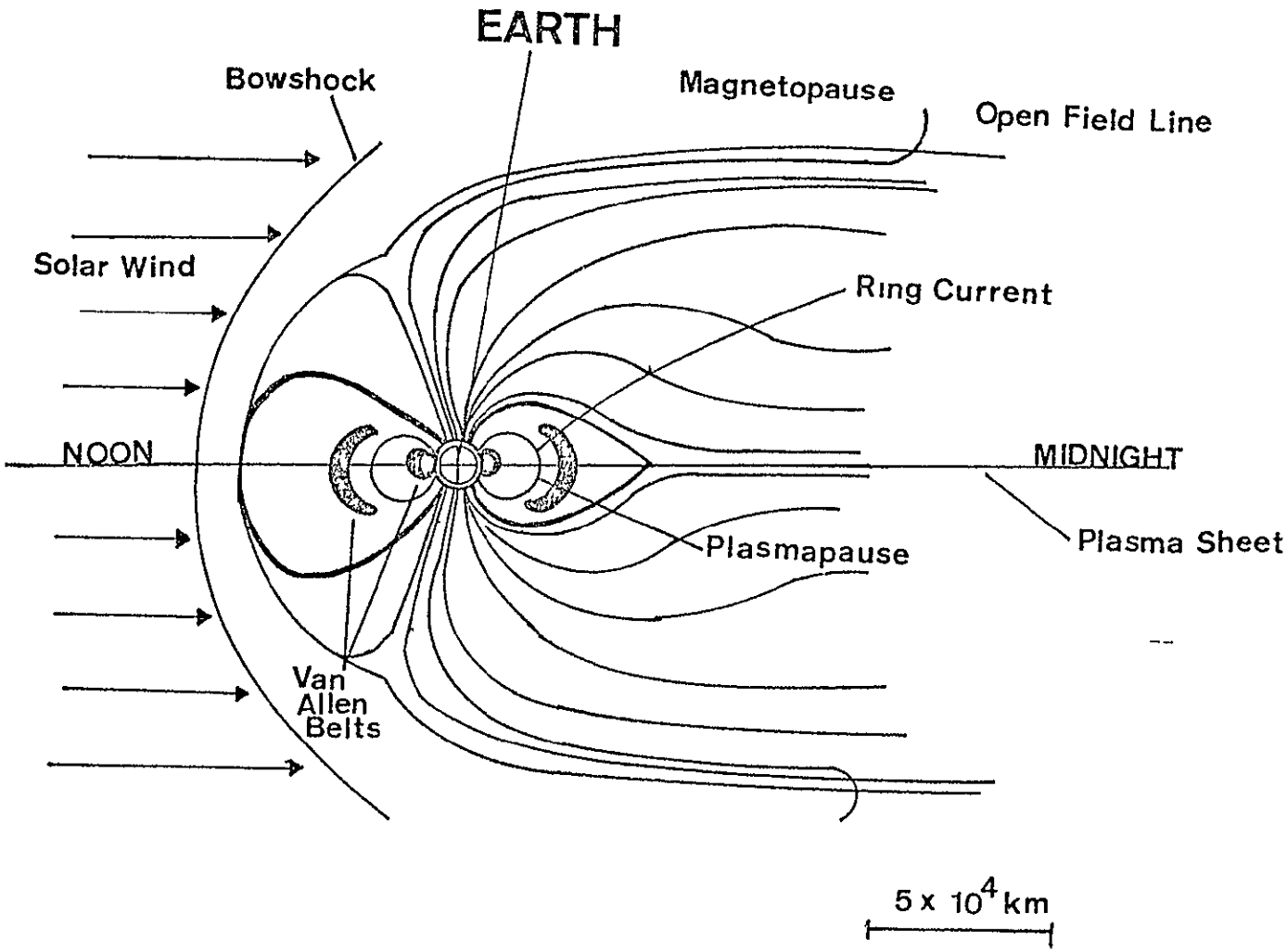

Figure 2.1.7. Magnetosphere Section Through Noon-midnight Plane (Ref. 10).

to create regions on the earth where the B field lines lead directly to interplanetary space (open field lines) allowing the easy exchange of plasma between the ionosphere and distant regions.

Surrounding the magnetopause at distances of the order of 2-3 R_e from it lies what is known as the bow shock front. This is a boundary within which the solar wind has changed from a cold smoothly flowing plasma to the hotter turbulent magnetosheath plasma. The shock front is analogous to that which occurs when an ordinary fluid such as air or water flows supersonically past an obstruction. Within this front the directed energy of the flow has been converted into randomly directly turbulent and thermal energy.

The observed complex phenomonology of the MS involves the interaction of the solar wind and IMF with its particle populations via the electric fields set up and electric currents flowing. Referring to Figures 2.1.6, 7 and Table 2.1.1, we take note of three main charged particle reservoirs. The plasmasphere is cold and dense by magnetospheric standards ($n \sim 100\text{-}1000\ cm^{-3}$, $T \sim .1\text{-}1$ eV) and consists of electrons, protons and heavy ions which boil up out of the ionosphere. There is a large amount of particle interchange between the plasmasphere and ionosphere [7] proceeding continuously. Referring to Eqn. 11 of section B we note that ~50% of the effluent from the orbit raising mission is deposited in the plasmasphere. The effluent plasma bears close resemblance to the ambient plasma and may participate in magnetospheric processes in a similar manner (except possibly for fast ions from bombardment ion thrusters).

The plasma sheet is a broad region of dilute, "warm" ($n \sim 1\ cm^{-3}$, $T \sim 1\text{-}5$ KeV) plasma about 5-10 Re thick lying in the equatorial plane extending from the dawn side to the dusk side of the tail and many earth

	Magnetic Field (gauss)	Approximate Particle Energy (eV)	Particle Density (cm^{-3})
Magnetopause	$5x10^{-4}$	1000	10
Solar Wind	$5x10^{-5}$	100 (electrons) 1000 (protons)	5
Plasmasphere	$3x10^{-3}$	1	100
Ionosphere	.5	1	10^5
Van Allen Belts	--	10^6 (electrons)	10^{-4}
Ring Current Belt	$2x10^{-3}$	5000	1
Plasmasheet	$5x10^{-4}$	1000	1

Table 2.1.1 Magnetospheric Parameters (Ref. 10)

radii down the tail. At its earthward end it terminates in a horseshoe shaped region with the tips reaching into the northern and southern auroral zones of the ionosphere. The plasma sheet plasma is regarded as originating mostly as solar wind plasma that has by various mechanisms penetrated the magnetopause and heated, although some scientists feel that it may be fed by the ionosphere. During times of magnetic disturbance some of the plasma sheet drifts directly toward the earth, gaining energy and ending up populating the third major particle reservoir, the trapped particle belts. The belts contain, in addition to the ever-present low energy plasma of ionospheric origin, high energy particles (~1 KeV - $\gtrsim$100 MeV) which are magnetically trapped, bouncing back and forth along B field lines and drifting in longitude around the earth, Figure 2 1.6. The very high energy (> 30 MeV) trapped particles are deposited when neutrons produced by high energy collisions of cosmic ray particles with the atmosphere decay into protons and electrons. The population of the trapped particle belts varies in time. During geomagnetically active periods hot plasma sheet particles are energized and injected, and perhaps local particles are energized, and are trapped. Some of them become untrapped and precipitate into the atmosphere. Some continue to diffuse earthward, gaining energy in the process. The inner region, which contains the protons of cosmic ray origin plus these energetic plasma sheet particles is rather stable in time and is known as the Van Allen Belt, Figure 2.1.7.

The radiation environment in this region is intense enough to be damaging to life and materials, such as solar cells and thus any process that might modify the radiation would be important. In 1965 an atomic bomb was exploded in the Van Allen region[12] (Project Starfish) and the high energy electrons from this explosion persisted for many years, far longer than anticipated.

Finally there is the polar cusp plasma reaching the earth on magnetic field lines leading directly from interplanetary space. It flows down from the plasma mantle, a thin sheet of plasma lying just inside the magnetopause.

The electric currents flowing in the MS determine the B field through Ampere's law

$$\vec{\nabla} \times \vec{B} = \frac{4\pi}{c} \vec{J}$$

The strong deviation from a dipole field may be regarded as due to these currents. On the other hand, knowing the magnetic field, it is possible to infer the currents. Likewise electric fields $\vec{E}$ are related to the flow velocity $\underset{\sim}{v}$ of low energy plasma by

$$\vec{v} = c \frac{\vec{E} \times \vec{B}}{B^2} .$$

Currents and flows during undisturbed times are approximately orthogonal to $\vec{B}$ because trapped plasma rapidly comes to equilibrium along B lines, which must therefore be equipotentials.

There exists at present only a crude picture of the currents that must exist. The magnetopause current varies strongly with time because the polar wind and the B field just outside the magnetopause is highly variable. On the average it is directed from dawn to dusk on the day side. This current must exist to account for the difference in B inside and outside the magnetopause. How the current is closed is not known for sure. It may join up with the neutral sheet current system. The neutral sheet is a very thin region lying in the equatorial plane and dividing the tail into its northern and sourthern halves. Current must be flowing from dawn to dusk to account for the different directions of B in the northern and southern regions. It presumably flows around the magnetopause forming two

closed loops when looked at endwise.

One theory of this current[13] depends on the E field that must exist in interplanetary space due to the motion of the solar wind plasma through the IMF given by

$$E = -\frac{v_s \times B_{IMF}}{c}$$

and which points in the dawn to dusk direction. It is surmised that this induction field penetrates the MS and causes current to flow on loops of non zero conductivity. Current can flow across the neutral sheet because there $B \cong 0$, which allows current flow parallel to E. This current flow may also be supported by plasma density gradients. It then joins with the surface currents flowing across the top and bottom of the tail. In a sense we can regard the MS as a load on the solar wind electric dynamo, and current flow across the neutral sheet constitutes a loss mechanism, Figure 2.1.8. The cross tail E field is considered to be very important in the creation of the energetic particle populations. One mechanism for particle energization says that the small net northward B component combined with E can E x B drift the plasma toward earth. This drift energizes a particle of charge q adiabatically because the magnetic moment $= q\frac{W_\perp}{B}$ where $W = \frac{1}{2}m\, v_\perp^2$ ($v_\perp$ is the particle velocity component normal to B) must remain constant and B increases on approaching earth. The plasma flow pattern may be summarized by saying that plasma flows down the tail near the surface and back towards earth in the plasma sheet within the tail as shown schematically in Figure 2.1.9.

The third major current system is the ring current, Figure 2.1.6. It is doughnut shaped and flows around the earth in circles lying parallel to the equatorial plane. This current flows from dusk to dawn on the sunward

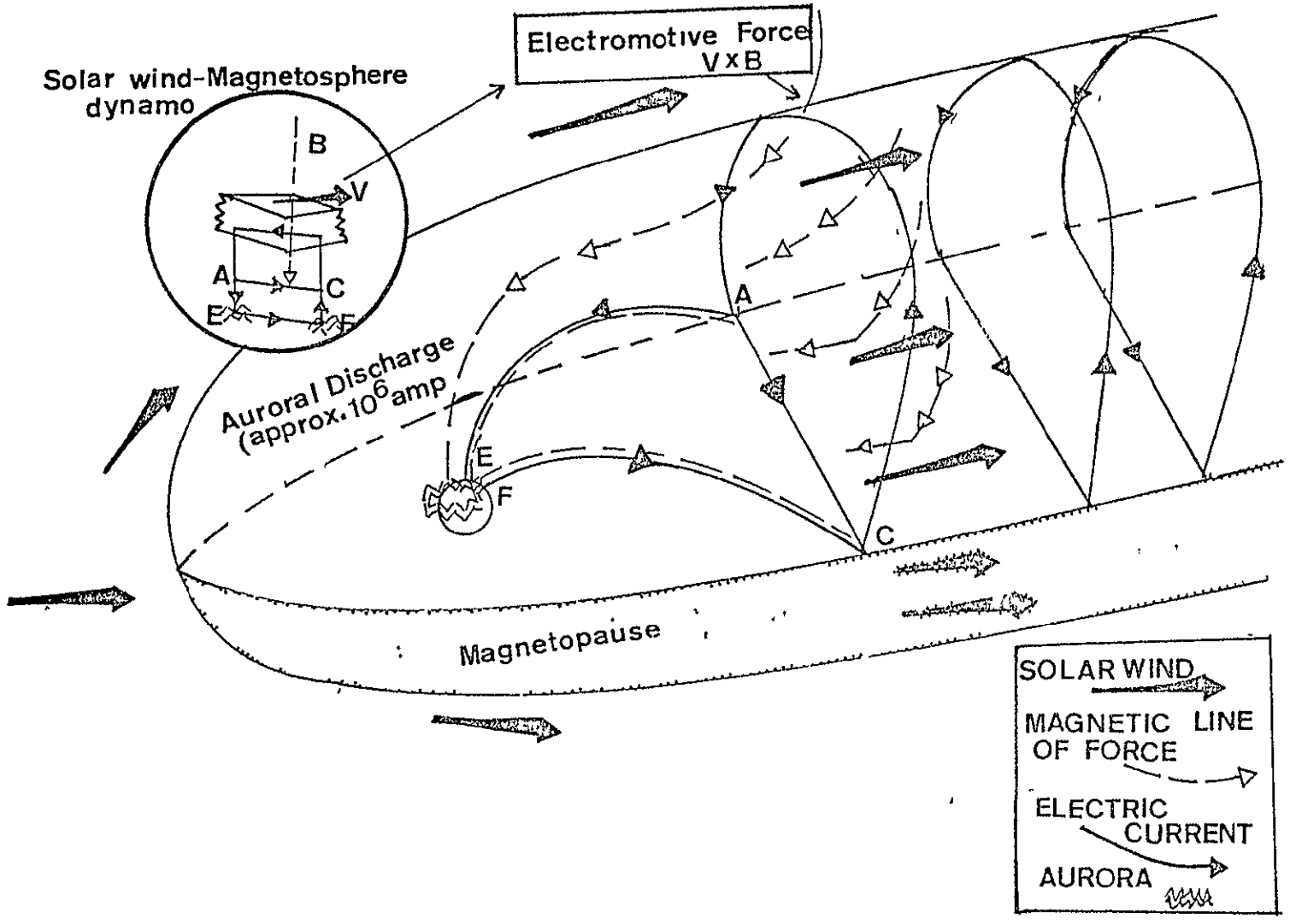

ORIGINAL PAGE IS OF POOR QUALITY

Figure 2.1.8 Solar Wind Dynamo Circuit (Ref.10).

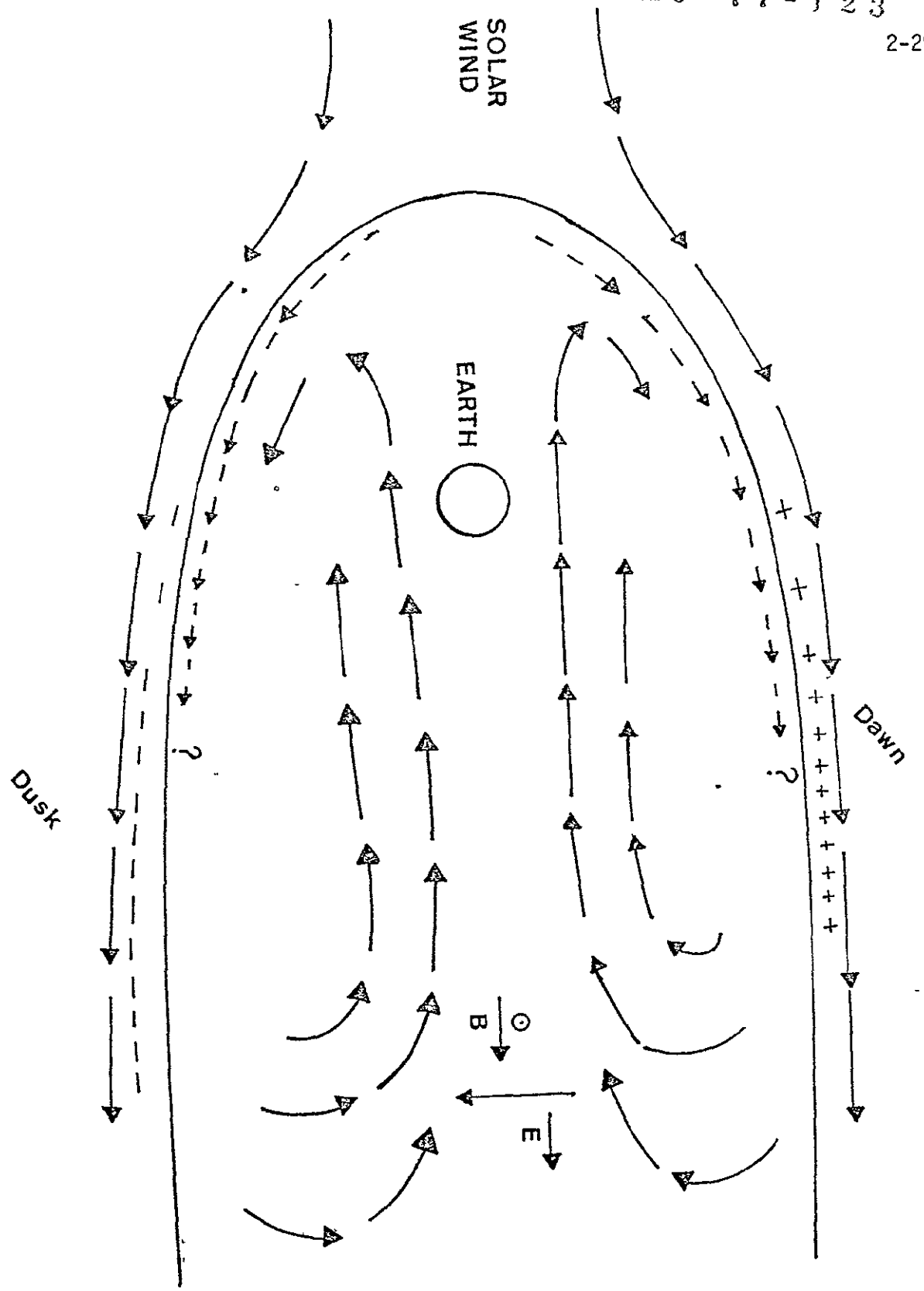

Figure 2.1.9 Large Scale Plasmasheet Convection.

side and thus tends to cancel the magnetopause current and add to the neutral sheet current. The current carriers are 1-20 KeV charged particles, protons, electrons and some alpha particles, trapped on closed B lines and it flows because particles slowly drift, compared to their bounce motion parallel to B, around the earth longitudinally due to the fact that B is not uniform. The protons and electrons drift in opposite directions but the protons drift faster, and in the direction opposite to the E x B drift. This is because the gradient B drift speed of particles depends on their Larmor radius which is much larger for protons than for the electrons since the protons are much heavier.

The field aligned or Birkeland currents, Figures 2.1.8, 10 flow down field lines from the plasma sheet to the ionosphere during times of geomagnetic activity They will be discussed in the section on magnetic storms.

The magnetospheric electric field pattern in the equatorial plane, insofar as it is known, is represented by the equipotential plots such as that[14] shown in Figure 2.1.11. These equipotential lines are also the flow lines for very low energy plasma since for this plasma

$$\vec{v} = c\,\frac{\vec{E} \times \vec{B}}{B^2} = -\,c\,\frac{\vec{\nabla}\phi \times \vec{B}}{B^2} \quad .$$

The flow paths above and below the equator may be inferred by noting that B field lines are equipotentials, at least during quiet times. The gross features of this pattern can be understood by superposing a uniform dawn to dusk E field with the radial co-rotational E produced by the rotation of the earth's dipole field given by $E = -\frac{r\Omega \times B}{c}$ where r is the distance from the rotation axis and Ω is the rotation frequency. The dotted segments in Figure 2.1.9 indicate only possible flow paths as these areas

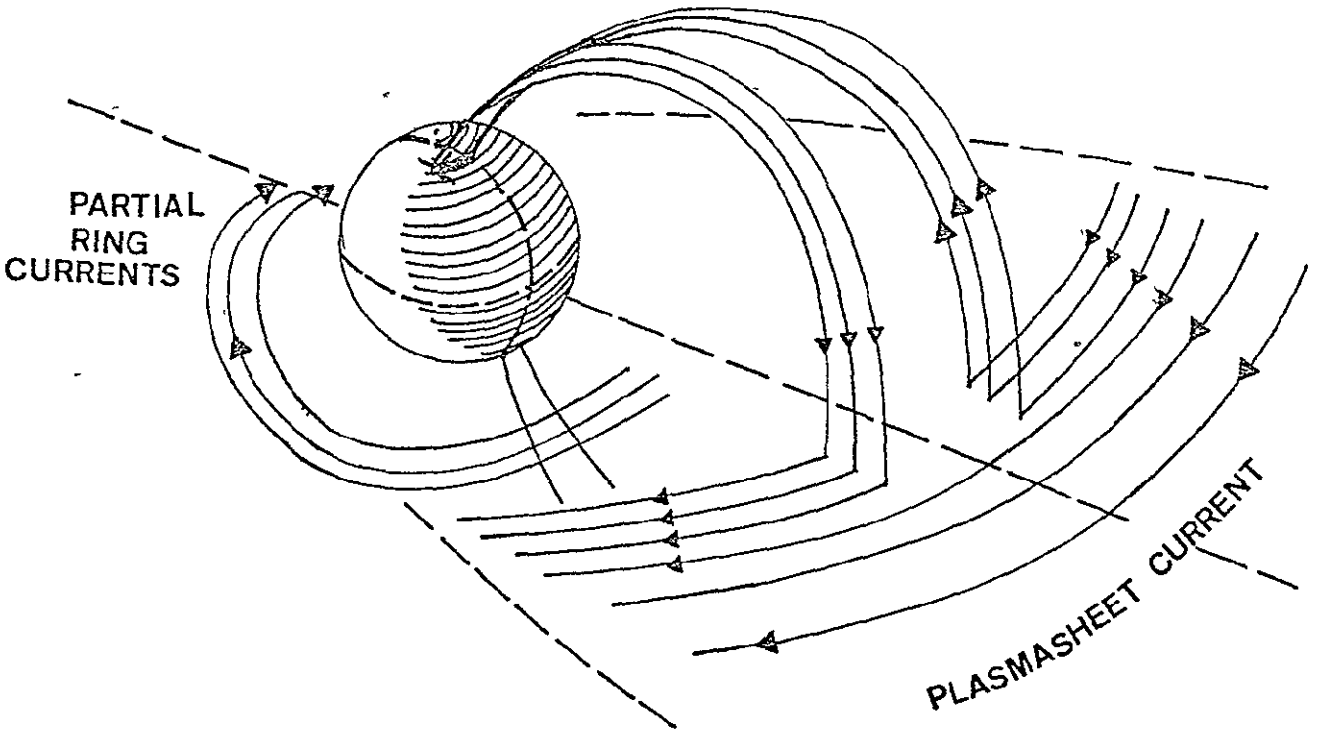

Figure 2.1.10 Field Aligned Currents.

ORIGINAL PAGE IS
OF POOR QUALITY

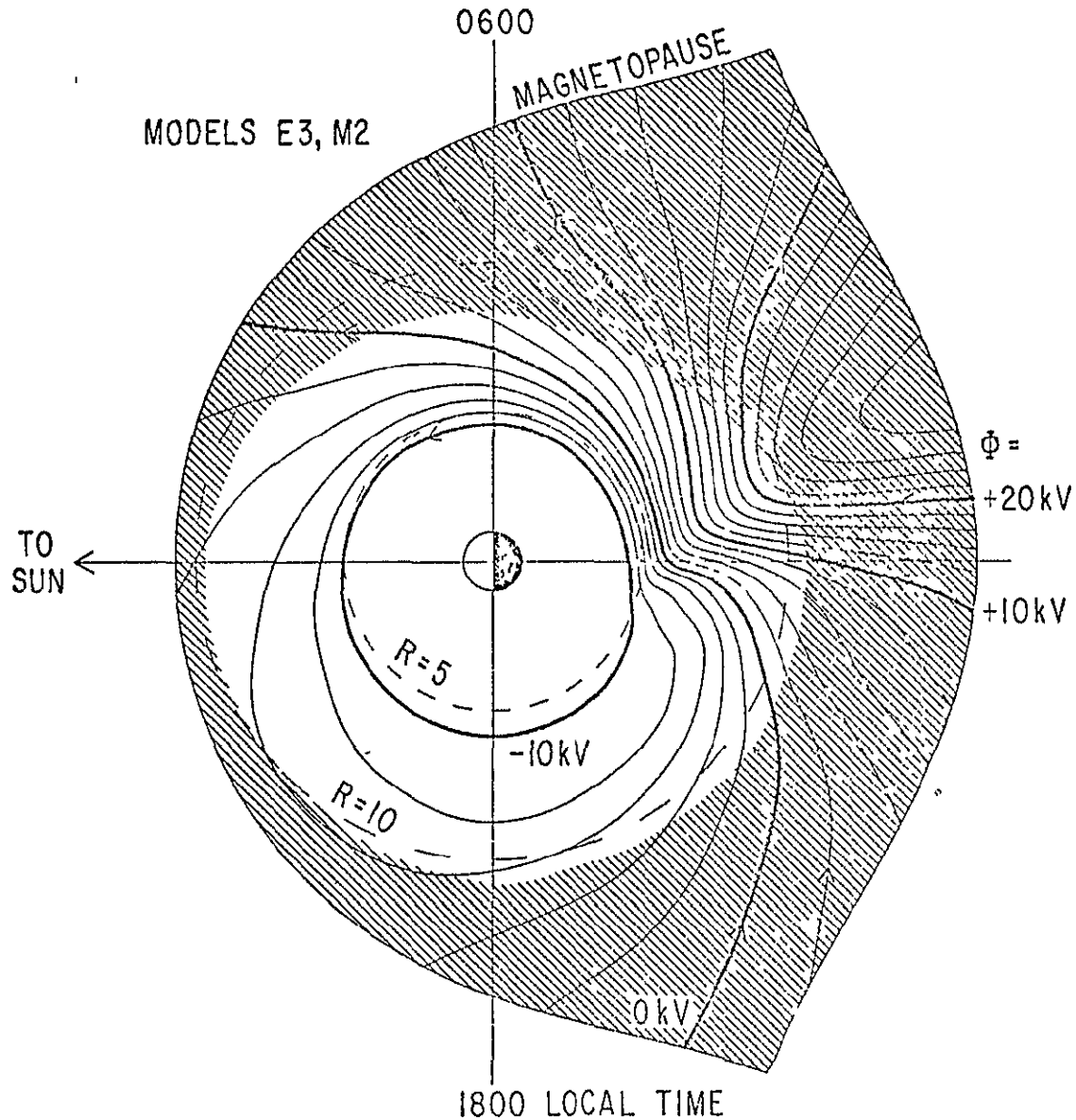

Figure 2.1.11 Magnetosphere Electric Equipotentials (Ref. 14).

ORIGINAL PAGE IS
OF POOR QUALITY

are not well understood. In particular it is not known whether there exist closed loops in the pattern outside of the plasmasphere region. This could be an important issue because the density of cold plasma continuously deposited on them might tend to build up over a period of time. The natural mechanisms for deposition into and loss from the magnetospheric convection pattern are not presently well known and thus it is not possible to determine with certainty the ultimate fate of large amounts of artificially injected plasma. Some conjectures are given immediately below.

The electric field pattern of Figure 2.1.11 is basically responsible for the non-circular shape of the plasmasphere boundary, the plasmapause. Outside the plasmapause the plasma is diffuse and hot ($n \sim 1\ cm^{-3}$, T in KeV region) due to heating while it is convecting in from the far tail regions or due to local heating mechanisms. Cool populations can also be found here. On the other hand the dense, cold ($n \sim 100\text{-}1000\ cm^{-3}$, $T \approx 1eV$) plasmasphere plasma corotates with the earth on closed equipotentials.

The sharp inward boundary of the hot convecting tail plasma occurs because the increasing B field keeps energetic particles from approaching too closely to the earth since their drift motion is in part determined by B. There exists a so-called forbidden region, Figure 2.1.12. The sharp density decrease of the cold plasma pause plasma is another matter. This may be explicable by reference to the so-called "polar wind."[7] The polar cap is defined as the ionospheric region which intercepts field lines leading far down the tail and ultimately into interplanetary space. This allows ionospheric plasma to escape rather easily, the polar wind flow, and would result in a sharp density gradient at the boundary between the closed lines and the open lines, thus explaining the plasmapause In fact, the plasmapause is equatorward of the closed field line boundary. Due to

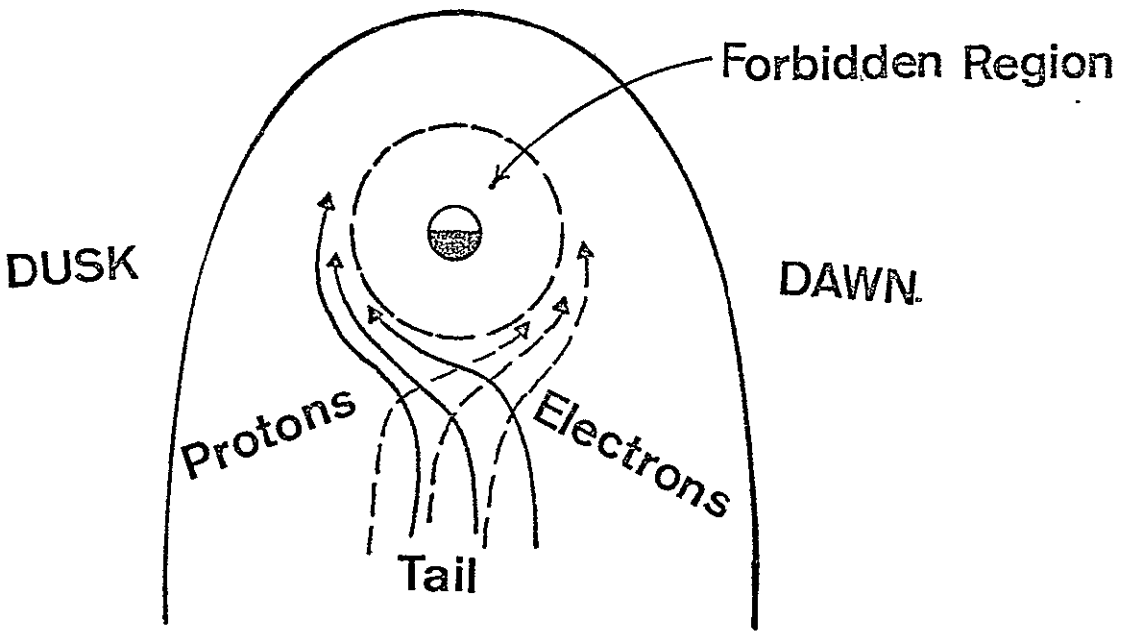

Figure 2.1.12 Forbidden Region.

the lack of symmetry in the polar region E field plasma can be convected from closed B lines to open B lines, Figure 2.1.13. It's input from the ionosphere is not rapid enough to refill these lines, and the density remains low. We mention this because the same process could constitute a rapid loss mechanism for plasma effluent deposited on the closed lines outside the plasmapause, particularly at geosyncronous orbit.

The magnetic substorm is the single most important instability of the magnetosphere. The MS gradually stores in its tail some 10^{22} ergs of energy drawn from the polar wind and earth's rotation and releases it rather explosively into the polar atmosphere. This results in the well-known auroral phenomena[15], intense magnetic activity and intense fluxes of high energy particles at high altitudes (e.g. GSO). All of these could have environmental consequences which are discussed in Section E. Thus it will be important to understand in what way effluent deposition might offset substorm activity.

Substorms occur as isolated events, every few days or hours, or may occur in rapid sequence They can result from a shock wave triggered by a solar flare, a change in the solar wind pressure, or a change in the IMF. During quiet times normal flucturations in the southward component of the IMF and in the solar wind fluxes generate corresponding fluctuations in the ionospheric current system, and plasmasheet particles are precipitated at a steady rate into the ionosphere. Many scientists believe some substorms are triggered when the IMF turns southward, in turn increasing the cross tail E field. Or it may be that when the IMF is directed more southward substorms are more likely to be triggered by solar wind fluctuations. In any case, a southward turning of the IMF and solar wind fluctuations are certainly correlated with substorms.

ORIGINAL PAGE IS
OF POOR QUALITY

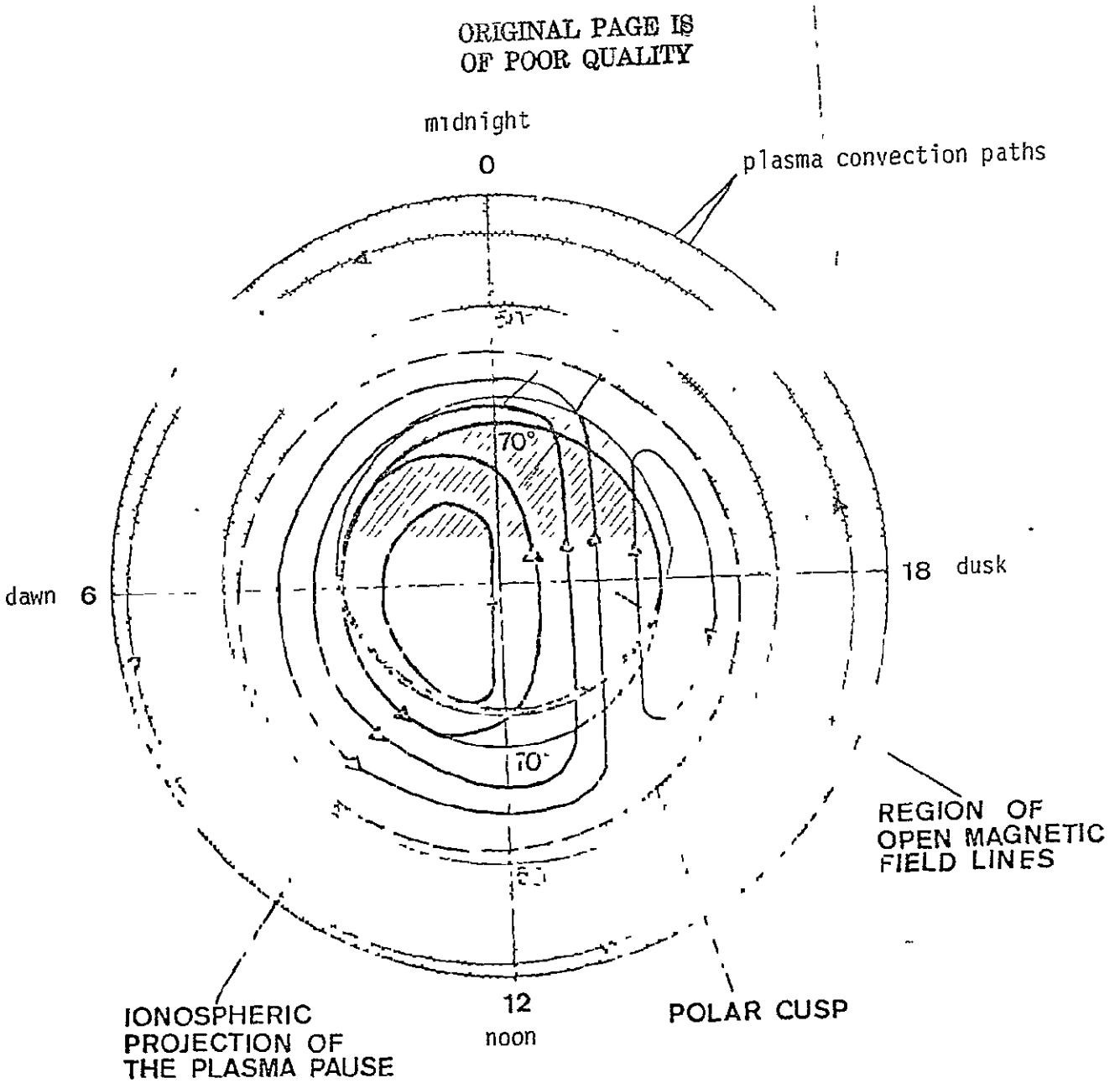

Figure 2.1.13 Electric Equipotentials In North Polar Cap Region(Ref. 7).

The release of energy in a substorm results essentially from the non-balance of convection rates on time scales shorter than the typical quiet time reaction times of the MS-ionosphere system To understand substorm phenomena it may be helpful to focus on the large scale MS current systems, which carry current in response to the "$v_s \times B_{IMF}$ solar wind electric dynamo", Figure 2.1.8. An increase in the driving voltage increases the currents. But it may also overload the circuit in the sense that instabilities are caused which can drastically increase the resistivity in a local region. This may cause a large release of energy in this region. Also the disruption of the current flow will cause voltages to be developed across other paths that normally do not carry much current.

Substorms tend to proceed in well-defined stages although this is not always the case. There may be a "growth phase" in which the magnetosphere is compressed due to increased solar wind pressure, the sunward magnetopause is pushed towards earth, and the tail B field lines are stretched. This B field deformation stores energy. On many occasions this energy may be dissipated and nothing drastic happens. However, if a certain not-well-understood threshold is reached, an explosive chain of events may be triggered. There exists controversy as to whether a well-defined growth pattern exists. This starts the "expansion phase", called that because the dipolar part of the B field expands. This seems to be triggered by the disruption of the previously enhanced neutral sheet current whose collapse begins near earth and propagates down the tail. It is thought that the neutral sheet current is redirected along B lines down to the auroral region of the ionosphere, Figure 2.1.8, 10, and back out again. The current segment that is set up in the ionosphere is known as the

auroral electrojet. The existence of field aligned currents was originally inferred by Birkeland who noted that they would explain the magnetic disturbance pattern caused by the auroral electrojet. This current path diverts energy down to the atmosphere causing optical radiation from atoms excited by incoming electrons, increased ionization and heating. At the same time plasma sheet particles are convected towards earth and their energy can increase by many tens of KeV. Fluxes of KeV particles observed at geosyncronous altitude are sufficient to cause spacecraft charging with the possibility of malfunction Some of the plasma sheet particles that gain energy as they are convected towards earth become trapped on closed field lines. (Those at higher latitudes can be precipitated in the auroral region). These, plus others that may have been energized due to local acceleration processes, increase the ring current. This new current tends to reduce the B field which had been previously compressed during the growth stage; it is said that the field "expands". Finally a "recovery phase" sets in. The ring current decays because the extra particles are precipitated into the atmosphere. This causes B to return to normal.

In section F we shall discuss the sort of local processes involved in substorm activity which might be affected by plasma effluent.

E. THE MAGNETOSPHERE AND THE ENVIRONMENT

We shall identify here some environmental consequences of certain processes of the MS. In the following section we point out possible ways in which these processes may be influenced by SSPS effluent.

Perhaps the main environmental function of the MS is the shielding of the atmosphere from direct collisional interaction with the solar wind. About 98% of the solar wind energy is deflected. It also shields the

stratosphere from high energy proton fluxes from solar flares. However, as has been explained, this deflection is accomplished by the earth's dipole field, whose source is currents deep within the earth. Thus this major function would not be impaired by effluent. There do exist, however, many environmental consequences of magnetospheric processes. These divide into effects on spacecraft and personnel in the vicinity of earth, and terrestial effects. The high level of radiation in the Van Allen belt is injurious to life and degrades parts of satellites, and solar cells. The hard component of Van Allen radiation, which lies rather close to earth, remains fairly constant during substorm activity. Below 30 MeV the radiation belts are filled with particles that have drifted in or been energized during substorm activity. These populations are affected by diffusion processes that depend on the ambient cold plasma density. It has been suggested theoretically that increased cold plasma density lowers the maximum number of trapped particles, and thus the radiation level might be reduced. Also during substorm activity intense fluxes of hot plasma (10 KeV) are observed to be generated. These cause satellites to charge up, which is detrimental to their operation. Finally it has been pointed out that density changes in the upper atmosphere due to auroral activity could alter the drag forces on low polar orbit satellites, affecting their orbital stability.

The terrestial effects of magnetospheric activity are many; some are harmful and some beneficial. These seem mostly to be associated with processes that deposit particles and energy in the atmosphere. A beneficial effect is that precipitation of particles in the polar regions keeps the ionization level high enough so that polar communication continue during winter darkness, when solar ionization is reduced. On the other hand,

during storm activity the ionization level at lower latitudes can be increased enough to impair shortwave communications. Also the magnetic perturbations at the earth's surface during storm activity have been known to affect power networks. Distances inferred by aircraft navigation aids are affected by substorms.

The above effects are well known and can be understood in terms of the magnetospheric activity that generates them However there exists an increasing body of evidence that atmospheric weather is affected by geomagnetic activity, which is in turn affected by solar activity. The studies in this area have been predominantly correlative[16], and there exists very little in the way of known mechanisms which could be analyzed in terms of their modification by SSPS effluent. In view of the potential seriousness of weather modification effects we shall discuss some of the evidence for their existence.

Study of the correlation between solar activity and the weather goes back many years. The supposed correlations might result from variations in the solar photon flux hitting the earth directly and over which the magnetosphere would have no influence. They might also result from variations in the solar wind particle flux or solar magnetic field as mediated by the magnetosphere. Since the solar wind energy flux is very small[17] compared to that from solar photons, it is reasonable to ask how the solar wind could possibly influence atmospheric activity, which is known to respond to the photon energy flux The answer might be that large amounts of potential energy are stored in the atmosphere owing to the pressure, temperature and moisture gradients that are continually being built up and dispersed. Thus there is the possibility that relatively small amounts of energy deposited locally could trigger the release of stored

energy if the atmospheric configuration there were not very stable.

An interesting historical study of solar activity and the weather was performed by Jack Eddy of the University of Colorado[18]. Historical evidence shows that during a seventy year period beginning in about 1645 sunspot activity was almost zero. This period is known to solar physicists as the "Maunder Minimum". During this time the solar corona, that is the cloud of ionized gas that surrounds the sun and expands outward forming the solar wind was also missing, and there was very little auroral activity. This period was also very cold, and is referred to as the "little ice age."

There are many recent studies showing direct correlations between atmospheric weather and magnetic activity. An interesting example is the work of W. O. Roberts and R. H. Olson[19] who studied the development of low pressure trough systems in the North Pacific and North American region. They find that troughs which enter (or are formed in) the Gulf of Alaska two to four days after a sharp rise in geomagnetic activity tend to be of larger than average size. The intensity of a trough is measured by its "vorticity area index", which is the area of the trough over which the absolute vorticity $\geq 20 \times 10^{-5}$/sec plus the area over which the vorticity $\geq 24 \times 10^{-5}$/sec. Some results of this study are shown in Figure 2.1.14. During the three to five days after the "geomagnetic key day" the troughs preceeded by a sharp rise in geomagnetic activity have on the average some 40% larger vorticity area index than troughs preceeded by a ten day geomagnetically quiet period. Other investigators have found similar results. Roberts and Olson[20] have suggested a possible mechanism for the observed effects. They think that the intense fluxes of particles precipitated in the auroral zone during geomagnetically active periods could cause ionization in the upper atmosphere. The ions could form the nuclei of

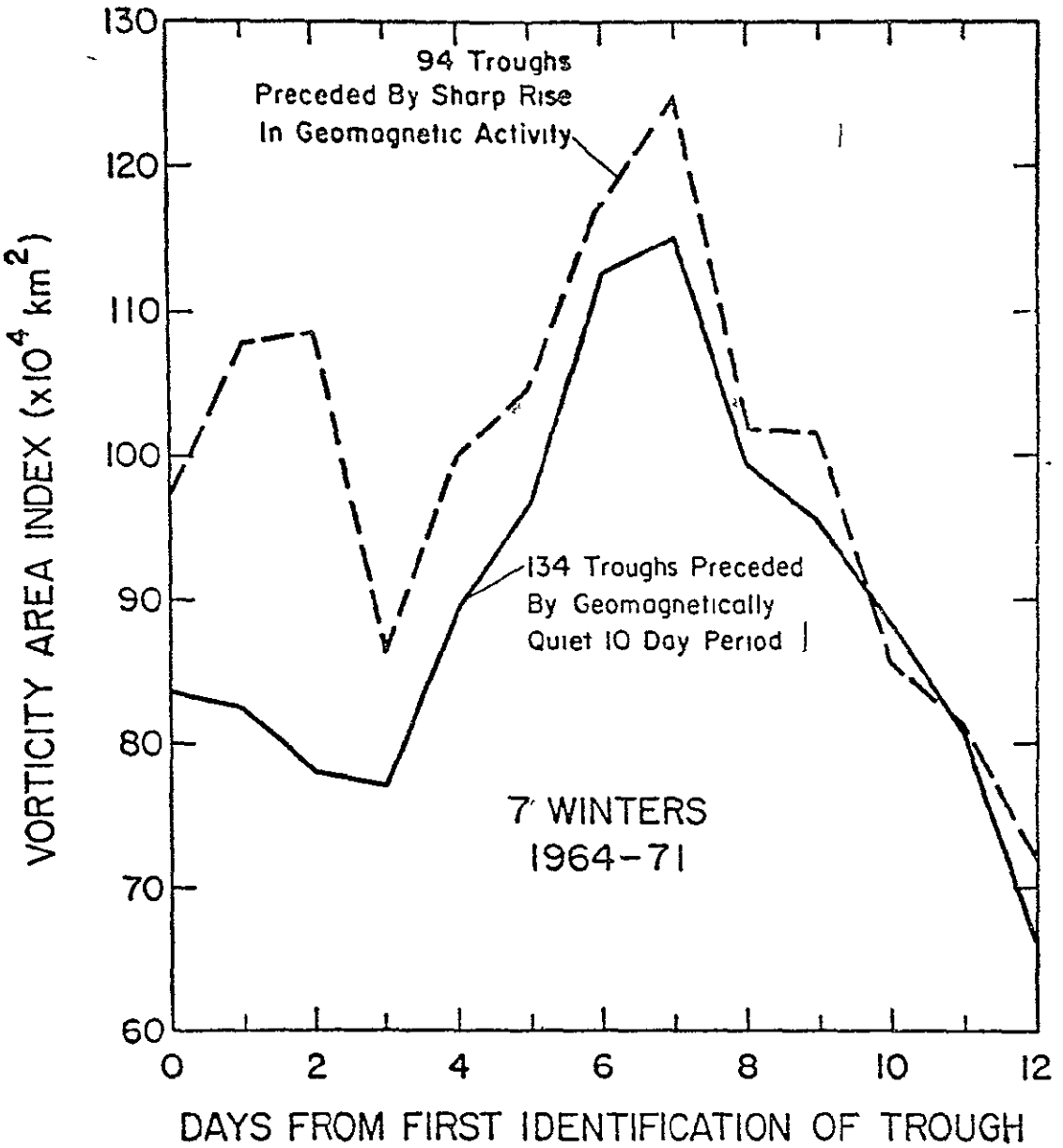

Figure 2.1.14. Atmospheric Vorticity and Geomagnetic Activity. (Ref. 19, 20)

accreting water particles which would form high altitude cirrus clouds. These clouds would blanket the earth, reflecting radiation coming from the ocean, and heating the area with energy that normally would be radiated into space. Thus a small energy input could release a large amount of energy.

These indications of weather perturbations resulting from geomagnetic or its associated auroral activity are presently rather subtle, and causal relationships barely established. On the other hand, their long-term significance might be very great. In view of the fact that weather effects could result from magnetospheric activity, and many ionospheric, atmospheric and terrestial magnetic effects are known to result from this activity it would seem very important to focus on how SSPS plasma effluent might alter this activity In our view this is a most crucial area for further study.

F. PLASMA EFFLUENT CONVECTION AND INTERACTION

It is widely held that the density N_c and ions species of ambient cold plasma of the type that will be deposited by SSPS thrusters have much to do with magnetospheric functioning and substorm phenomena in particular. The most common type of mechanism which affects magnetospheric behavior is called wave particle interaction, or instability What happens here is that particles within the trapped hot particle population can have velocities parallel to B of such a value that they interact reasonantly with a plasma wave propagating along B. The result can be that these hot particles may become untrapped, and precipitate into the ionosphere. Since the wave velocities depend on N_c, this density tends to have control over these precipitation phenomena. Indeed experiments have been proposed to trigger wave-particle instabilities simply by releasing small amounts of cold plasma from satellites.

In seeking the relationship between cold plasma deposition and magnetospheric activity it will be worthwhile to keep in mind some general questions. We recall that the occurrence of substorms is strongly correlated with a southward turning of the interplanetary magnetic field and an increase of the solar wind flux, both of which apparently build up the energy stored in the MS Then for some reason the energy is very suddenly released. On the other hand, the time scale of some important processes involving wave particle interaction, such as the establishment of an equilibrium distribution of ring current protons in the trapped particle belts, is a few hours. Thus an important question would seem to be whether the effluent will change the quiet time large-scale particle fluxes and electric currents. Changes in these could affect both the sensitivity of the MS to solar wind perturbations, and the intensity of the response once a substorm begins

We feel that the next logical step in analyzing the effect of effluent on the MS is to attempt to establish a realistic plasma effluent density profile and its fluctuations in time and space. For this it will be necessary to pick a particular thruster, probably the MPD arcjet, and determine as well as possible its plume properties. It will also be necessary to choose a sequence of missions, for example, the one proposed in the JSC Study[1] From these it should be in principle possible to determine a source function for ionized plasma, that deposited directly plus that deposited by photoionization of neutrals.

This plasma will then disperse in response to electric fields, pressure gradients, collisions and so forth. As a first step, one might consider separately convection within and outside of the plasmasphere, treating the plasmapause as fixed in space and time, which it is not. It

bf

seems likely that plasma deposited outside will disperse rapidly being convected to and perhaps lost, through the magnetopause boundary and being spread over a large volume. The situation within the plasmasphere would be different. Deposited plasma tries to come to equilibrium with the ionosphere. In this case one might have a critical height similar to that occurring in the exosphere above which the plasma responds only to the average electric and magnetic fields, and below which collisions with neutrals become important. There has been recent theoretical effort in solving this type of problem[7,23] and this should be applicable to the effluent.

The effects caused by effluent could be of two types: response to a long-term and probably smoothly varying cloud of plasma that develops over a period of time from more than one SPS, and local effects that could take place as an SPS passed by and deposited a dense cloud of plasma. The long-term ambient cold plasma could alter quiet time magnetospheric parameters, such as trapped particle fluxes, and could also modify wave particle processes during substorms. A scenario for a localized process might be as follows. We take note of the fact that there may exist small quiet time currents along B field lines. If cold plasma is suddenly deposited, an unstable spectrum of waves could grow up due to resonant wave particle effects or due to the local inhomogenity created. This wave spectrum might increase the resistivity at this point ("anomalous resistivity"). This can cause a large voltage drop to develop quickly along the B field here, the deposition of LI^2 circuit energy in this localized region, and consequent possible disruption of the current flow. Or the potential drop might simply accelerate particles. It would seem that the best way to approach this type of phenomena would be to keep

track of plasma deposition experiments and calculations as they are carried out. It appears that this will be an active area of research.

Large-scale changes due to modification of N_c are probably amenable to calculation. One type of calculation would be directed towards determining modifications of high energy particle fluxes. These tend to be determined by N_c through "pitch angle diffusion" Righthand polarized electromagnetic whistler waves exchange energy with trapped electrons of appropriate speed. Left-hand polarized ion-cyclotron waves exchange energy with protons. These interactions are possible whenever the frequency of the wave as seen by the bouncing particle is an integral multiple of the particle's cyclotron frequency. This can lead to an instability in the behavior of trapped particles with the wave amplitude growing exponentially while the particles undergo pitch angle scattering in such a way as to line up with B and precipitate into the atmosphere. This process continues until the flux of resonant particles levels off at a certain maximum value permitted for stable trapping; this value is proportional to N_c[21]. For this wave particle instability to develop two conditions must be met· the hot particle pitch angle distribution must be anistropic, peaking at 90° to B, and the particles' initial energy must surpass a critical value E_c given roughly by

$$E_c = B^2/(8\pi N_c) \quad .$$

This demonstrates that as N_c increases the number of susceptible particles increases. Figure 2.1.15[8,25] shows a plot of E_c as a function of altitude using the natural N_c. The above formula indicates that E_c increases as N_c increases which indicates that slower particles would be untrapped. This may be true for electrons. The correct analysis shows that if one adds cold plasma with heavy ions the wave particle instability is quenched[24],

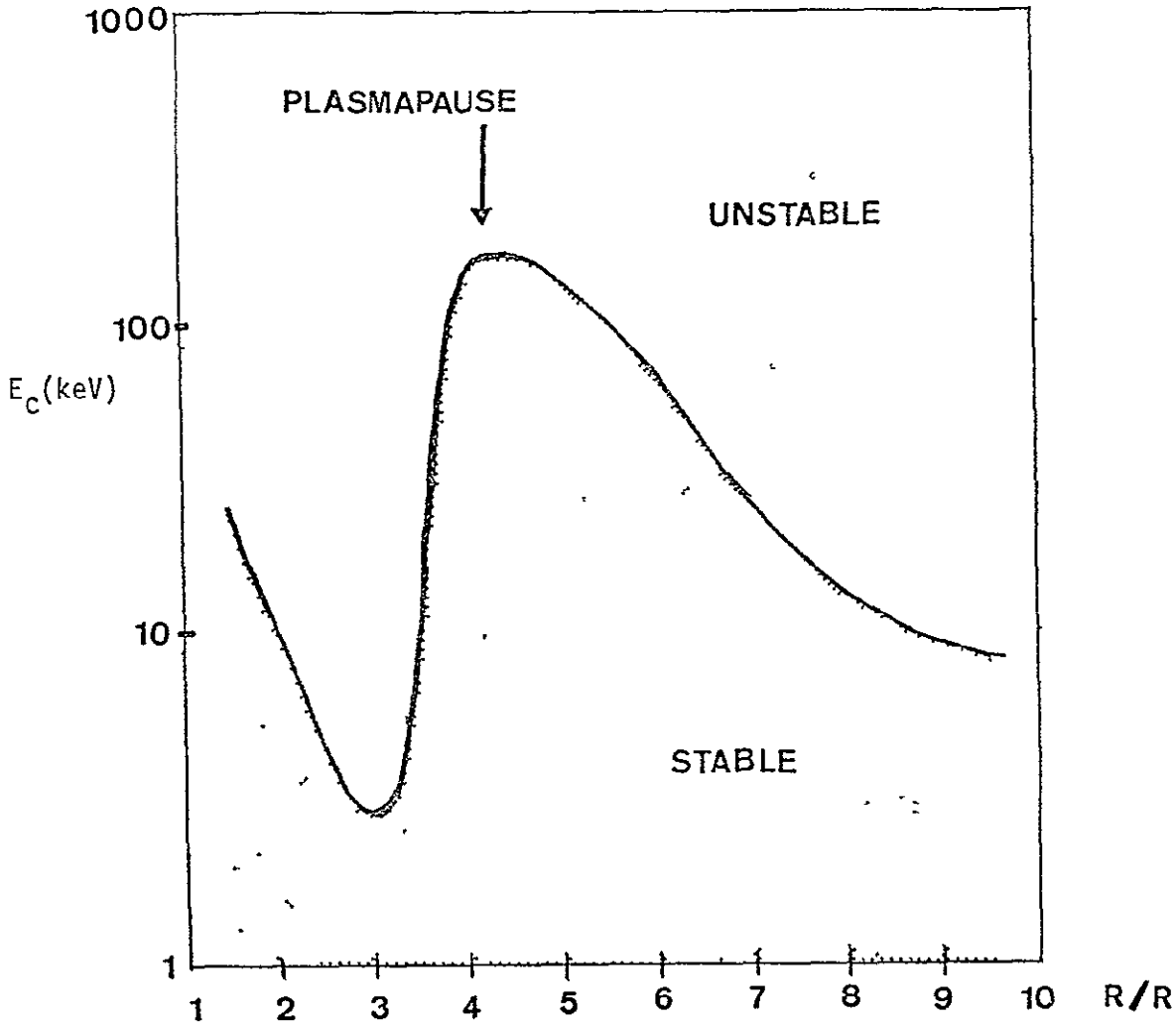

Figure 2.1.15 Critical Energy For Wave-Particle Instability (Ref. 25).

which raises the trapped proton flux. This comes about because the wave phase velocity for important frequencies can be increased by the heavy ions. Learning how curves such as Figure 21.15 are modified by the effluent plasma would be a worthwhile goal for theoretical analysis.

In the following we estimate very crudely the alteration in plasma density in the vicinity of GSO due to photoionization of the slow neutrals deposited by stationkeeping. The amount of slow neutrals deposited by 100 SPS is, Section A,

$$\frac{dN}{dt} \cong (3 \times 10^5)\ (\beta \sim .1)\ (100)\ \text{gm/day} = 5.78 \times 10^{23}\ \text{atoms/sec}$$

A rough estimate of the volume over which they might be spread can be made by referring to Fig. A.1. Assuming a velocity of 10^4 cm/sec the neutrals' orbits would probably distribute them in a tubular ring of major radius that of GSO, $r \sim 4 \times 10^9$ cm, and minor radius $a \sim 2.5 \times 10^8$ cm. The ring has volume $V = 2\pi^2 ra^2 \sim 5 \times 10^{27}$ cm.^{3} Thus neutrals are deposited at the rate

$$S_n = 1.15 \times 10^{-4}/\text{cm}^3\text{-sec.}$$

The rate equations describing the densities of neutrals and ions are

$$\frac{\partial n_n}{\partial t} = S_n - \frac{n_n}{\tau_i}$$

$$\frac{\partial n_i}{\partial t} = \frac{n_n}{\tau_i} - \frac{\overline{v}}{a} n_i$$

The ratio $\overline{v}/a$ represents crudely the amount of time a typical ion remains in the volume, and τ_i is the photoionization time. The largest characteristic velocity for these particles is the E x B drift velocity $\overline{v} \sim 10^6$ cm/sec. In equilibrium $\frac{\partial}{\partial t} \to 0$ and the ion, electron density is

$$n_i = \frac{a}{v} s_n \sim 3 \times 10^{-2}/cm^3 .$$

This is safely below the ambient density. However the estimate is very crude and we have not answered the question of where the plasma goes after it is created. This calculation illustrates some considerations that will be involved in a correct calculation, and hopefully indicates the type of answer that will be found.

BIBLIOGRAPHY

1. Initial Technical, Environmental and Economic Evaluation of Space Solar Power Concepts, NASA, Lyndon B. Johnson Space Center, Houston, Texas, Aug. 31, 1976.

2. The Solar Energy Spectrum, H. H. Malitson, Sky and Telescope 29, p. 162 (1965).

3. Photoionization Processes in Gases, G. Marr, Academic Press, 1967, p. 125.

4. Satellite Environment Handbook, Johnson, F. C., Stanford University Press (1961).

5. Space Physics, White, S., Gordon and Breach, New York (1970).

6. L. Spitzer, in The Atmospheres of the Earth and Planets, G. Kuiper, Ed., Univ. of Chicago Press (1952).

7. Aeronomy, Parts A, B, P. Banks and G. Kockarts, Academic Press, New York (1973).

8. Juan G. Roederer, Science, Jan. 1974, p. 17.

9. Lief Svalgaard, Geomagnetic Responses to the Solar Wind and to Solar Activity, Institute for Plasma Research, Stanford University.

10. S. Akasofu, L. Lanzerotti, Physics Today, Dec. 1975, p. 28.

11. Cosmical Geophysics, Ed. A. Egeland, O. Holten, A. Omholt, Universitets forlaget, Oslo (1973).

12. The Radiation Belt and Magnetosphere, Hess, W. N., Blaisdell (1968).

13. Electric Current Structures of the Magnetosphere, H. Alfven, in Physics of the Hot Plasma in the Magnetosphere, Ed., B. Hultquist, L. Stenflo, Plenum, New YOrk.

14. McIlwain, C. E., Plasma Convection in the Vicinity of the Geosyncronous Orbit, in Earths Magnetospheric Processes, D. Reidel, Dordrecht, Netherlands (1972).

15. Auroral Phenomena, B. J. O'Brien, Science, Vol. 138, p. 449, April 1965.

16. Solar Activity and the Weather, J. Wilcox, Stanford University Institute for Plasma Research, Report No. 544, Stanford University.

17. D. M. Willis, the Energetics of Sun-Weather Relationships Magnetospheric Processes, Journal of Atmospheric and Terrestrial Physics 38, p. 685 (1976).

18. Nova, Television Documentary, WGBH, Boston, J. Eddy, Sci. Am., May 1977.

19. Roberts, W O. and Olson, R. H., J. Atmos. Sci. 30, p 135 (1973).

20. Roberts, W O. and Olson, R. H New Evidence for Effects of Variable Solar Corpuscular Emission on the Weather, Rev. Geophys. and Space Phys., p. 731-740, 1973.

21. Artificial Enhancement of Energetic Particle Precipitation through Cold Plasma Injection· A Technique for Seeding Substorms?, N. Brice, Journal of Geophysical Research 25, p. 4890 (1970).

22. Magnetospheric Dynamics with Artificial Plasma Clouds, J. M. Cornwall, Space Science Reviews 15, p. 841 (1974).

23. Exospheric Models of the Topside Ionosphere, Lamaire, J. and Sherer, M., Space Science Reviews 15, p. 591, (1974).

24. Electromagnetic Ion-Cyclotron Instabilities in Multicomponent Magnetospheric Plasmas, J. M. Cornwall and M. Schultz, Journal of Geophysical Research 76, p. 7791 (1971).

25. R. M. Thorne, in Critical Problems of Magnetospheric Research, E. R Dyer, Ed., IUCSTP Secretariat, National Academy of Sciences, Washington, D.C., p. 211.

26. Massey, H. S. and Smith, R. A., Proc. Roy. Soc. 142, p. 142 (1933).

27. Statement of Work, JPL Subcontract 954663 under Contract NAS 7-100: JPL Interoffice Memo to Irving Stein from W. Phillips and E. Pawlik, 383 EC-76-708, 23 July, 1976.

APPENDIX A -- Orbits of Neutral Effluent

In this appendix we analyze the orbits of neutral effluent atoms whose velocities are less than escape velocity. These remain on bound elliptical orbits.

It is assumed that the neutral atoms are emitted from an SPS in a circular orbit of radius r, whose velocity is thus $v_{SPS} = \sqrt{K/r}$. The tangential velocity of the neutral atom is

$$v_n = v_{SPS} - v_{ex} \cos\theta \quad ,$$

where v_{ex} is the speed of the effluent and θ is its angle of emission with respect to the SPS motion. The minimum and maximum radial extent of the neutral atom orbit is

$$r_{max,min} = a\ (1 \pm \varepsilon)$$

where ε is the ellipticity

$$\varepsilon = \left(1 + \frac{2EL^2}{m^3K^2}\right)^{\frac{1}{2}}$$

and

$$= \left|\frac{K}{2E}\right| \quad .$$

The formulas for E and L are

$$E = \frac{1}{2} m\ v^2 - \frac{K}{r} = \frac{1}{2} m \left\{ (v_{SPS} - v_{ex} \cos\theta)^2 + v_{ex}{}^2 \sin^2\theta - \frac{K}{r} \right\}$$

$$L = mrv_\theta = mr \left(v_{SPS} - v_{ex} \cos\theta \right) .$$

For particles emitted tangential to the SPS orbit r_{max} is equal to r. In Fig. A.1 we show the range in radius of the orbits of neutral atoms emitted tangentially. The outer point of each radial bar is where the particle is emitted and the inner point is the minimum. We find that these ranges are

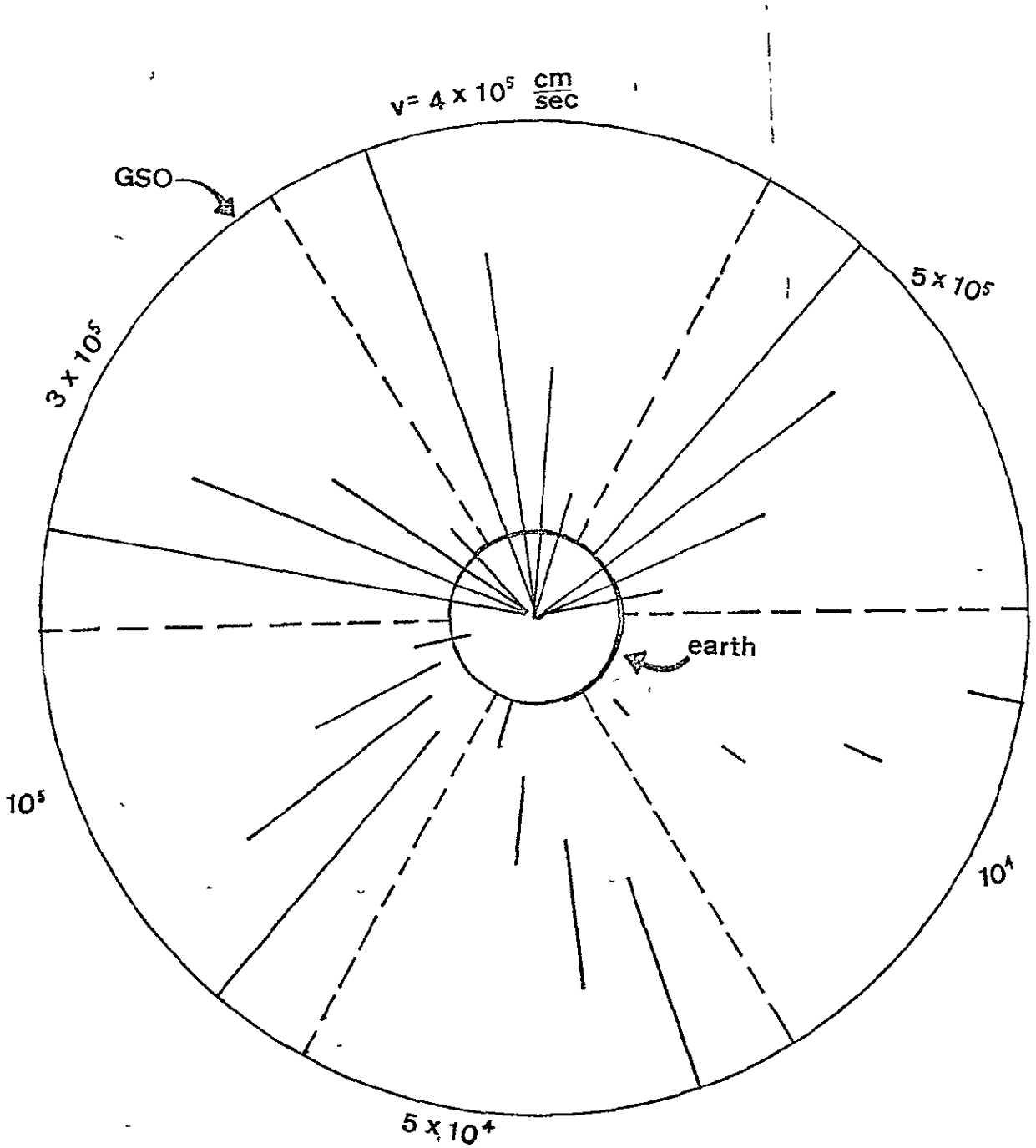

Figure A.1. Neutral Effluent Trajectories. The outer limit of a bar is at the radius at which the effluent is deposited, and the inner limit is at the minimum radius.

not substantially altered with angles of emission θ up to 15°. The high velocity orbits (v_{ex} = 3,4,5 x 10^5 cm/sec) correspond to chemical thrusters of specific impulse I_{sp} = 306, 408, 510. The low velocity orbits would be typical of the slow neutral argon atoms emitted by the MPD thruster. Fig. A.1 makes the point that the chemical thruster neutrals might hit the atmosphere on the first orbit, whereas the slow MPD neutrals would be deposited in a disc coinciding with the orbital plane. These results will have to be checked using more realistic models of the exhaust plumes.

2.2 BIOLOGICAL CONSEQUENCES OF SPS REFLECTED LIGHT

INTRODUCTION

A proposed group of space solar power satellites (SPS's) would appear as stationary light sources in the night sky. Each SPS would appear approximately as bright as the planet Venus; 100 of them may have a total light reflection with intensity up to that of a half-moon. In addition, each single SPS may briefly (for a few minutes up to an hour) reflect with the brightness of a full moon or more during orbit maneuvers. In this section of the report, some possible biological consequences of these additional light sources are discussed. (A) Effects on the daily and seasonal photoperiodicity of plants and animals, (B) effects on celestial orientation of migrating birds and other users of the night sky patterns, and (C) effects on animal behaviors such as nocturnal predation which correlate with the available intensity of light. Following the description of each effect, the significance of the effect is discussed. A preliminary evaluation of the effect is made, and some further studies are suggested.

A. PHOTOPERIODICITY

Description of the effect

Plants and animals undergo daily cycles of activity. The correct timing of these cycles depends on sampling the intensity of available light, although other features of the environment, for example temperature, may provide additional information. The light levels used as reference points are not the bright levels of the day (greater than 100 lux) but rather the dim levels (1 to 10 lux) before sunrise and after sunset (Bünning, 1972). These light levels are the least sensitive to weather factors such as cloudiness and are therefore reached at nearly the same time in each solar day.

Bünning (1972) theorizes that the light threshold of 1 lux found in many plants may have evolved to avoid interference from moonlight which can reach levels up to 1 lux. Additional nocturnal light sources contributing a few tenths of a lux or more (such as the SSPS's) could add enough to the lunar light to trigger the daily "clock" of plants and animals.†

Plants and animals also measure day-length to initiate seasonal behaviors such as reproduction and migration. The mechanism for photoperiodic regulation of budding in some plants has been described (Wareing, 1953). Extra light from SSPS's could appear to these organisms as longer days, delaying the recognition of an approaching winter or prematurely signaling the onset of spring. Some plants may, for instance, be fooled into budding too early in the year, before the danger of frost is past. The light levels used as reference points are again in the range of 1 to 10 lux and may be of short duration. For instance it has been shown that the eclosion time of fruit flies can be affected by 15-minute pulses of light in the 1 to 10 lux range (Chandrashekaran & Loher, 1969).

Significance

Disruption of daily and/or seasonal cyclic activity in some plants or animals could have a large impact, especially in agriculture. There could be confusion in daily cycles leading to less than optimal use of sunlight for growth and development. There may be a general loss of synchrony in some reproductive cycles leading possibly to more disperse fruition times. In the extreme, premature germinations or buddings could occur, leading to losses of entire crops or harvests.

† Several animals have light intensity thresholds of 0.1 lux (e.g., the sparrow, (Menaker, 1968)). These animals presumably avoid moonlight interference by reacting in dark places at night (Bunning, 1972).

Disruption for animals in the wild would mean confusion in daily wake-up time, and possible wrong cues for mating or migration times. The daily vertical migration of many plankton is synchronized by reference light intensities (Enright, 1967). The importance of these organisms to the marine food chain makes disruption of their normal migratory pattern a serious consideration

Evaluation

Some comparison can be made with animals and plants living in arctic regions where in summer months the light intensities never reach the normal reference levels of 1 to 10 lux. These organisms are still capable of using light intensity information in conjunction with the dramatic temperature changes to coordinate their daily cycles (Swade and Pittendrigh, 1967). Yet they are not capable of the time coordination required for more complex developmental processes which take place in other latitudes (Bünning, 1972). It should be noted that successful arctic adaptations are the result of a slow selective process rather than a sudden environmental change as could be produced by the SSPS's.

Other useful comparisons can perhaps be made with plants and animals already living in an environment with extra light sources, such as near cities.

Further studies

More information is needed on the light intensity thresholds for photoperiodic regulation of various plants and animals. Agricultural simulations could presumably be done both in the field and under more controlled laboratory conditions. In either case, different intensities and durations of artificial light could be tested for their effect on daily and seasonal photoperiodic regulation.

Measuring these effects on animals in the wild will be much more

difficult. Laboratory simulations on plankton and small mammals should give some idea of the magnitude of the problem. Again, attention needs to be given to both daily and seasonal photoperiodic regulation.

B. CELESTIAL ORIENTATION AND NAVIGATION

Description of the effect

Several animal species make use of the night sky for migration and orientation. Migrating birds use star information as part of their navigation system (Emlen, 1975) Beachhoppers apparently use the lunar arc as a reference for correctly moving parallel to the water line (Enright, 1972). Several intertidal organisms probably use moonlight for tide synchrony--definite moonlight responses have been found in the marine insect Clunio (Neumann, 1972) -- although a careful distinction must be maintained between tidal and moonlight effects. Additional nocturnal light sources could interfere with the mechanisms of navigation and migration in some of these celestially-orienting species.

Significance

A disruption of the navigational mechanism in any migrating species could threaten the existence of that species. Continuously incorrect orientation in species like the beachhopper would put those species at a severe disadvantage.

Evaluation

In migrating species, the pattern of the night sky is only part of the navigational system. Many birds make substantial use (many researchers believe primary use, e.g., Wiltschko, et. al., 1971 and 1975) of the earth's magnetic field for navigational information, although this is still open to some

question (Emlen, 1970). There is recent evidence that some night-migrating birds can orient in the absence of both star information and magnetic field information (Rabol, 1975). Star information apparently adds to the information gained from the earth's magnetic field (and possibly other information), but is not crucial to successful orientation. (Bird-migration would otherwise be totally dependent on clear skies).

Other species may also have back-up orientation systems Research at Scripps Institute of Oceanography has shown that beachhoppers can make use of stationary floodlamps for orientation in preference to use of their lunar tracking system (Hartwick, 1975).

Further studies

Some research on bird orientation using artificial star patterns has already been done (Wallraff, 1969, Terhune, 1972). Simulations could easily be done in a planetarium using the proposed distribution of SSPS's as they may appear in the spring and fall skies.

C. NOCTURNAL BEHAVIORS AFFECTED BY MOONLIGHT

Description of the effect

Much of the behavior of nocturnal animals can be expected to be affected by the visibility of the environment. In the case of moonlight this has been shown to be true in many species, influencing behaviors such as predation, reproduction, and general activity levels. Additional light sources such as SSPS's can also be expected to affect these light-sensitive behaviors.

Moonlight increases the vulnerability of salmon to both trout (Ginetz and Larkin, 1976) and sculpin (Patten, 1971). Other observations on salmon have shown that salmon will cease spawning during a lunar eclipse (Reimers, 1967) -- this suggests the possibility that "false moonlight" could instigate a spawning period. Some crustaceans apparently synchronize their molting

with a lunar light cycle (Reaka, 1976).

Moonlight seems to make some smaller mammals inactive, perhaps due to fear of predation. Woodrats (Wiley, 1971), kangaroo rats (Lockard and Owings, 1974), and 12 nocturnal species of desert rodents (O'Farrell, 1974) were all shown to be less active on moonlit nights. No such effect was found in the activity of white-tailed deer in Texas (Michael, 1970). Some nocturnal mammals respond to moonlight with heightened activity rather than diminished activity (Erkert, 1974).

Insects show several moonlight-dependent behaviors. The number of insects caught in traps will generally depend on moonlight. Species studied include the bullworm moth (Nemec, 1971) and scarab beetle (Gruner, 1975) both of which were trapped less frequently on moonlit nights. Sexual activity in the bullworm moth was also inhibited by moonlight (Nemec, 1971). On the other hand, more Prays Citri males were caught in female-baited traps on moonlit nights (Sternlicht, 1974). Mosquito biting has a complex relationship with moonlight (Davies, 1975).

Plankton can apparently make use of lunar light to avoid predation (Cheng and Enright, 1973).

Significance

Several insect pests are among those animals affected by moonlight. The possibility that reflected light from SSPS's may affect their reproduction or flight activity must be considered.

Effects on plankton, because of their food-chain importance, must also be carefully considered.

Depletion of economically important species (e.g., salmon) by increased nocturnal predation is a serious possibility. Shifts in the

predator-prey balance for many species, ranging from plankton to the big cats, may result from a significant increase in nocturnal light.

Evaluation

Care should be taken to differentiate lunar effects produced specifically by increased nocturnal illumination from other lunar effects resulting from physical interactions other than light Many lunar effects on marine species can be attributed to tidal relationships rather than moonlight (e.g., Pearse, 1972). Gerbils show a lunar-day periodicity which is a result of sensing weak geoelectromagnetic fields produced by lunar phase (Stutz, 1974). Obviously, additional nocturnal light sources will have no effect on animal behaviors dependent only on lunar position.

Further studies

More information is needed on the intensity (and duration) thresholds of those behaviors which are correlated to moonlight levels. A more precise relationship between light levels and success of predation for nocturnal hunters is needed. The light-dependence of reproduction and other activity needs to be more clearly defined for insects and other animals.

TABLE 2.2.1

Biological Effects of SSPS Light Reflection

A. Priority Rating (1 = highest, 3 = lowest)

1. Photoperiodicity

   a. Daily (1)

   b. Seasonal (1)

2. Celestial orientation (3)

3. Nocturnal behavior affected by moonlight

   a. Predator-prey balance (2)

   b. Pest activity and reproduction (2)

   c. Other light-dependent nocturnal activity (3)

B. Ease and Time-estimate for Further Studies

1. Photoperiodicity

   a. Daily - easy for plants and small animals, 2-6 months, difficult for larger animals, 3-12 months.

   b. Seasonal - moderate for plants and small animals, 1-2 years; difficult for larger animals, 1-2 years.

2. Celestial orientation - easy, 2-6 months.

3. Nocturnal behaviors affected by moonlight - easy to difficult depending on species (smaller, more localized species generally easier), 2-12 months.

BIBLIOGRAPHY

Bunning, E. (1972). Symptoms, problems and common features of circadian rhythms in plants and animals. In Circadian Rhythmicity, Proceedings of the International Symposium on Circadian Rhythmicity, Wageningen, the Netherlands, April 1971, pp. 11-32 Centre for Agricultural Publishing and Documentation, Wageningen, Netherlands.

Cheng, L and Enright, J. T (1973). Can halobates dodge nets. II. By moonlight. Limnol. Oceanogr. 18 (4), 666-669.

Chandrashekaran, M. K. and Loher, W. (1969). The relationship between the intensity of light pulses and the extent of phase shifts of the circadian rhythm in the eclosion rate of Drosophila pseudoobscura. J. expl. Zool. 172, 147-152.

Davies, J. B. (1975) Moonlight and the biting activity of Culex-Portesi and Culex-taeniopus diptera culicidae in Trinidad forests. Bull. Entomos. Res. 65 (1), 81-96.

Emlen, S. T. (1970). The influence of magnetic information on the orientation of the indigo bunting Passerina-cyanea. Anim. Behav. 18, 215-224.

Emlen, S. T. (1975). The stellar-orientation system of a migrating bird. Sci. American 223, (2), 102-111.

Enright, J. T. and Hamner, W. M. (1967). Vertical diurnal migration and endogenous rhythmicity. Science 157, 937-941.

Enright, J. T. (1972). When the beachhopper looks at the moon the moon compass hypothesis. In Animal Orientation and Navigation. (ed. by Galler, et. al.) Scientific and Technical Information Office, NASA sp-262.

Erkert, H. G (1974). The effect of moonlight on the activity of nocturnal mammals. Oecologia (Berl.) 14 (3), 269-287.

Ginetz, R. M. and Larkin, P. A. (1976). Factors affecting rainbow trout Salmo-gairdneri predation on migrant fry of sockeye salmon, Oncorhynchus-nerka. J. Fish. Res. Board Can. 33 (1), 19-24.

Gruner, L (1975) Activity of the adults of West-Indian scarab beetles studied by light and chemical trapping. Ann. Zool. Ecol. Anim. 7, 399-423.

Hartwick, P. F. (1975). Orientation behavior in beachhoppers of the genus Orchestroidea· Capacities and strategies. Ph.D. Thesis, Univ. of Calif. San Diego.

Lockard, R. B. and Owings, D. H. (1974). Moon-related surface activity of bannertail (Dipodomys-spectabilis) and Fresno (dipodomys-nitratoides) kangaroo rats. Anim. Behav 22 (1), 262-273.

Menaker, M. (1968). Extraretinal light perception in the sparrow I. Entrainment of the biological clock. PNAS 59, 414-421.

Michael, E D. (1970) Activity patterns of white-tailed deer in south Texas. Tex. J. Sci 21, 417-428.

Nemec, S J (1971). Effect of lunar phases on light trap collections and populations of bullworm moths. J. Econ. Entomol. 64 (4), 860-864.

Neumann, D. (1972). New experiences on the control of the lunar swarming times of Clunio populations. Chironomus 1, 88.

O'Farrell, M. J. (1974). Seasonal activity patterns of rodents in a sagebrush community. J Mammal. 55 (4), 809-823.

Patten, B. G. (1971). Increased predation by the torrent sculpin, Cottus-rhothems, on coho salmon fry, oncorhynchus-kisutch, during moonlight nights J. Fish. Res. Board Can 28 (9), 1352-1354.

Pearse, J. S. (1972) A monthly reproductive rhythm in the diadematid sea-urchin, Centrostephanus-coronatus. J. Exp Mar. Biol. Ecol. 8, 167-186.

Rabol, J. (1975). The orientation of night migrating passerines without the directional influence of the starry sky and or the earth magnetic field. Z. Tierpsychol. 38 (3), 251-266.

Reaka, M. L. (1976) Lunar and tidal periodicity of molting and reproduction in stomatopod crustacea: a selfish herd hypothesis. Biol. Bull (Woods Hole) 150, 468-490.

Reimers, P. E. (1967). Cessation of chinook salmon spawning during a lunar eclipse. Oregon Fish. Comm. Res. Briefs 13, 125.

Sternlicht, M. (1974). Effects of moon phases and of various trap colors on the capture of Prays-citri males in sticky traps. Phytoparasitica 2, 35-40.

Stutz, A. M. (1974). Lunar day variations in spontaneous activity of the Mongolian gerbil. Biol. Bull. (Woods Hole) 146, 415-423.

Swade, R. H. and Pittendrigh, C. S (1967). Circadian locomotor rhythms of rodents in the arctic. Am. Nat. 101, 431-466.

Terhune, E. C. (1972) Operant conditioning as a means of testing the ability of white-crowned sparrows to discriminate star patterns. J. Exp. Biol. 56, 755-768.

Wallraff, H. G. (1969) The orientation of birds under natural and artificial star patterns: training experiments with mallards. Zool. Anz. Suppl (32), 348-357.

Wareing, P F. (1953). Growth studies in woody species. V. Photoperiodism in dormant buds of Fagus Sylvatica. Physiol. Plant. 6, 692-706.

Wiley, R. W (1971) Activity periods and movements of the Eastern woodrat, Neotoma-floridana. Southwest Nat. 17, 43-54.

Wiltschko, W., Hoeck, H & Merkel, F. W. (1971) Outdoor experiments with migrating European robins in artificial magnetic fields. Z. Tierpsychol. 29, 409-415.

Wiltschko, W and Wiltschko, R. (1975) The interaction of stars and magnetic field in the orientation system of night migrating birds. II. Spring experiments with European robins, Erithacus-rupecula. Z. Tierpsychol. 39, 265-282.

2.3 IMPACT OF THE SSPS ON EARTH-BOUND ASTRONOMY

INTRODUCTION

Considerable study has been devoted to the feasibility of proposals to place as many as one hundred satellite power stations into geosynchronous orbit over the western hemisphere by the year 2020 to meet a substantial portion of the projected power requirements of the United States at that time. A single such SPS may have a light collecting area of order 140 km^2 for converting solar radiation to microwaves which would be directed onto a collecting "rectenna" on the earth's surface[1].

The total flux of solar radiation over this light collecting area is almost 200 gigawatts. The microwave beam would carry a power of order 10-20 gigawatts to the collecting array at the earth's surface whose area would be of order 100 km^2. A portion of the power intercepted by the satellite would be scattered or reflected by its surface (probably about 10% of the incident flux) which could easily make it the brightest celestial object in the night sky discounting the moon. Most of the collected power would be re-radiated diffusely in the far infrared region of the spectrum, making the SPS very bright at far infrared wavelengths as well.

In this study we will consider the potential impact of these satellites on ground-based astronomical observations. We discuss four main considerations: (1) The intensity of visible sunlight scattered or reflected by the SPS, (2) diffuse night sky illumination by this scattered light; (3) the intensity of diffuse thermal radiation emitted by the SPS at far infrared wavelengths; and (4) interference with radio observations.

It is anticipated that proposed SPS systems will present serious problems of night sky illuminations for astronomers working at visible and shorter wavelengths, and possibly more serious problems at radio wavelengths.

Further study of these problems is recommended in areas enumerated in the summary and conclusions of this study.

A. Visual Brightness of the SPS

A single SPS in geosynchronous orbit 35870 km above the earth's surface with a cross-section area of 140 km^2 viewed normally to its collecting surface occupies a solid angle

$$\Omega = 1.1 \times 10^{-7} \text{ ster} = 1.3 \text{ (arc min)}^2.$$

The fraction of light it reflects can vary considerably, but may be as low as 10%, for example for silicon treated with antireflection dielectric coatings. If the reflection is completely diffuse, so that the specific intensity of the reflected light is independent of the viewing angle, then this special intensity is given by

$$\bar{I} = \frac{L_0 A}{(2\pi\tau_0)^2} = 43 \frac{\text{Watt}}{m^2 \text{ ster}}$$

Here L_0 is the solar luminosity, 3.83×10^{26} watts, A is the diffuse reflectivity of the collecting surface (assumed to be 10%) and τ is the distance from the sun to the SPS (taken to be the earth-sun distance of 1.5×10^{11}m). Note that we are treating the specific intensity as the amount of power over the entire solar spectrum incident on a unit surface area per unit solid angle of directions from which the radiation comes - those directions being assumed about normal to the receiving surface. Then, multiplying by the solid angle, Ω, occupied by an SPS, we see that a single SPS viewed normally will illuminate the earth's surface with a flux of

$$F = \Omega I = 4.7 \times 10^{-6} \frac{\text{watt}}{m^2} .$$

If we assume the reflectivity of the SPS to be independent of the wavelength of the incident radiation, then its color will be identical to that of the sun. The rule for computing the apparent magnitudes of the SPS from those of the sun is

$$M_{SPS} = M_{\odot} + 21.15 .$$

The U, B, and V magnitudes of the SPS would be

$$U = -4.91,$$

$$B = -5.04,$$

$$V = -5.69.$$

For comparison, the values for Venus at elongation are[2]

$$U = -2.93,$$

$$B = -3.43,$$

$$V = -4.22.$$

The bolometric magnitude (corresponding to the integrated flux of 4.7×10^{-6} watt/in^2) of one SPS is -5.67.

A single SPS of the sort we have considered would therefore appear brighter than any other celestial object in the night sky with the exception of the moon which, when full, has a visual magnitude of $V_D = 12.73$.

The integrated light from about a hundred such objects distributed across the celestial equator in the western hemisphere would scatter sufficient light to illuminate the night sky noticeably. If distributed evenly over 12 hours in longitude they would scatter 64 times as much light into the earth's atmosphere as a single SPS viewed normally at the anti-solar position. The integrated magnitude of these would be 4.5 less (thus brighter) than that of the single one. For example,

$$V\ (100\ \text{SPS's}) = -10.19$$

which is about the same magnitude as a first-quarter moon, or about a tenth the brightness of a full moon.

B. Night Sky Illumination

The main concern of earth-based astronomy at visible wavelengths regarding the SPS is night sky illumination due to Rayleigh scattering of light (reflected to the earth from the SPS) by air molecules, and diffuse scattering by aerosols and dust. These effects are strongly dependent on atmospheric conditions and vary strongly with wavelength. In relatively clean dry air, continuum extinction due to scattering is at least 15% at 5500 Å (the effective wavelength of the V filter) and about 40% at 4250 Å (a standard photographic effective wavelength). About half of this scattered light propagates toward the ground to form the diffuse sky illumination, the other half is scattered back into space. (Only a minor portion of the atmospheric opacity is due to absorption.)

In Figure 1 we compare the night sky brightness increase due to the SPS with that of the unilluminated night sky, the sky illuminated by the full moon, and the surface intensity due to the Milky Way and other sources. We express these intensities in units of the equivalent intensity of a single tenth magnitude star per square degree of solid angle; (a tenth-magnitude star is about the faintest star one can see through a good pair of six-power binoculars, and the full moon occupies a solid angle of about 0.2 square degrees.)

While the sky brightness due to a large number of SPS's is perhaps an order of magnitude less than that due to the full moon, it is several times that of the unilluminated night sky. The problem is more serious at the blue end of the spectrum, and no doubt even more serious for the ultra-violet region for which we do not have an estimate here. It is, of course, more serious yet for air that is not particularly clean in which case scattering at the red end of the spectrum becomes more significant.

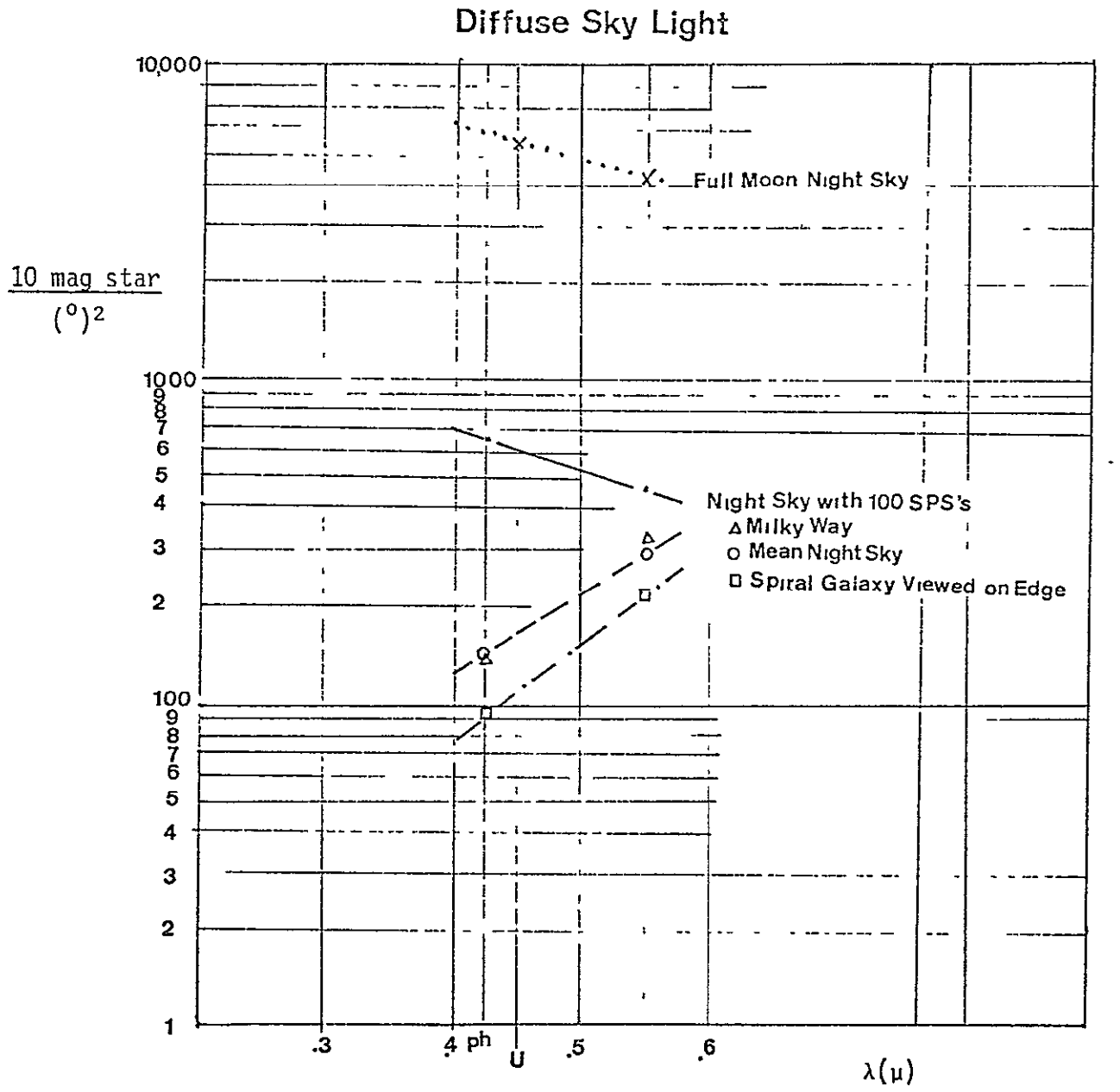

Figure 2.3.1. Diffuse Sky Light.

ORIGINAL PAGE IS
OF POOR QUALITY

The albedo of the earth's surface has been taken to be zero in the foregoing considerations. In places where it is high, for example large snow-covered regions, the sky illumination will be perceptibly greater than the values we have shown

C. Suppression Techniques

Diffuse sky illumination from a large number of SPS's will certainly cause serious problems for ground-based astronomy unless the diffuse reflectivity of the SPS can be reduced by at least one or two orders of magnitude. The use of anti-reflection techniques may be unable to reduce the total reflectivity of the light-collecting surfaces to less than 10%. However, it should be possible to reduce the diffuse reflectivity considerably by making all reflecting surfaces optically smooth, so that reflection is primarily specular, and flat enough that this reflection can be directed away from the earth with only small adjustments in orientation. It would be desirable to reduce the diffuse reflectivity of a single satellite to as small as 0.1% if possible, giving it a visual magnitude of -0.5 which is about the same as the brightest stars in the night sky.

It should be noted that if the specularly reflected light from a single SPS were directed onto the earth's surface (as may happen inadvertently during passage through the anti-solar point near the equinoxes) then it could become as bright as V = -14.7, about six times as bright as the full moon.

Such an intense source could conceivably damage the eye if looked at directly for many seconds.

Another possible consideration would be the length of time over which a surface can retain optical smoothness in the space environment.

The practical limit to how low the diffuse scattering from a surface can be probably depends almost entirely on how clean it can be kept from surface blemishes, either caused during manufacture or by subsequent degradation in the space environment.

D. Thermal Emission at Infrared Wavelengths

A single SPS absorbs about 170 gigawatts of radiant energy from the sun, about 7% of which is radiated to the earth in microwaves. The remaining 160 gigawatts must be disposed of by means of diffuse thermal emission -- most efficiently by black-body radiation at infrared wavelengths. The black-body temperature necessary for radiating this amount of energy from an area of 280 km^2 (140 km^2 on each side) is determined by the Stephen-Boltzmann law to be about 320°K. The black-body spectrum corresponding to this temperature reaches a maximum at a wavelength of about 9μ.

The specific intensity of radiation emitted by such a black body into a narrow wavelength band of width $\Delta\lambda$ is given by the Planck function:

$$B_\lambda(T)\Delta\lambda = \frac{2hc^2}{\lambda^5}\left(\exp[hc/\lambda kT] - 1\right)^{-1}\Delta\lambda.$$

For T = 320°K this takes the form

$$B_\lambda(320°K)\Delta\lambda = 10.05\,\frac{\Delta\lambda}{\lambda^5}\left(\exp\,[45/\lambda] - 1\right)^{-1}\frac{\text{Watt}}{m^2(\text{arc min})^2}$$

where the wavelengths λ and $\Delta\lambda$ must be expressed in microns. For wavelengths considerably longer than 10μ the Rayleigh-Jeans approximation becomes accurate:

$$B_\lambda(320°K) \rightarrow 0.196\,\frac{\Delta\lambda}{\lambda^4}\,\frac{\text{Watt}}{m^2\,(\text{arc min})^2}$$

In Table 1 we show the intensities of this radiation for various wavelengths in bandwidths, $\Delta\lambda$, for which $\Delta\lambda/\lambda = 0.2$ (typical of broadband filters used in far infrared photometry). Here $\bar{I}$ is the specific intensity of the radiation integrated over the band $\Delta\lambda$ which is centered about the wavelength λ (that is, the intensity emitted by a square-arc-minute solid angle of the source's area); $\bar{F}$ is the total radiation flux emitted in the band $\Delta\lambda$, m is the total infrared magnitude of the source, and m′ the magnitude of a portion of the source viewed with a 10 arc sec x 10 arc sec aperture (which is typical of the focal plane apertures used in present infrared astronomical techniques).

Since present-day far-infrared detectors can easily detect a power of 10^{-12} watt in less than a second, the sources shown here would be easily seen even by a small telescope. The SPS would once again be the brightest night sky object with the exception of the moon at 10μ. The moon has a specific intensity about equal to that of the SPS throughout the infrared, but it occupies a much greater solid angle.

Even many hundred SPS's should not be expected to cause a detectable sky illumination at far infrared wavelengths. The main component of sky radiation in this region of the spectrum is thermal emission from the lower atmosphere; the Rayleigh scattering cross-section of air molecules and particles in many orders of magnitude less than at visible wavelength. (Even the solar 10μ flux does not illuminate the sky detectably at that wavelength, so that when visual references are not needed, far-infrared photometry can be done in the daytime).

The effect of alternative power generating schemes in which the waste heat is radiated from either a smaller area, or a less emissive surface is to raise the effective temperature of the surface, so that the

Table 2.3.1

SPS Infrared Fluxes

$\lambda(\mu)$	$\Delta\lambda(\mu)$	$\bar{I}\ \frac{\text{Watt}}{m^2(\text{arc min})^2}$	$\bar{F}\ \frac{W}{m^2}$	m'	m'
5	1	3.96×10^{-7}	4.68×10^{-7}	-11	- 7
10	2	2.23×10^{-6}	2.90×10^{-6}	-16	- 12
20	4	1.48×10^{-6}	1.92×10^{-6}	-18.5	- 14
1000	200	4.5×10^{-11}	5.85×10^{-11}	-24	- 20
Total	∞	1.82×10^{-5}	2.36×10^{-5}	- 7.4	-3.2

power is radiated predominantly at shorter wavelengths. Of course, the total power radiated is the same for a given collecting surface.

E. Radio Astronomy

It is in radio astronomy that the SPS seems bound to have the greatest negative impact. At the contemplated transmission frequency, 2.45×10^9 Hz, an isotropic source emitting monochromatically a small fraction of a watt from geosynchronous orbit is quickly detected. Thus it appears that a single 10^{10} watt source would be large enough to affect the entire radio band if even only a small fraction of its power were distributed throughout it.

As an example we consider a radio telescope with a beam solid angle of 100 (arc min)^2 and a system temperature of 20°K receiving over a bandwidth $\Delta\nu = 10$ MHz at or near the frequency $\nu = 2.45 \times 10^9$Hz. Such a system should detect a black body which occupies a solid angle about equal to that of the beam and whose temperature is equal to the system temperature with a signal to noise of about unity in a time $\tau = 1/\Delta\nu = 10^{-7}$ sec.[3] The flux produced by such a black body is determined by the Rayleigh-Jeans formula to be

$$B_\nu(T)\Omega\Delta\nu = \frac{2kT^2}{c^2}\Delta\nu\Omega = 3 \times 10^{-18}\ \frac{\text{watt}}{\text{m}^2}$$

This is about 10^{-4} times the total solar flux in this same 10 MHz band.[4] A satellite in geosynchronous orbit radiating isotropically a power of only 0.05 watt would produce this flux at the earth's surface.

Even if the antenna is not pointed directly at the source, it sees a small fraction of the former signal through diffraction side-lobes and scattering. We assume that the antenna response when pointed far from the source is of order 2×10^{-6} times the main beam response. (This would mean

that about 80% of the power received from an isotropic background was received through the main lobe.) Then we see that a flux of 1.5×10^{-12} watt/m^2 in the receiving band would be detected in $\sim 10^{-7}$ seconds regardless of where the antenna were pointed. (If we assume the ground to have a reflectivity of unity for microwaves, then we find that a 12 kilowatt isotropic source in geosynchronous orbit would produce this flux at the earth's surface.)

However, if one integrates the power received for a much longer time interval than $1/\Delta\nu$, the interference threshold becomes considerably lower. The threshold for detection is proportional to $(\tau\Delta\nu)^{-1/2}$, where τ is the integration time, so the interference flux for a 10 second integration time is 1.5×10^{-16} watt/m^2 which would be provided by a 1.2 watt isotropic source in geosynchronous orbit. (For antennas of comparable beam width, but greater side-lobe responses the interference flux can be lower; for an isotropic antenna it would be 3×10^{-17} watt/m^2, one fifth of the value above for which we assumed that only 20% of the power received from an isotropic background came in from outside the main beam.) Since the transmitter is a coherent source, possibly fluctuating with time, and moving across the celestial sphere, and the side-lobes of radio antennae fluctuate spatially, one cannot treat this interference as random noise which can be accounted for statistically by integrating for a long time.[5] We expect that a transmitter emitting isotropically only a few tenths of a watt from geosynchronous orbit will interfere with detection of sources at the transmitter frequency which normally require more than 10 seconds of integration time to detect.

Glaser et.al.[6] (1974) have estimated the noise flux levels from the SPS in the neighborhood of the fundamental which they assume to be at

3300 MHz. They assume the noise from a single amplitron to be radiated coherently over the one meter dimension of an amplitron. So instead of being radiated isotropically, the noise is beamed toward the earth with a gain of order 10^3. With present-day technology it appears inevitable that the noise flux even from a single SPS would inundate the entire band between 2200-4200 MHz. In the band ± 100 MHz about the intended transmission frequency the noise flux would be about 10^9 times the 1.5×10^{-16} watt/m^2 threshold for a 10 MHz band.

The loss of this large segment of the radio spectrum clearly cannot be welcome amongst radio astronomers. Thus a high priority should be assigned to developing the technology to reduce this loss-band to a more acceptable level. According to Glaser et.al., expected improvement in filter design will reduce this noise flux by many orders of magnitude, narrowing the loss-band to as small as 200 MHz. In their summary they anticipate that the interference with radio astronomy will be slight (with the parenthetical qualification of < 2700 MHz). In fact it is doubtful that the permanent loss of the 3200-3400 MHz window of the microwave spectrum will be this well received, but if this projection is not overly optimistic then it can conceivably be considered acceptable.

Besides sideband noise in the neighborhood of the fundamental transmission frequency, one needs to consider harmonics. The second and third harmonics of the fundamental transmitted by the amplitron are expected to be of order 10^{-5}-10^{-6} the power of the fundamental. Therefore one would expect these to exceed the threshold in some bandwidth, probably narrower than that about the fundamental, unless they can be properly filtered. The actual behavior of these and higher harmonics depends on

their phase coherence with the harmonic emission of other amplitrons.

In summary, the problems presented by the SSPS to radio astronomy are potentially quite serious and deserve serious consideration. Particular emphasis should be placed on reducing sideband noise to well below the levels attainable with present technology, and to minimizing emission of harmonics.

C-2

GR

BIBLIOGRAPHY

1. G. D. Arndt from Initial Technical Environmental & Economics Evaluation of SPS Concepts, NASA, 1976.

2. C. W. Allen, Astrophysical Quantities, Athalone Press, London, 1973 (3rd edition)

3. J. D. Kraus, Radio Astronomy, McGraw-Hill, New York 1966.

4. M. Kundy, Solar Radio Astronomy, Interscience, New York, 1965.

5. W. Coles, Private Communication.

6. P. E. Glaser, O. E. Maynard, J. Mackovciak and E. L. Ralph, Feasibility Study of a Satellite Solar Power Station, NASA, 1974.

2.4 CATASTROPHIC FAILURE AND DEBRIS

INTRODUCTION

Here we consider possible magnetospheric environmental perturbations resulting from a failure in the SSPS system. It is difficult to see how SSPS failure might affect the magnetospheric environment other than by the dispersal of materials resulting from the failure of a single SPS or as the result of collision with another SPS or different type of satellite. Another possibility is the electromagnetic radiation pollution that might result from the uncontrolled broadcasting of an SPS with disabled control system. This problem and its remedy are probably best left to groups studying microwave system design and radio interference. Since we shall then focus on the debris problem it is natural to include in this discussion debris that might result from normal SSPS operation and from construction.

In considering the "pollution of space" two general goals for further work are important. One is to delineate the effects of particles of various sizes and compositions on the magnetosphere, on other SPS', and on other satellites. Qualitative aspects of such a division are present in Section A. A second important factor to be addressed is the subsequent concentration or dispersal of the materials emitted. This is discussed in Section D, where we consider effects of some of the forces affecting the orbits of emitted particles.

In addition to the above, we consider briefly SPS collision, Section B, effects of rupture of argon propellant tank, Section C; small particles, their orbits, optical effects and methods of controlling their dispersal, Section D.

A. PARTICULATE PROPERTIES

An important objective of theoretical and experimental study as SSPS development proceeds should be to identify sources of particulate emissions and their effects on SPS' and other satellites. For example, one goal of space

construction experiments should be to determine the pollution potential of the various alternative technologies. It could well turn out that small particulate emissions will constitute virtually no problem at all. Experienced NASA personnel have suggested that this may be the case on the basis of experience with the Apollo and Skylab projects On the other hand, the SSPS system involves many large satellites in close proximity, over a period of at least thirty years. It seems evident that as the use of space for industrial purposes becomes more commonplace, problems concerning orbital debris will have to be addressed. Some work to examine these problems is under way at Langley Research Center.[1]

In the following we consider qualitatively sources and effects of materials that might be emitted in SSPS operations, mainly in terms of size. Composition is also an important factor. Quantitative estimates of some materials are made in Ref. 2,13. The general types of particles are:

1. Large chunks of material that can collide with an SPS and disable some important apparatus, penetrate a living space or fueltank, or damage some important surface. These might result from collision, or breakage in construction or docking operations.
2. Smaller size particles that might become inserted in the works of some mechanical device causing either undue friction and wear in the case of very small particles or jamming of moving parts by larger particles. An example of the second would be the failure of a docking hatch to seal properly because of particles deposited on a joining surface. Sources of these particles might be the same as in item 4.
3. Liquid droplets and frozen liquid droplets. These might be frozen Argon pellets from a fuel spill, low volatility components of

spilled lubricants or residues of effluent from certain types of chemical thrusters, and perhaps waste liquids dumped into space. The effects of such liquids might be either physical damage in the case of frozen pellets, the coating of optical surfaces, or sticking of mechanical apparatus by heavy residues.

4. Very small particles result from a meteoroid impact, sputtering from charged particle impact, mechanical friction, erosion of surfaces due to thermal and mechanical stresses, erosion of ion thruster electrodes; construction processes such as welding, sawing, grinding and filing These might stick to optical surfaces, marring their ability to transmit or reflect light. Examples might be solar energy concentration and absorption surfaces and windows which must remain transparent. In this connection we note that tests have demonstrated that solar cells can still function well even after being coated with residues or suffering surface degradation such as caused by meteoroids.[3] This is because the light is scattered at the damaged surface but still transmitted. On the other hand, similar degradation of surfaces that are supposed to provide specular reflection, such as solar collectors, could be more serious. Very small particles could conceivably form a cloud around the SPS, cutting off some fraction of the sunlight. We shall present estimates showing that emission of enough material to do this is very unlikely.

5. Single atoms, molecules, and charged particles are in profusion by chemical and ion thrusters. They also result from evaporation of liquids and outgassing and sublimation of solids. The neutrals can charge exchange within the thruster beam forming a plasma which can cause solar arrays to draw excessive electron current.[4] This

problem is currently under study by NASA Lewis Research Center; possible effects in the context of SSPS operations should be analyzed. Whether this process can cause two SPS' to interact should be examined; it probably cannot since they are some 350 km apart. Neutral atoms and molecules might stick to cold shaded surfaces. The effect of atomic particles on the magnetosphere itself is the subject of Section 2 1

The quantitative assessment of particle types, sizes and effects is an important object for further study.

B. CATASTROPHIC FAILURE-COLLISION

The type of catastrophic failure we consider is that in which violent physical damage is in some way involved. Another type of catastrophic failure might be that in which the power collection or broadcasting systems are disabled but the SPS poses no danger to itself or any other SPS. The first type will naturally require a large source of energy and momentum, and the SSPS must be examined for such sources Possibilities are rupture or penetration of a pressure vessel, breakage of structural members that operate under stress, extra stresses that might result if some structural component fails due to its heating up because of loss of thermal control. Probably the most likely source of extraneous momentum is the failure of the stationkeeping thruster system, which must reliably provide well controlled impulses during the whole time the SPS is in orbit. In this regard there are several important questions concerning SSPS design. These are. 1) Is SPS attitude and orbit control independent of control of the power broadcasting system? 2) Will each cluster of thrusters be controllable separately from the others? 3) Will each cluster of ion thrusters (if these are used) obtain its electric power and propellant locally, and independently of the others? 4) Could "space tugs" be developed to take over control of a disabled SPS in time to avert collision? 5) Would independently operable "one shot" chemical thrusters for collision avoidance be a workable concept? Calculations combining the SPS orbit equations with the probability of thruster failure will be required.

The problem of collision avoidance has been recognized in several SSPS studies.[5,6] In particular, solar radiation pressure causes variations in the eccentricity of the orbit. An optimum eccentricity $\varepsilon \sim .04$ has been proposed in Ref. 5. Viewed by an observer on the earth, a satellite with eccentricity ε will appear to move across the sky on a "small" ellipse of major axis

length $\ell = 4r\varepsilon \sim 6746$ km, where r is the radius of GSO (see below). Since the SPS' are only about 370 km apart a change of .0043 or ~10% in ε could cause the orbits to intersect.[5] A simpler example of a collision scenario is the following. Imagine the SPS' are all in circular orbits, and an extraneous momentum is applied to one along the direction of motion, tending to decrease its velocity and raise the orbit by an amount Δr. At GSO $v = \sqrt{K/r} = 3.075 \times 10^5$ cm/sec. If we ask that the orbit be raised by an amount that collision can occur and the SPS not pass one another we should take $\Delta r \sim 10$ km. The velocity is lowered by about 36 cm/sec which would cause the SPS' to collide in about 260 hours, probably time enough to take corrective action. The size of momentum impulse ΔP_{coll} required for this collision can be calculated from the change in angular momentum of the orbit

$$\Delta L = r\Delta P = \Delta(Mvr) \tag{2.4.1}$$

which gives $\Delta P_{coll.} \sim 1.7 \times 10^{12}$ dyne-sec. This is only about .8% of the yearly station-keeping requirement of $\Delta P_o \sim 2.16 \times 10^{14}$ dyne-sec ($\Delta v \sim 46$ m/sec), and one could easily imagine it being applied during some catastrophic incident. It corresponds to ten MPD thrusters ($\dot{m}$ = 15.6 gm/sec, v_{ex} = 20 Km/sec) operating for about 1.5 hours. An important point is that since stationkeeping requirements are small the extraneous impulse that might cause collision is also small.

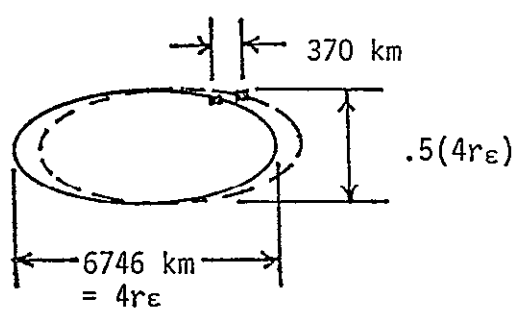

SPS orbits viewed in earth rotating frame.

C PROPELLANT TANK RUPTURE

The rupture of a liquid propellant tank and release of propellant into vacuum can transfer momentum to the SPS. We attempt to ascertain here what ΔP the rupture of a vessel containing liquid argon might provide. We also consider what then might happen to the argon released. We have not examined the situation where propellants such as H_2 and O_2 which can chemically react are released.

We assume that Ar could be stored in liquid form at atmospheric pressure if it could be kept out of the sunlight, properly insulated and perhaps refrigerated. Its temperature might be somewhere near the atmospheric pressure boiling point T ~87.3° K.[7] We also assume that for some reason the tank ruptures and some fraction of its surface area is directly exposed to the nearly perfect vacuum of outer space. The escaping Ar will exert an impulse which we shall attempt to estimate by two methods. If liquid Ar had very large thermal conductivity (which is not the case), or were in a container that could easily conduct heat to all regions such as a pipe, the momentum transfer would be provided by the boiling off of individual atoms at the exposed surface. This would progress until heat removal caused the freezing of the Ar at ~83.8°K; the vapor pressure then decreases rapidly. For an example we have taken 1.0 m^3 of Ar and assumed a hole 100 cm^2. (This is about 640 pounds and represents ~.64% of the yearly stationkeeping propellant requirement of ~10^5 pounds). The energy and particle fluxes may be estimated by assuming they are given by a half-Maxwellian distribution emerging from the surface, corresponding to temperature T and with particle density $n_o = P_v/kT \sim 8.33 \times 10^{19}/cm^3$, where P_v is the vapor pressure at atmospheric pressure, $P_v \sim 10^6/dyne/cm^2$, and does not vary much between boiling and freezing. We are thus using a detailed balance argument to obtain the efflux of particles which really depends

only on the liquid temperature. We are overlooking the effect of collisions which cause some particles to bounce back to the liquid and thus probably overestimating the net fluxes. The number and energy fluxes are

$$\Gamma_{n,\varepsilon} = n_o \left(\frac{m}{2\pi kT}\right)^{3/2} \int_0^\infty v^2 dv \int_0^{2\pi} d\Phi \int_0^{\frac{\pi}{2}} d\theta e^{-\frac{1}{2}mv^2/kT} (v \cos\theta)$$

$$\times \{1, \tfrac{1}{2}mv^2\} \qquad (2.4.2)$$

or

$$\Gamma_n = \frac{n_o v_o}{\sqrt{\pi}}, \quad \Gamma_\varepsilon = \frac{2kT}{\pi} n_o v_o \qquad (2.4.3)$$

where $v_o = \sqrt{\frac{2kT}{m}} \cong 1.9 \times 10^4$ cm/sec.

Using T = 87°K we obtain the numerical values $\Gamma_n = 8.93 \times 10^{23}$ atoms/cm^2-sec, $\Gamma_\varepsilon = 2.27 \times 10^6$ erg/cm^2-sec. Assuming surface area 100 cm^2 and using the density of liquid Ar 1.4 gm/cm^3 and its heat capacity $c \sim 6$ calorie/mole-°K = 6.23×10^6 erg/gm-°K (Ref. 7) one finds that enough heat is carried away to freeze the whole tank in $T \sim 135$ seconds, during which 0.005 of the fluid is evaporated. The momentum transfer during this period is $\Delta P \sim m v_o \Gamma_n T \sim P_v \cdot 100$ cm^2 · T = 1.35×10^{10} dyne-sec, or about 1% of the ΔP_{coll} computed in B. This calculation assumed very good heat conductivity so that the surface does not freeze while the rest remains liquid, and that no heat flows in from external sources.

The heat flow equation

$$\nabla^2 T = \frac{c\rho}{K} \frac{\partial T}{\partial t} \qquad (2.4.4)$$

where the heat conductivity $K \sim 125$ mwatt/meter-°K = 1.25×10^4 erg/sec-cm-°K[7] gives the scale time for temperature equilibration

$$\tau \sim \frac{c\rho L^2}{K} \sim 700\ L^2 \text{ sec.} \qquad (2.4.5)$$

For L = 1 meter $\tau \sim 7 \times 10^6$ sec >> T. This can have two consequences. First, the fluid near the rupture may freeze rapidly, because energy is being extracted only from the fluid near the rupture, and perhaps seal it. Also fluid in the warmer regions can boil because the static pressure is released. Both of these phenomena are observed when liquids are pumped on for cooling purposes An interesting illustration of the effect of thermal conductivity occurs when liquid He^4 is pumped on. Above the λ point at 4.2°K the liquid actively boils, but when the λ point is reached it immediately becomes quiet due to the large increase in heat conductivity.

Another way to estimate the momentum impulse is to assume that the fluid in the tank farthest from the rupture remains at its original temperature and vapor bubbles form which drive the rest of the fluid out. A crude model would say that all of the fluid is driven out under atmospheric pressure. In this case the energy expended is given to fluid kinetic energy, i.e.,

$$P \cdot A \cdot L = \frac{1}{2} MV^2 \qquad (2.4.6)$$

where $A = 10^4 cm^2$, L = 100 cm and $M = 1.4 \times 10^6$ gm. This gives $V = 1.2 \times 10^3$ cm/sec and $\Delta P = MV = 1.7 \times 10^9$ dyne-sec.

The maximum of the ΔP we have estimated is only about 1% of ΔP_{coll}. On the other hand we have only guessed at the relevant parameters and made only a first attempt at understanding the physics of the situation. Thus we feel that propellant tank rupture as a source of uncontrollable momentum transfer should be examined further. If problem areas are uncovered, storage of argon in solid form might be considered; since its freezing temperature is close to the boiling point the extra effort to store it this way might be small and the reduction in dispersal worth the extra effort. Also if liquid storage is used it might be worthwhile to provide good thermal connection between all parts of the vessel to reduce boiling so that less fluid is expelled.

Frozen argon droplets associated with a fuel spill could be a hazard to the SPS where they originate or to another SPS. We present here some very tentative analysis of this possibility.

Consider a just frozen argon sphere of radius r and mass $m = \frac{4}{3}\pi r^3\rho$, and assume that it absorbs some fraction γ(50% say) of the solar flux f = .14 watt/cm^2 hitting it. At the same time it loses energy and mass due to sublimation at the surface. We shall assume again large heat conductivity although this is probably not correct for droplets larger than a few millimeters (Eq. 2.4.5). The rate of change of temperature is

$$\frac{dT}{dt} = \frac{1}{Mc}\frac{dQ}{dt} = \left(\frac{4}{3}\pi\rho r^3(t)\right)^{-1}\left(\frac{dQ_s}{dt} + \frac{dQ_\varepsilon}{dt}\right) \tag{2.4.7}$$

with the heat fluxes given by

$$\frac{dQ_s}{dt} = \pi r^2\gamma f \tag{2.4.8}$$

$$\frac{dQ_\varepsilon}{dt} = -4\pi r^2\Gamma_\varepsilon = -4\pi r^2(P(T)/kT)\cdot kT\sqrt{\frac{2kT}{m}}, \tag{2.4.9}$$

P(T) is the vapor pressure at temperature T. Note that both heat flux terms have the same r dependence. Mass evaporates off at the rate

$$\rho\frac{d}{dt}\left(4\pi r^3(t)\right) = -4\pi r^2 m\Gamma_n = -4\pi r^2\frac{M}{\sqrt{\pi}}\left(\frac{P(T)}{kT}\right)\sqrt{\frac{2kT}{m}} \tag{2.4.10}$$

These equations may be summarized as

$$\frac{dr}{dt} = -\frac{m}{\rho\sqrt{\pi}}\sqrt{\frac{2kT(t)}{m}}\;\frac{P(T)}{kT} \tag{2.4.11}$$

$$\frac{dT}{dt} = \frac{3}{\rho c r(t)}\left[\frac{1}{4}\gamma f - \frac{2}{\sqrt{\pi}}P(T)\sqrt{\frac{2kT(t)}{m}}\right], \tag{2.4.12}$$

and can be solved analytically if a form for P(T) is given. Near the freezing point, where P ~.1 atm., the evaporation term dominates the temperature equation. By consulting vapor pressure tables[7] we find that the heat

absorption balances the evaporation term somewhere in the neighborhood of $T_o = 40°K$ ($P \sim 10^{-5}$ atm = 10 dyne/cm^2). If the pellet is hotter in the center heat will convect to the surface and be expelled by an increase in the evaporation term until the whole droplet reaches a quasi-equilibrium at T_o. Then

$$\frac{dr}{dt} = \frac{-m}{\rho\sqrt{\pi}}\sqrt{\frac{2kT_o}{m}}\,\frac{P(Te)}{kT_e} \sim -5.7 \times 10^{-4}\,\frac{cm}{sec}\ , \qquad (2.4.13)$$

giving a time 2.4 hours for a 10 cm diameter sphere to evaporate. If it had been expelled in a fuel tank rupture with $V \sim 10^3$ cm/sec $\sim$ 40 km/hr (Eq. 2.4.6) it would take ~ 9 hours to reach another SPS. More detailed analysis in the future will show whether a fuel spill incident might cause damage to an adjacent SPS. If the velocity V we have used is correct such pellets could apparently damage the SPS of origin.

Two other effects of spilled argon should be considered. As has been discussed in Section 2.1 neutral argon is converted to plasma by photoionization, with possible consequences for magnetospheric functioning. A second possibility is adhesion of argon to cold shaded surfaces such as windows. If there were no heat input its vapor pressure would become so low that it might stay around for a long time, and special measures would be required to remove it.

D SOLID PARTICULATES

Solid particulates could constitute a long term impairment to the functioning of an SPS for reasons mentioned in A. There are four important areas that must eventually be investigated quantitatively:

1. Sources, types, and quantities of particulates emitted;
2. the concentrations that will build up and possible dispersal effects,
3. effects of particles of various size and composition on operation of SPS and other satellites; and
4. possible methods of control of particulates should they turn out to be a problem.

There is little, if any, knowledge concerning items 1. and 3., since even the grossest features of the SSPS have not been decided.

On the other hand, it is not too early to become aware of the issue and to analyze SSPS alternatives in terms of particulate effects. It is in principle possible to calculate particulate distributions in space if a given source distribution is assumed. The source might be estimated by theoretical analysis, and experimental data as it becomes available.

Possibly whatever is deposited will tend not to disperse, but to concentrate in GSO. A cloud of dust and debris in a perfectly spherical 1/r potential will, over a long period of time, dissipate energy due to viscous drag forces, at the same time conserving angular momentum. The minimum energy configuration has all matter moving with the same speed in a thin circular ring (in this configuration there are no longer any drag forces). Also along the GSO orbits there exist shallow potential wells in the earth rotating frame arising from the non-spherical corrections to the shape of the earth.[5] This causes the SPS' to oscillate about a stable equilibrium point in the rotating frame and might also have the effect of trapping particulates in the

longitudinal direction. On the other hand, the other perturbations such as luni-solar effects and radiation pressure might disperse the particles. For example solar radiation can push very small particles, $r \sim 10^{-5}$ cm, completely out of the solar system.[8] Due to the unique nature of the GSO stable points it will probably be appropriate to consider space here as an important and limited resource.

For very small bits of material that acquire charge electric forces could play a role. We consider three possibilities: 1) They might be affected by the magnetospheric electric field. 2) Charged particulates might interact with an SPS that is itself charged due to magnetospheric substorm activity. 3) Electrostatic methods might be used to clean up particulates.

To examine 1) we consider aluminum spheres, $\rho \sim 2.7$ gm/cm^3, of mass M which have acquired charge from 10V to 10kV, during a magnetospheric substorm. Their radius as a function of mass is $r = \left(\frac{3M}{4\pi\rho}\right)^{\frac{1}{3}} = 445M^{\frac{1}{3}}$ (gm) and their charge is given by $q = r\Phi = 14.7M^{\frac{1}{3}}$ esu at $\Phi = 10$kV. A typical value of the magnetospheric electric field is 1 mV/meter = 3.33×10^{-8} stat volt/cm,[14] so the electric force on the particle if $F_e = 4.9 \times 10^{-7}\ M^{\frac{1}{3}}$ dynes. The earths' gravitational force at GSO and the sun's gravitational force at 1 a.u. are $F_{g-e} = 22.4M$ dynes and $F_{g-s} = .593$ M dynes. The solar radiation pressure at 1 a.u. is $\left(\frac{1}{c}\right)$ .14 watt/cm^2 = 4.67×10^{-5} dyne/cm^2 giving for the radiation force $F_{sp} = 2.9 \times 10^{-5}\ M^{2/3}$ dynes. In Figure 2.4.1 accelerations of particles as a function of radius are plotted. We see that only for very small particles do the radiation pressure and electric forces become important. For a 10kV particle the earth gravitational force and electric force become equal at $r \sim 6.6 \times 10^{-5}$ cm. Such a particle accelerated through 50kV, roughly the

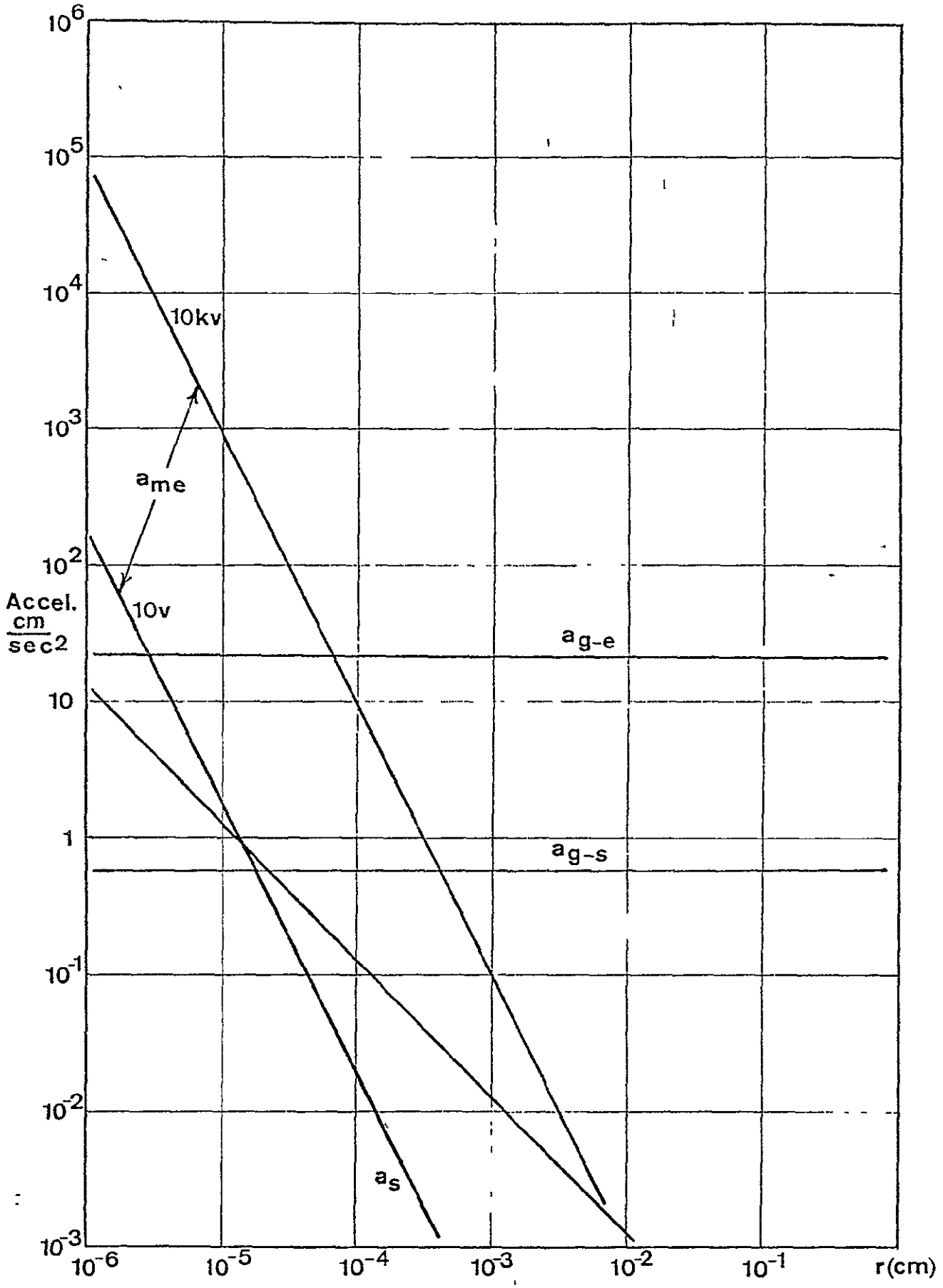

Figure 2.4.1. Debri Particle Orbit Contributions.

voltage that exists across the magnetosphere, would acquire velocity $5 \times 10^5 \frac{cm}{sec}$ in about 5.5 hours. This is of the order of orbital velocities and is smaller than typical meteoroid velocities of $2\text{-}4 \times 10^6$ cm/sec. The rate of charge deposition on a surface by magnetospheric electron fluxes is at most $\sim 10^{-9}$ amp/cm^2 = 3 esu/cm^2 -sec giving a time 15 hours for the above particle to charge to 10kV. Before it could be charged to 10kV it would most likely be exposed to sunlight where the surface photoemission is important. This rate is something like 12.5 esu/cm^2-sec, meaning that a 10kV particle would discharge in a few hours. In general it does not appear that the voltages necessary for particulate motion to be strongly affected by magnetospheric electric fields can be attained. On the other hand, Figure 2.4 1 indicates that electric and radiation forces could be a significant perturbation for particles less than a micron in size and charged in the neighborhood of 100V.

In the absence of intense electron fluxes particulates can charge positive by photo emission to energies of the order of the emitted electrons ~10V. Although they would not be strongly affected by the magnetospheric electric field they might tend to migrate towards negatively charged SPS surfaces. We leave open the question of how the particulates might be charged positive near a negatively charged SPS surface. They could perhaps drift to a shaded region from a sunlit region after a substorm has subsided. We assume that the SPS surface is charged to 1 kV with respect to the surrounding plasma, its electric field extends out a Debye length, ~100 m, from the surface. This field is a factor 10^4 greater than the magnetospheric electric field. Again with the assumption of aluminum density we have calculated the perpendicular outward velocity a particle of radius r, charged to 10 V, would need to escape the SPS finding $V_{es} = .139/r$ (cm) cm/sec. It seems that only very small particles are affected very much. Further consideration may show that even though they tend

to migrate towards surfaces other processes intervene to remove them.

If particulates are emitted in a localized region, such as in the operation of some construction machine, electrostatic methods might be used to control them. If aluminum spheres charged to 1 kV, say by an electron gun, pass between parallel plates charged to 1 kV the maximum time for them to be drawn to one of the plates is 142.7 r (cm) sec. This indicates that fairly large particles, perhaps up to .01 cm, could be collected efficiently at the source. We have also examined the possibility of using electrostatics to collect particles from large distances. The 100 m Debye length is a limiting factor. Charging particles with an electron beam and attracting them to a small three-dimensional region appears impractical due to the $1/r^2$ falloff of the Coulomb field. Very large, light planar sweeping grids, propelled by thrusters, might be a workable method. Another possibility is to use high power lasers to destroy debris that threatens the SPS.

Aside from contact interaction with satellite surfaces and mechanisms, particulate matter will interact with the various forms of electromagnetic radiation present. These include solar radiation, the SPS microwave power beam and its attendant phase control reference beam, radio communications signals, radar ranging apparatus, and possibly laser beams for communications and ranging. Estimates below indicate that such problems will be minimal.

There exists a large well-developed body of knowledge concerning the scattering and absorption of electromagnetic radiation by bits of matter[9,10,11]. This theory could be applied to virtually any distribution of particulates once the distribution is given. The ability of a particle to remove power from the incident wave is described by its extinction cross section $\sigma = \varepsilon/I_0$ where I_0 is the incident intensity and ε is the power removed. It is the sum of the scattering cross-section σ_s, describing power redirected by the particle, plus

the absorbtion cross-section σ_a describing power absorbed and converted into thermal energy. In the limit of incident wavelength long compared to particle size the scattering cross-section reduces to the Rayleigh cross-section

$$\sigma_R = \frac{8\pi}{3} \left(\frac{2\pi}{\lambda}\right)^4 |\alpha|^2 \xrightarrow[\lambda \to \infty]{} 0$$

where α is the electric polarizability of the particle. The polarizability depends on the particle properties and exhibits large values at the resonance frequencies. This is responsible for oscillations with frequency of the magnitude and polarization of the scattered wave. Extinction cross-sections tend to maximize for particle size of the order of the incident wavelength at a value of the order of the geometrical cross-section. For spheres it asymptotically approaches $2\pi r^2$ as $\lambda \to \infty$. The actual energy removed from the beam is $\pi r^2 I_0$, the factor of two discrepancy being known as the extinction paradox[11].

Using the geometrical cross section it is possible to assess crudely three phenomena that might disrupt SPS operations: the extinction of sunlight by particulates, scattering of the microwave beam, and the heating of bits of material in the beam. We imagine the particles are spherical of aluminum density. Their projected area in terms of their mass is $\sigma = \pi r^2 = (3M/4\pi\rho)^{2/3} = .623M^{2/3}$. We ask what mass of these particles is required to extinguish 10% of the sunlight. If there are N of them in a 1 cm^2 column we require $N\sigma = .1$. Their mass is $MN = \frac{.1M}{\sigma} = .16M^{\frac{1}{3}}$ gm/cm^2, or taking the SPS area to be 100Km^2 the total mass is

$$M_t = 1.6 \times 10^{13} M^{\frac{1}{3}} \text{ gm.}$$

Even using particles with radius 5×10^{-5} cm, a typical sunlight wavelength, we find the total mass required to reduce the sunlight by 10% to be about

1.8×10^6Kg. This is about 4% of the SPS mass. If this much mass had been eroded from the SPS' they would be inoperable anyway.

Erosion of surfaces by meteoroids and sputtering are two sources of particulates. It can be seen fairly easily that they will not produce anything like the above amount if dispersed uniformly. These processes do, however, degrade optical surfaces and their ejecta could impair the SPS in other ways.

The impact of meteoroids on a surface erode some one hundred times the mass of the meteoroids themselves.[12] The flux is given by [8]

$$\log_{10} I(m) = -17.0 - 1.70 \log_{10} m,$$

where I(m) is the average number of impacts/m^2-sec by particles of mass greater than m grams (it is a sensitive function of altitude). This translates to I(m) $= 10^{-17} m^{-1.7}$, which when differentiated gives for the flux of particles of mass m

$$dI(m) = -1.7(10^{-17}) m^{-2.7} dm$$

To find the total mass we multiply by m and integrate from $m = 10^{-10}$ to $m = 10^{-5}$, giving for the total mass impacting

$$\frac{dM}{dt} = -1.7 \times 10^{-17} \int_{10^{-10}}^{10^{-5}} m^{-1.7}\, dM \sim 2.5 \times 10^{-10} \text{ gm/m}^2\text{-sec.}$$

Using twice the SPS frontal area and the ratio 100 for the ejecta mass we find the total mass ejected to be 1.5×10^5 kgm/year. This number could in ten years become roughly comparable to that given above. However the ejecta will emerge with an angular distribution; it seems unlikely that enough would collect in the column above the light collecting surface to obscure the sunlight. Nevertheless it seems like a large amount, ~ 400 kgm/day, and its

fate will have to be determined.

Sputtering, the removal of minute chunks of matter from a surface by charged particle impact, also constitutes a source of particulates. A typical rate for the sputtering of iron by solar wind particles at 1 a.u. is[8] $.48 \times 10^{-8}$ cm/year. This might be increased somewhat for the softer SPS materials exposed to magnetospheric conditions. At this rate about 50 kgm/year would be ejected. Erosion of material by meteoroid impact and sputtering is probably more significant for its direct effect on the SPS, than for optical extinction by the eroded material.

We can make a simple estimate of the density of ejected material and compare it to the ambient density of meteoroid material. The average meteoroid velocity is $v \sim 2 \times 10^6$ cm/sec The flux as calculated above is

$$\frac{dM}{dt} = 2.5 \times 10^{-14} \text{ gm/cm}^2\text{-sec} = \rho_m v_m$$

giving $\rho_m \sim 10^{-20}$ gm/cm^3. The mass ejected from 100 SPS' per year is $\sim 10^{10}$ gm. If we assume the meteoroid energy is uniformly distributed among the ejecta we find the debris velocity $v_D = .1 v_m = 2 \times 10^5$ cm/sec. We shall attempt a crude estimate of the volume over which they might distribute themselves If they were emitted tangentially to the SPS trajectory their radial range might be something like 5 earth radii, Section 2.1 - Figure A.1. We imagine that they fill a donut-shaped region of minor radius $a \sim 2.5\ R_e = 1.6 \times 10^9$ cm, and major radius $r \sim 4R_e = 2.5 \times 10^9$ cm. The volume they fill is thus

$$V \sim (2\pi r)\ (\pi a^2) \sim 10^{29} \text{ cm}^3.$$

Thus debris density builds up at the rate $\dot{\rho}_D \sim 10^{-19}$ gm/cm^3-year, compared to $\rho_M = 10^{-20}$ gm/cm^3. This might indicate that SSPS operations would give rise to a fairly dense man-made "meteoroid belt". Further study should be carried out to determine the correct density and velocity distributions.

Finally we consider effects on the microwave power beam. From the above it is clear that very small particles will not affect the beam if their amount is anything like what we have calculated above. It is hard to imagine how, during normal operation, material straying into the beam would be sufficient to deflect or extinguish it.

We can roughly estimate the maximum temperature to which foreign bodies might heat due to exposure to the beam. At the maximum temperature of the body thermal emission equals energy absorption. The absorption we assume to be a factor a of the total incident energy, where a is the absorbtivity of the material at microwave frequency. The heat flow balance condition is

$$a\, I_0\, \pi\, r^2 = 4\pi\, r^2\, e\sigma T^4 ,$$

or

$$T = \left(\frac{I_0 a}{4e\sigma}\right)^{\frac{1}{4}} = 258\left(\frac{a}{e}\right)^{\frac{1}{4}} {}^\circ K,$$

where e is the average emissivity over a black body spectrum, $I_0 \sim .1$ watt/cm^2, and $\sigma = 5.67 \times 10^{-5}$ erg/(cm^2-sec-°K^4) is the Stefan-Boltzmann constant. For dielectric materials, paints and rough surfaces, e is in the region of .3-1. If we assume that the absorption is maximum, a = 1, we find T ~ 350°K. Polished metals have small e ~.02 - .08 but their absorption is small as well. It is given by $a = \frac{1}{2}\frac{\omega\delta}{c}$ where $\delta \sim 10^{-4} - 10^{-3}$ cm is the skin depth at 3 GHz and c is the speed of light. Substitution shows that polished metals will tend to remain cool, the heat input being dominated by the solar flux. There appears to be no danger that stray materials would melt in the microwave beam.

BIBLIOGRAPHY

1. Research and Technology Objectives and Plans Summary, W77-70277, p. 42, 1977.

2. Behavior of Materials in Space Environments, L. D. Jaffe, J. B. Rittenhouse, ARS Journal 32, 320, 1962.

3. Robert Naumann, George C. Marshall Space Flight Center.

4. The Interactions of Solar Arrays with Electric Thrusters, H. R. Kaufman and G. C. Isaacson, AIAA Paper No. 76-1051, Electric Propulsion Conference, Key Biscayne, Fla , November 1976.

5. Initial Technical, Environmental and Economic Evaluation of Space Solar Power Concepts, Vol II, IV - A-3-8, Lyndon B. Johnson Space Center, August 31, 1976.

6. Arthur D. Little, Inc., "Feasibility Study of a Satellite Solar Power Station", NASA CR-2357, NTIS N74-17784, February 1974.

7. Argon, Helium, and the Rare Gases, G. A. Cook, Ed., Interscience Publ., 1961.

American Institute of Physics Handbook, McGraw-Hill Book Co., 1972

8. Satellite Environment Handbook, Ed. F. S. Johnson, Stanford University Press, 1965.

9. Principles of Optics, M. Born and E. Wolf, Pergammon Press, 1970.

10. Light Scattering by Small Particles, H. Hulst, Wiley, 1964.

11. Radiation and Optics, Stone, J. M., McGraw-Hill, 1963.

12. D. H. Humes, Langley Research Center, private communication.

13. R. J. Naumann, Skylab-Induced Environment, Progress in Astronautics and Aeronautics 48, p. 383, 1976.

14. During a substorm the field could go as high as 10 mV/meter; this fact will not change the commentary in the text.

2.5 SATELLITE INDUCED PROCESSES

INTRODUCTION

There are three ways in which a satellite can influence the environment through which it travels, aside from the deposition of material: 1) It may produce directly electromagnetic radiation; 2) its physical motion through the surrounding medium, plasma and neutral, alters the medium particle distributions, and 3) this can then generate plasma electromagnetic disturbances. The direct EM radiation, typically microwave power beam and communication signal frequencies will be high enough to pass through the plasma, barely affecting it. Whether or not this is the case for the power beam passing through the ionosphere is still problematical, and we discuss this in Section 2.6. The type of processes we shall discuss here are the "satellite induced processes", those caused by the motion of the satellite through the medium.

Two possible "environmental" consequences of these processes are the alteration of the particle environment in the vicinity of other satellites by emission of disturbances by an SPS, and the production of electromagnetic interference. Consequences for the SPS itself are changes in its particle environment, and forces and internal stresses on the SPS physical structure. These forces, known as "drag forces" because they act opposite to the direction of motion, have been studied for a long time in connection with smaller satellites. They are caused by a number of different physical mechanisms. These are the same that produce the plasma disturbance. Momentum and energy extracted from the satellite motion goes into plasma motion. For this reason it will probably be most efficient in the future to study satellite induced processes not only as an environmental problem, but also at the same time to examine effects on

the SPS itself. We feel that the environmental consequences of satellite induced processes could be minimal. The drag forces on an SPS during construction in low earth orbit and during orbit raising may be important.

There are basically three types of drag force exerted on a satellite by the surrounding medium. 1) Neutral drag[1,2] (or aerodynamic drag), the force that results from the impact of neutral particles on the front surface. 2) Charged particle drag,[2,3,4,5] the force that results from direct impact of charged particles on the front surface, plus that resulting from the deflection of charged particles by electric fields surrounding the satellite. This second is sometimes called "coulomb drag", or "electrohydrodynamic drag". 3) Induction drag.[3,5,6,7,8,9] currents induced by satellite motion through magnetic field and fed by the surrounding plasma interact with the magnetic field producing a drag force.

A. PARTICLE DRAG FORCE AND WAKE

As a satellite with velocity V moves through a stationary medium more particles impact on the front side with higher velocity than on the rear. These particles may be reflected, absorbed, or perhaps reemitted with a different velocity. In any case the satellite experiences a drag force. This force is most simply understood when the background gas is neutral and V is extremely large compared to the thermal speed $v_n = \sqrt{\frac{2kT_n}{m_n}}$ of the neutrals. In this case the satellite simply sweeps up all the particles in its path leaving a tubular void behind it. Eventually the void fills in due to the thermal motion. Results of density calculations for $V/v_n = 8$ (Ref. 2, p. 58) for satellites of various shapes are shown in Figure 2.5.1. The calculations have assumed that the neutral particle mean free path is large compared to the satellite size. This is fairly

ORIGINAL PAGE IS
OF POOR QUALITY

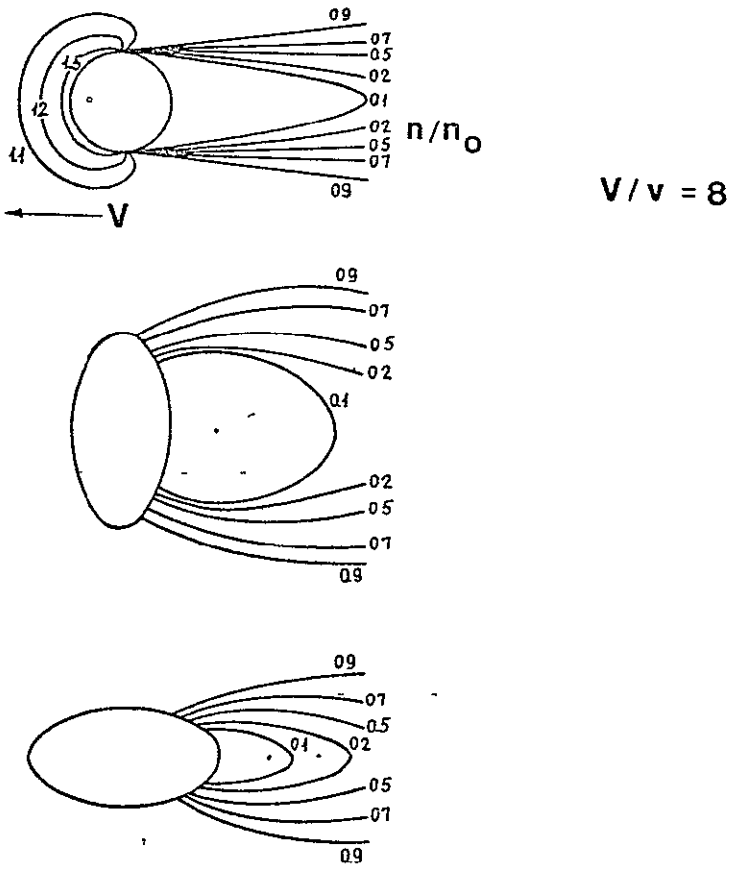

Figure 2.5.1 Density Perturbation Near Fast Moving Body(Ref. 2)

well satisfied for the neutrals at LEO (Table 1). A simple approximate expression for the neutral drag force F_n may be derived by assuming that all the particles impact the front surface with velocity -V. The momentum transfer to the satellite is

$$F_{Dn} = n_n m_n AV^2 C_D .$$

A is the satellite frontal area, n_n and m_n are the particle number density and mass, and C_D is the "drag coefficient", a number of order unity. At LEO the neutral density is some 500 times that of the charged particles and they account for most of the drag.

As altitude increases the neutral density decreases more rapidly than the ion density, they become equal at about 1200 km. The motion of the charged particles is more complicated than that of the neutrals owing to the earth magnetic field and satellite electric field. In Table 1 we show important particle properties at three altitudes. We see that at 500 and 1000 km v_i, $v_n < V \ll v_e$ and at GSO $V \sim v_n$, v_i, $v_e \gg V$. At GSO the particle drag forces are essentially nonexistent, due both to the rarity of the neutrals, and the rarity and high speed of the charged particles.

In the regions where $V < v_i$ the charged particle drag formula is almost the same as that for the neutrals

$$F_{DC} = m_i n_i V^2 A' ,$$

the drag being provided by the massive ions. A is a modified area that depends on the floating potential of the satellite ϕ_s[3,5]

$$A' \cong A\left[1 + \left(\frac{2e\phi_s}{m_i V^2}\right)\right] .$$

It takes account the modification of ion motion due to the electric field surrounding the satellite. ϕ_s is acquired because of the difference in

		Number Density		Mass Density		Satellite	Temp.	Thermal Speed (cm/sec)		
Alt(km)	Alt(cm)	Neutrals	Ions	Neutrals	Ions	Speed(cm/sec)	^{o}K	Neutral	Ion	Electron
500	6.9×10^{8}	6×10^{7} O	2×10^{5} O^{+}	1.3×10^{-15}	5.3×10^{-18}	7.6×10^{5}	1300	1.1×10^{5}	1.1×10^{5}	2×10^{7}
1000	7.4×10^{8}	2×10^{5} O	7×10^{3} O^{+}	5.3×10^{-18}	1.9×10^{-19}	7.35×10^{5}	1300	1.1×10^{5}	1.1×10^{5}	2×10^{7}
5000	1.14×10^{9}	2×10^{3} H	5×10^{3} H^{+}	3.3×10^{-21}	8.3×10^{-21}	5.92×10^{5}	1300	4.6×10^{5}	4.6×10^{5}	2×10^{7}
10000	1.64×10^{9}	5×10^{2} H	5×10^{3} H^{+}	8.3×10^{-22}	8.3×10^{-21}	4.94×10^{5}	1300	4.6×10^{5}	4.6×10^{5}	2×10^{7}
15000	2.14×10^{9}	2×10^{2} H	2×10^{3} H^{+}	3.3×10^{-22}	3.3×10^{-21}	4.32×10^{5}	1300	4.6×10^{5}	4.6×10^{5}	2×10^{7}
35800	4.22×10^{9}	30 H	1-5 H^{+}	5.0×10^{-23}	$\gtrsim 4 \times 10^{-24}$	3.07×10^{5}	1300 H 10^{7} H ,e	4.6×10^{5}	$\gtrsim 4 \times 10^{7}$	2×10^{9}

	Debye	Magnetic	Drag Force*(dynes)			Solar
	Length(cm)	Field(gauss)	Neutral	Ion	Induction	Pressure
500	.5	.25	10^{8}	3×10^{5}	3×10^{6}	4.7×10^{6}
1000	3.0	.2	3×10^{5}	10^{4}	8×10^{4}	4.7×10^{6}
5000	3.5	.055	--	--	?	4.7×10^{6}
10000	3.5	.018	--	--	?	4.7×10^{6}
15000	5.5	8.3×10^{-3}	--	--	?	4.7×10^{6}
35800	$\sim 10^{4}$	1.1×10^{-3}	--	--	$< 10^{4}$	4.7×10^{6}

*Drag forces computed using A $10 km^{2}$.

Table 2.5.1 Drag Forces and Magnetospheric Parameters.

flux of electrons and ions, and is also influenced by photoemission. Its value is typically -(.3→.6) volts at lower altitudes compared to $\frac{1}{2} m_1 V^2$ ~ 5eV. Detailed calculations[5] have shown that potential corrections to the drag force on large satellites are typically a few percent. Thus it is reasonable for estimates to set $A' = A$.

The most apparent effect on a satellite of the drag force is its decrease of radius, which speeds up the satellite and increases the drag force. The rate of change of radius depends on F_D divided by the mass M, and so drag forces are most effective for very light satellites with large frontal area, such as the SPS. The collector area of an SPS is some 100 km^2. For purpose of discussion we note that on the average it will not always be facing in the direction of motion and in LEO and during orbit raising may not be fully erected. Thus we take A ~10 km^2 as the frontal area and $M = 50 \times 10^6$ kg. A typical research satellite might have A ~1m^2 and M ~250 kg. The area to mass ratios are respectively 2 cm^2/gm and 4×10^{-2} cm^2/gm. It would seem that drag forces could easily be 50 times more effective on an SPS. Also if the center of mass did not coincide with the center of area torques could develop. At LEO the neutral drag dominates. The force on a 10 km^2 area is $F_D \sim 1.5 \times 10^8$ dyne. This corresponds to 5 MPD thrusters ($\dot{M}$ = 15.6 gm/sec, v_{ex} = 20 km/sec) operating continuously and would change the radius at a rate ~5 km/day. A quantitative assessment of the drag forces as a function of altitude using a realistic SPS construction scenario and realistic SPS dimensions should be an object of further study.

When moving through the medium at supersonic speed the satellite leaves a characteristic "Vee" shaped wake, Fig. 2.5.2, which viewed in the satellite frame appears stationary. Its opening angle in the case of a

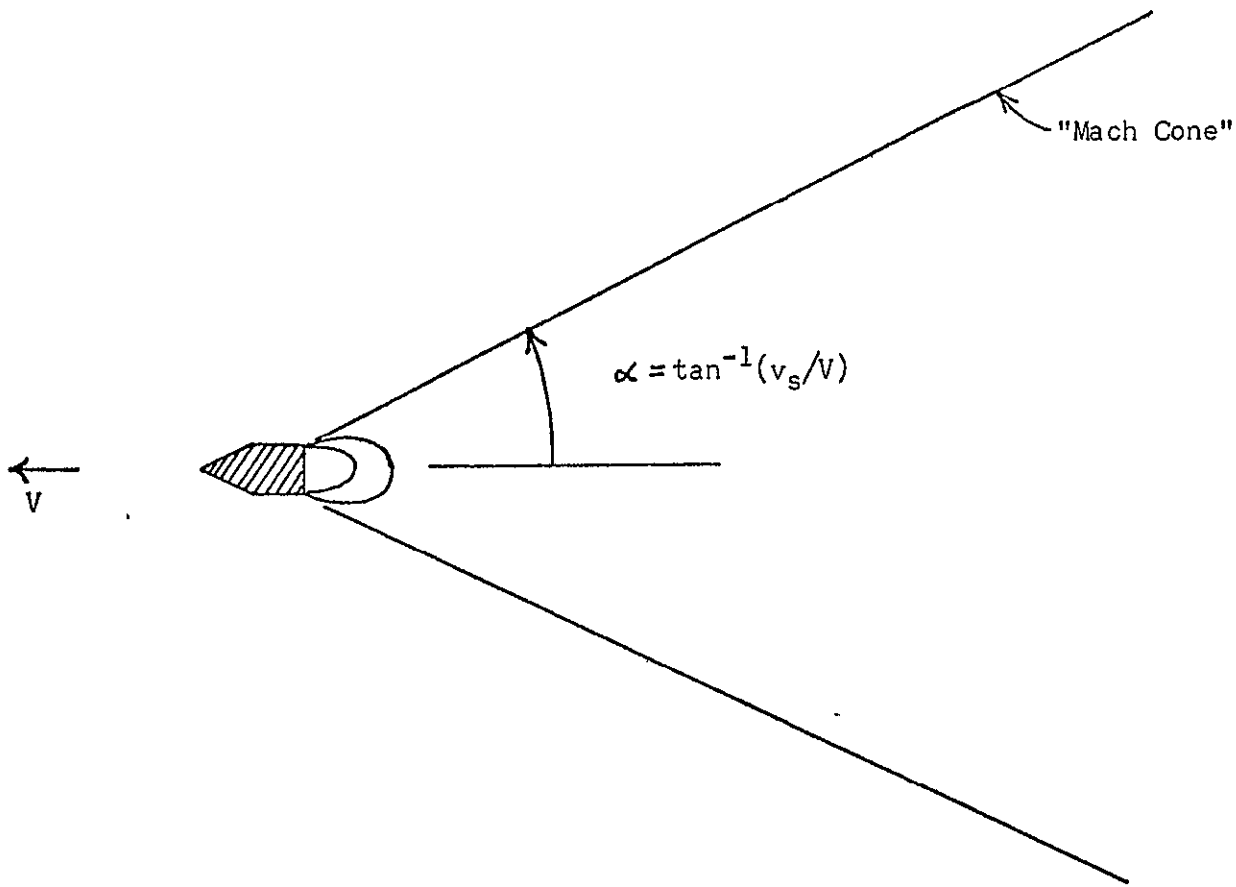

Figure 2.5.2. Far Zone Wake.

charged particle medium is $\alpha = \tan^{-1} \frac{V_s}{V}$. $v_s = \sqrt{kT_e/m_i}$ is the ion sound speed. With this disturbance is associated an electric field that should be considered. The "sonic boom" in the neutral medium should also be considered, but is probably not important since collisions will diffuse it. It is an interesting fact that in the case of a charged particle medium one finds a similar wake structure whether the mean free path is large or small[10] (that is whether the particles behave independently, or are in local thermodynamic equilibrium).

Extensive calculations have been performed on such wakes and the techniques could be adapted to SPS dimensions and surface properties. The ion trajectories are directly computed, including the magnetic field and some times satellite E field perturbations. Since $v_e >> V$ it is assumed that the electrons are in thermal equilibrium $n_e = n_i e^{e\phi/kT}$. Results of measurements of a near zone wake on the satellite Ariel 1[2,11] are shown in Fig. 2.5.3.

A long distance from the satellite the behavior of the wake depends strongly on whether or not a magnetic field is present. Figure 2.5.4 is a plot of the far zone on axis density perturbation with and without magnetic field. The formulas are respectively[2]

$$\left.\frac{\delta n_e}{n_e}\right|_{B\neq 0} = -\frac{\pi R^2 V}{r\, r_{Li} v_i} B_H\left(\theta, \frac{V}{v_i}\right) \tag{1}$$

$$\left.\frac{\delta n_e}{n_e}\right|_{B=0} = \frac{R^2 V^2}{r^2 v_i^2} B_o\left(\theta, \frac{V}{v_i}\right) \tag{2}$$

The satellite dimension is R, r is the distance, and r_{Li} is the ion Larmor radius. The functions $B_{o,H}$ give the angular dependence measured with

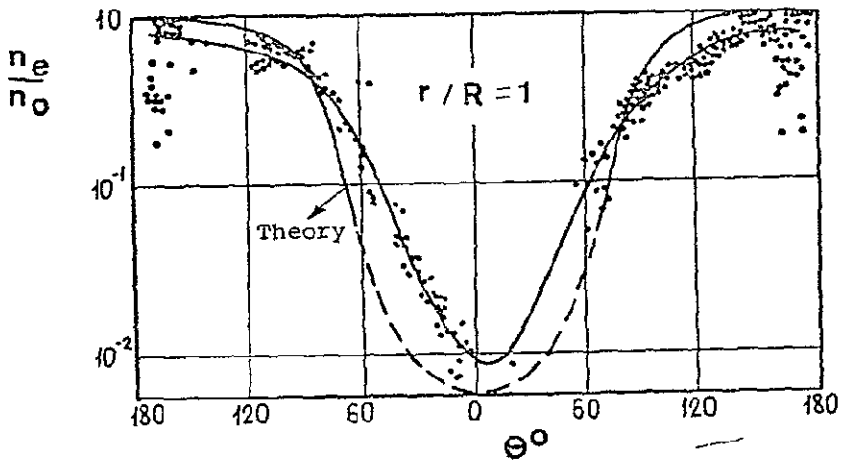

Figure 2.5.3 Near Zone Density Perturbation (Ref. 2,11)

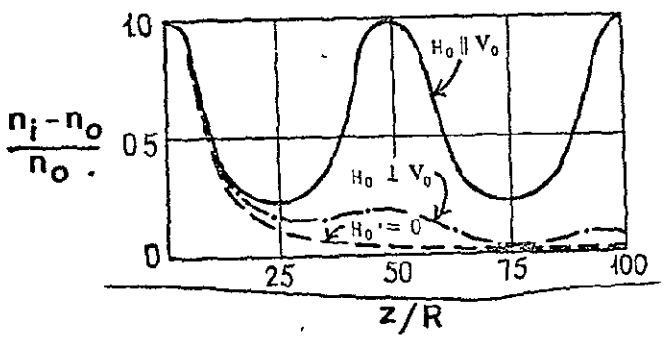

Figure 2.5.4 Far Zone On-Axis Density Perturbation (Ref. 2)

H_o = Magnetic Field

ORIGINAL PAGE IS
OF POOR QUALITY

respect to the satellite motion. Plots of the electric field are shown in Fig. 2.5.5[2] where the field is plotted on a radial plot as a function of angle. Since the wake is essentially an ion sound wave disturbance its propagation depends on the ratio of electron to ion temperature. For large T_e/T_i the "Mach cone" is sharp and for $T_e = T_i$ it becomes more diffuse, Fig. 2.5.6. The figures provided are intended to illustrate the phenomena only qualitatively.

The electric field in the wake may be found by noting that in an ion wave disturbance the potential is given by

$$\phi(\vec{r}) = \frac{kT_e}{e} \frac{\delta n_e}{n_e}$$

Differentiating Eqn. 1 we find the electric field signal strength

$$|E| = |\nabla\phi| = \frac{kT}{e} \frac{\pi R^2}{r^2 r_{Li}} \frac{V}{v_i} F(\theta) \quad .$$

The function $F(\theta)$ is shown in Fig. 2.5.5(c), its maximum value being about 4.0. The field has a rather complicated petal like structure. Using SPS and low earth orbit plasma parameters we find a field strength maximum ($F(\theta) \rightarrow 4$) of $E \sim 80/r^2$ volt/meter, where r is expressed in km. At r = 100 km the signal strength is of the order of 8 millivolt/meter. The static corotational E field

$$E_{CR} = - \frac{\Omega \times B}{c} r_{LEO}$$

is of the order of 7 millivolt/meter. This is the order of magnitude that is typically observed by sophisticated scientific instruments. Thus the far zone wake may be observable but should not be an important electromagnetic interference source. A more thorough evaluation should be made.

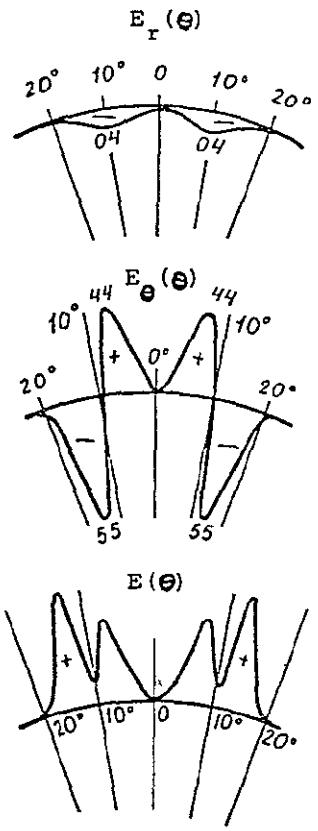

Figure 2.5.5 Angular Behavior of Far Zone Electric Field (Ref. 2)

ORIGINAL PAGE IS
OF POOR QUALITY

ORIGINAL PAGE IS
OF POOR QUALITY

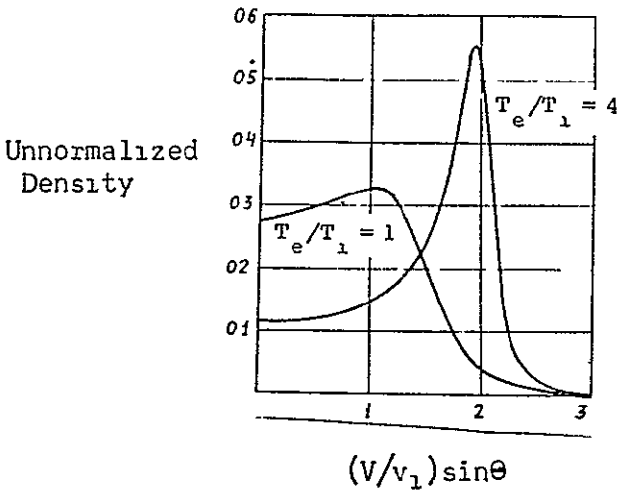

Figure 2.5.6 Effect of Temperature on Far Zone Angular Dependence (Ref. 2).

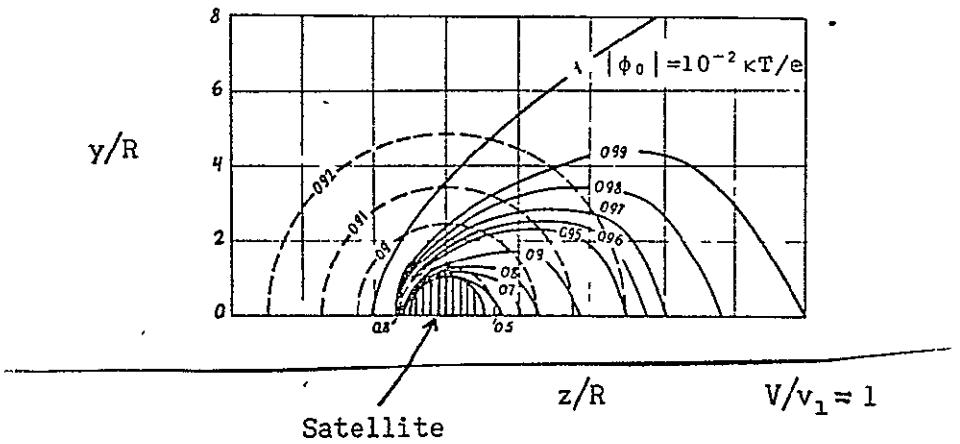

Figure 2.5.7 Equipotentials Around Slow Moving Satellite (Ref. 2)

At the altitude of GSO the situation is considerably different. The neutral particle density is about $100/cm^3$, too low to exert any appreciable drag. The charged particle density is also very low here, $\sim 1/cm^3$. The ion velocity here is of the order 10^7 cm/sec >> V, so that rather than a cone-shaped wake one gets simply a distortion of the spherical equipotentials surrounding a stationary object, along the line of motion. Calculations have been performed for the case of a sphere of radius $R \gg \lambda_D$, the Debye length. These give a disturbance of the form

$$\frac{n_e}{n_o} = \frac{n_e(r)}{n_o} + \frac{V}{v_1} f\left(\frac{r}{R}, \frac{e\phi_s}{kT}\right) \cos\theta .$$

$n_e(r)$ is the perturbed density that would obtain for a stationary satellite. Sample plots of the equipotentials are shown in Fig. 2.5.7, ($\frac{V}{v_1}$ at GSO is much smaller than used for this calculation).

It would appear that at GSO neutral and charged particle drag is negligible and the electrostatic potential perturbations will not propagate away from the satellite. These perturbations are very important on scientific satellites because they can distort measurements of the ambient plasma properties.

B. INDUCTION DRAG AND ALFVEN WAKE

When a conducting satellite moves through the earth's magnetic field an electric field

$$\vec{E} = -\frac{1}{c}\vec{V} \times \vec{B}$$

is induced in the satellite, polarizing it electrically, Fig. 2.5.8. Since the satellite is moving through a plasma current can flow in one end and out the other. This current $\vec{I}$ interacts with $\vec{B}$ producing the induction drag force

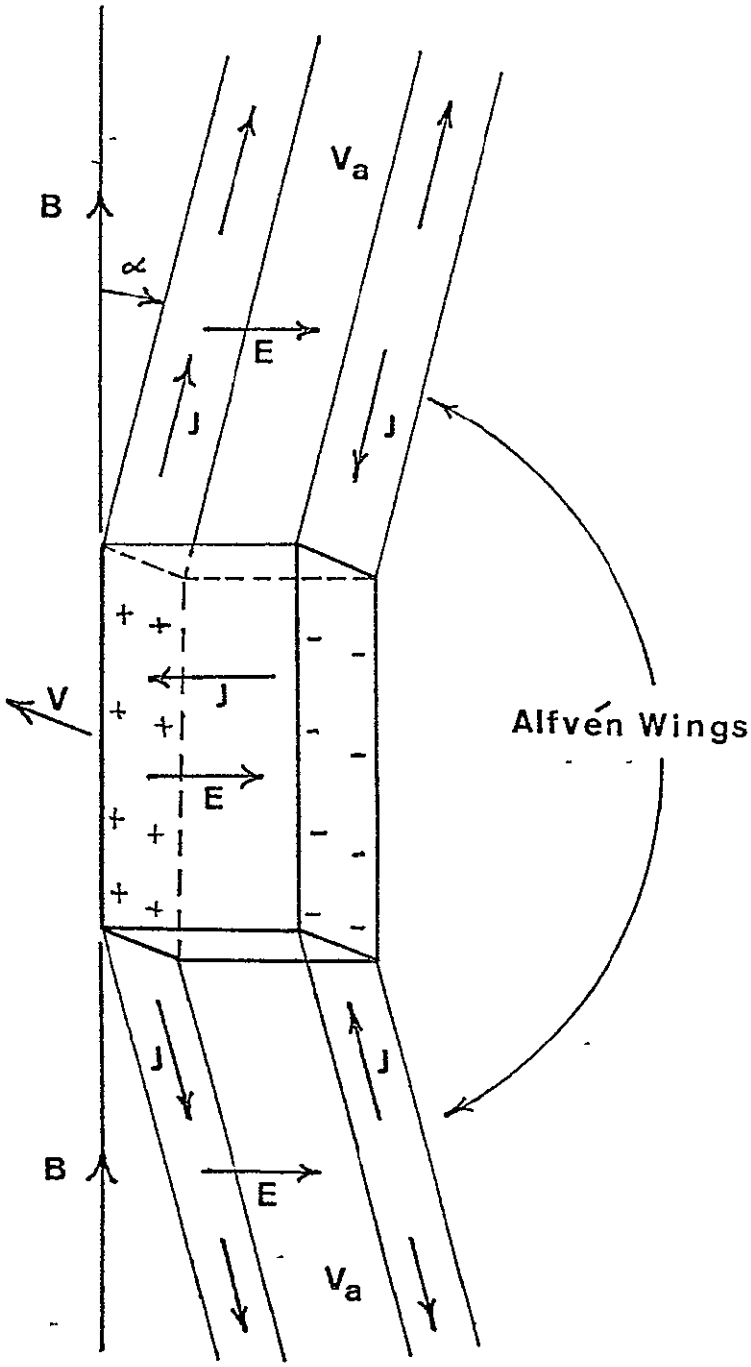

Figure 2.5.8 Moving Satellite and Alfvén Wake(Ref. 7)

$$\vec{F}_{DI} = \frac{\ell}{c} \vec{I} \times \vec{B} ,$$

where ℓ is the length of the current path. We assume that $\vec{V}$ is perpendicular to $\vec{B}$. The direction of $\vec{F}_{DI}$ implies that the direction of current flow is opposite to $\vec{E}$. This can be understood by noting that $\vec{E}$ is produced because plus and minus charges are separated by the $\vec{V} \times \vec{B}$ force, that is $\vec{E}$ is a Hall field. Current flows when an external load is connected. In our case the plasma is the load. Positive ions impact preferentially on the more negative part of the satellite and electrons on the positive part This reduces E and the V x B forces tend to restore $\vec{E}$.

Calculation of the current[5,6,8] depends on a number of factors, such as the satellite geometry, the ratio v_i/V, the satellite portential ϕ_s, and surface properties. At low altitude the ions move on essentially straight lines and impinge principally on the front portion of the satellite. The electrons travel along B and impinge principally on the more positive surfaces. The current is qualitatively indicated in Fig. 2.5.9. Detailed analysis[3,5,8] for the low altitude case reveals that I flowing through the satellite is ($V >> v_i$)

$$I = n_i eVA,$$

that is just the ion current impinging on the front surface. The drag force is

$$F = \frac{1}{c} n_i eVA\ell B .$$

The current density neV ~ 70 esu/cm^2-sec. For satellite dimensions at LEO we take A ~ 10 km^2 (see Section A) and ℓ ~ 500 m. With these parameters we find F_{DI}(LEO) ~ 1.7 x 10^6 dyne. This is about 1% of the neutral drag. Both drags are sensitive to the presented satellite area which we have no way of knowing. However the ratio is probably more or less correct.

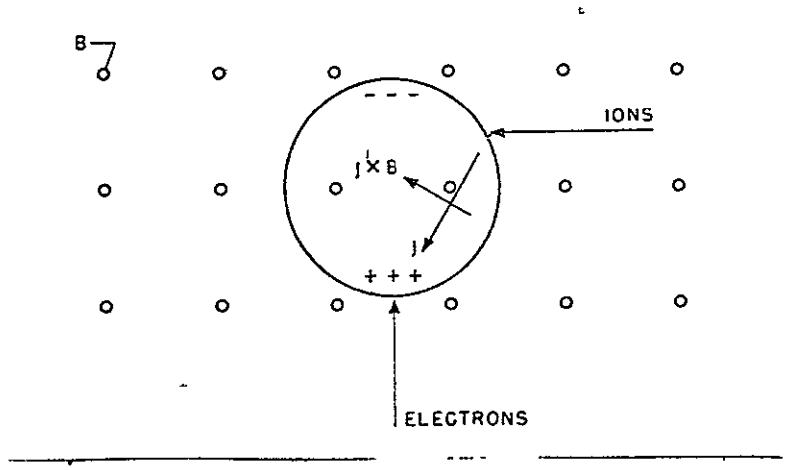

Figure 2.5.9. Induction Current Distribution (Ref. 5).

At GSO the current might have a maximum characteristic of the photoemission current 10 esu/cm^2-sec. If we simply substitute this in place of neV, multiply by 10 to take account of the fully erected area, and use $B = 7 \times 10^{-4}$ gauss at GSO we find F_{DI} (GSO) ~ 10^5 dynes. This is probably an overestimate since the current calculated exceeds the theoretical maximum proposed by Drell et.al. (Ref. 7, p. 3136) by a factor of ~ 10. In any case 10^4-10^5 dynes is fairly small. It represents a momentum transfer of about .2%-2% of that required for stationkeeping.

As the satellite moves along the polarization disturbance of the plasma that results from the satellite electric field and current propagates away from the satellite, along B in the satellite reference frame, Fig. 2.5 8. In the fixed frame the disturbance makes an angle $\alpha = \tan^{-1} (V/V_A)$, where the Alfvén velocity

$$V_A = \sqrt{\frac{B^2}{4\pi n_1 m_1}} \sim \begin{cases} 1.8 \times 10^7 \text{ cm/sec, LEO} \\ 6.8 \times 10^7 \text{ cm/sec, GSO} \end{cases}$$

Thus α is very small. In the ideal situation discussed by Drell, et.al. the electric field disturbance equals the induced E in the satellite

$$E \sim \frac{VB}{c} \sim \begin{cases} .1 \text{ volt/meter, LEO} \\ 2 \times 10^{-4} \text{ volt/meter, GSO} \end{cases}$$

The frequency typical of the disturbance is given by V divided by the satellite dimension, or something like .3/sec-15/sec, depending on satellite orientation. This is very low. Alfvén waves, which are what this wake is made up of, can penetrate to ground level after coupling to ordinary electromagnetic waves. Again the wake would probably be observable, but not a significant noise source. We do however recommend a review of the literature on observations of satellite wakes.

Finally we note that Drell, et. al.[7,13] have pointed out that if an external power source is available the current flow could be reversed and the induction force used for propulsion and maneuvering. This seems like an interesting possibility considering the large area to mass ratio of the SPS, and a quantitative assessment would be interesting.

C. ADDITIONAL TOPICS

There are two additional effects that may be of importance, and which we have not had time to investigate. 1) The wake structures produced may be unstable[2], and their decay could be a source of turbulence and EM signals of higher frequency than produced by the original wake, and 2) the charge disturbance may be a very effective radar scatterer[2] of cross-section much larger than that of the SPS itself. This could possibly impair precise radar ranging, 3) Selective amplification of certain wave modes due to the regular spacing of the SPS's could be a major problem. One result could be continual auroras at the foot of each SPS field line, and none elsewhere. This could upset magnetospheric dynamics and the flow of energy into the upper atmosphere at auroral latitudes.

BIBLIOGRAPHY

1. Chopra, K. P., Interactions of Rapidly Moving Bodies in the Terrestrial Atmosphere, Rev. Mod. Phys. 33, p. 153, 1961.

2. Al'pert, Y. L., Waves and Satellites in the Near Earth Plasma, Consultants Bureau, New York, 1974.

3. Brundin, C L , Effects of Charged Particles on the Motion of an Earth Satellite, AIAA Journal 1, p. 2529, 1963

4. de Leeuw, J H., A Brief Introduction to Ionospheric Aerodynamics, in Rarefied Gas Dynamics, Ed. C. L. Brundin, Academic Press, 1967.

5. Hohl, F. and Wood, G., Electrostatic and Electromagnetic Drag Forces on a Spherical Satellite in a Rarefied Partially Ionized Atmosphere, in Rarefied Gas Dynamics, Ed. J. A. Laurmann, Academic Press, 1963.

6. Chu, C. K. and Gross, R. A., Alfvén Waves and Induction Drag on Long Cylindrical Satellites, AIAA Journal 4, 2209, 1966.

7. Drell, S., Foley, H. and Ruderman, M., J. Geophys. Res. 70, p. 3131, 1965.

8. Beard, D. B. and Johnson, F. S., J. Geophys. Res. 65, p. 1, 1965.

9. Venkataraman, N. S. and Gustafson, W. A., the Journal of Astronautical Sciences 21, p. 99, 1973.

10. Kraus, L. and Watson, K., Plasma Motions Induced by Satellites in the Ionsophere, Phys. Fl. 1, p. 480, 1958.

11. Samir, U. and Willmore, A. P., Planet. Space Sci. 13, p. 285, 1965. See also Ballard, T., Medved, D., and Ballard, T., Jour. Astr. Sci. 18, p. 173, 1970; Samir, U. and Jew, H., Jour. of Geophys. Res. 34, p. 6819, 1972.

12. Tiuri, M. Radar Investigations of Worldwide Ionospheric disturbances Associated with Satellites, Nature 207, p. 1075, 1965.

13. Drell, S., Foley, H. and Ruderman, M., Drag and Propulsion of Large Satellites in the Atmospheric, An Alfven Propulsion Engine in Space, Phys. Rev. Letters 14, p. 171, 1965.

2 6 MICROWAVE POWER TRANSMISSION

INTRODUCTION

The microwave power transmission system used by an SPS will interact with the magnetospheric plasma. MAYA has identified two potential impacts associated with these interactions. First non-linear interactions, known as parametric instabilities, occur when a sufficiently intense electromagnetic wave propagates through a plasma. MAYA has performed an extensive bibliographic review of the literature of parametric instability. To date no serious impact upon either the magnetosphere or the microwave power transmission system has been shown to result from parametric instability. In addition, we have expended substantial effort, outside of the scope of this contract, on ionospheric interactions with the microwave beam, and while the case is much less clear-cut and deserves more study, no insurmountable problems have appeared.

A second impact which may be more problematic demands more study. In the operation of the self-phasing antenna system, it is assumed that the propagation medium is reciprocal and that its properties do not change significantly during a round trip transit time for a microwave signal. This round trip transit time is 0.3 seconds for an SPS at GSO. The total electron content and hence the plasma contribution to the index of refraction may exhibit significant change in 0.3 seconds. These changes may result from magnetic storms, solar x rays or micropulsations in the PC 1 band. A computer simulation of the phased antenna and intervening magneto-ionospheric plasma would enable a thorough study of these problems to be performed. (See Figure 2.6.1) Such a computer model would be a useful tool for the analysis of design trade-offs involved in the detailed

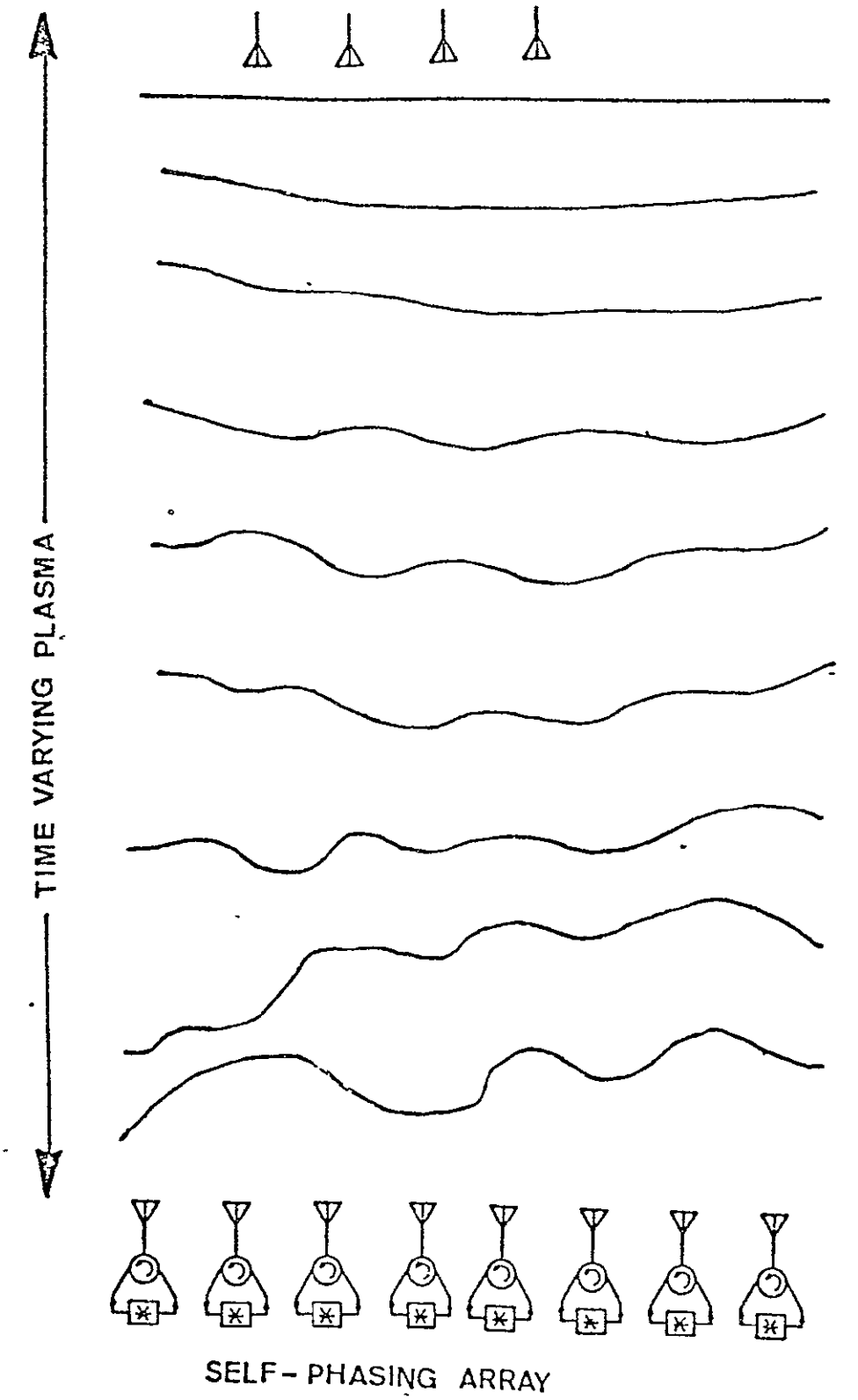

Figure 2.6.1. The microwave beam wavefront is distorted by passage through the magneto-ionospheric plasma. The selfphasing array is capable of restoring the wave phase distortions caused by spatial variations of the plasma. Dynamic response of the system to temporal variations of the plasma with periods of 0.3 sec or less must be examined.

design of such an antenna system. The model would draw heavily upon previous work by Johnson Space Center, JPL, and Raytheon for antenna and electronic systems definition but would include detailed modeling of the intervening temporal and spatial plasma variations as prescribed by MAYA.

A. PARAMETRIC INSTABILITY

Parametric Instability of an Intense Microwave Beam in the Magnetosphere

A decade of research has established theoretically and experimentally that many materials are unstable to the propagation of very intense electromagnetic radiation. A plasma is no exception. Parametric instability of an electromagnetic wave propagating through a plasma has been studied by a large number of physicists with interests in laser fusion, the heating of magnetically confined fusion plasmas, ionospheric modification and astrophysics. An extensive bibliography of the literature describing these parametric instabilities is included at the end of this section.

When an intense electromagnetic wave (the pump) is incident upon a plasma it will excite two new waves. If the amplitude of the incident wave is above a calçuable threshold then those waves will grow unstably. Schematically we may consider two processes:

Case 1. ("parametric decay")

$t \rightarrow \ell + \ell'$, the incident transverse electromagnetic wave t decays into two longitudinal plasma waves ℓ and ℓ'.

Case 2. ("stimulated scattering")

$t \rightarrow t' + \ell$, the incident transverse electromagnetic wave t scatters into another transverse electromagnetic wave t' and a longitudinal plasma wave ℓ

Consider a model equilibrium consisting of a uniform plasma and an external wave of amplitude E_o and frequency ω_o. Now if one perturbs this equilibrium with a density fluctuation

characterized by $(\omega,\underset{\sim}{k})$ then these fluctuations will be carried about by the oscillating electric field E_0 and will lead to currents at $\omega_0 \pm \omega$ and $\underset{\sim}{k}_0 \pm \underset{\sim}{k}$. Thus the low frequency fluctuations interact with the pump wave E_0 to produce sidebands about ω_0 and $\underset{\sim}{k}_0$. The sideband modes interact back upon the pump and produce forces acting at $(\omega,\underset{\sim}{k})$ upon the original perturbations. If the amplitude of the pump is greater than some threshold value (to be determined by calculation) then one finds that the perturbations grow exponentially. Energy is transferred from the pump into the plasma modes at $(\omega,\underset{\sim}{k})$ and into the sideband modes at $(\omega_0 \pm \omega, \underset{\sim}{k}_0 \pm \underset{\sim}{k})$. Such a linear calculation defines thresholds and illustrates the basic mechanism of instability. To determine the ultimate amplitude perturbations one must proceed to a nonlinear calculation and allow for either plasma nonlinearities, such as trapping, or pump depletion or both.

In Appendix B.1 we go through the details of this sort of linear calculation. Using these formulae we note that the wave energy is far above that necessary to stimulate either Brillouin or Raman scattering in a homogeneous plasma. We also indicate the growth rates which would obtain for these instabilities.

When a magnetic field is included a plasma admits to a formidable bestiary of different modes, e.g. electron Bernstein modes, ion cyclotron modes, upper and lower hybrid modes, etc. and each of these is a potential candidate for stimulated scattering. Even without the magnetic field there are the self-focusing, or filamentation modes to be considered. In this case plasma density striations are created in the direction perpendicular to the beam direction. Such striations have been observed in the ionospheric modification experiments and explained on the basis of parametric instability.

d. Linear Equations in a Spatially Homogeneous Plasma.

Consider a large amplitude plane polarized electromagnetic pump wave

$$\underset{\sim}{E}_o = E_o \underset{\sim}{e}_o \cos(\underset{\sim}{k}_o \underset{\sim}{X} - \omega_o t)$$

propagating in a homogeneous plasma. This wave will satisfy the usual homogeneous plasma dispersion relation

$$\omega_o^2 = \omega_p^2 + c^2 k_o^2$$

where $\omega_p^2 = \frac{4\pi n_o e^2}{Me}$ is the plasma frequency The equilibrium consists of electrons oscillating at the "quiver" velocity, $v_o = \left(\frac{eE_o}{Me\omega_o}\right)$ and of essentially stationary ions.

These processes come about because of the resonant interactions which can occur between three waves. Three wave resonant interactions are important whenever the phase matching conditions

$$\omega_o = \omega_1 + \omega_2$$

$$\underset{\sim}{k}_o = \underset{\sim}{k}_1 + \underset{\sim}{k}_2$$

are satisfied.

In general, the decay into longitudinal modes described by Case 1) will be important whenever the incident electromagnetic wave frequency, ω_o, is near to the frequency of a plasma mode, e.g. $\omega_o \simeq \omega_p$. If, however, $\omega_o >> \omega_p$ as is the case for a microwave beam propagating in the ionosphere, then Case 2) is important and we may anticipate enhanced scattering.

Case 2, enhanced scattering, may be further subdivided into categories according to the particular longitudinal plasma wave off of which the transverse wave is scattering. These are:

Case 2a) Scattering off of an electron plasma oscillation, known as Stimulated Raman Scattering (SRS)

Case 2b) Scattering off of an ion acoustic mode of the plasma, known as Stimulated Brillouin Scattering (SBS)

The microwave energy densities proposed by proponents of microwave energy transmission are well above the threshold for the production of both SRS and SBS in a spatially homogeneous plasma. As we shall show, it seems likely that the spatial inhomogeneity will quench the backscattered modes.

b. Effects of spatial inhomogeneity.

The spatial variation of the magnetospheric plasma can significantly modify the stability of the plasma to parametric excitation by a high frequency microwave beam. One has the geometry:

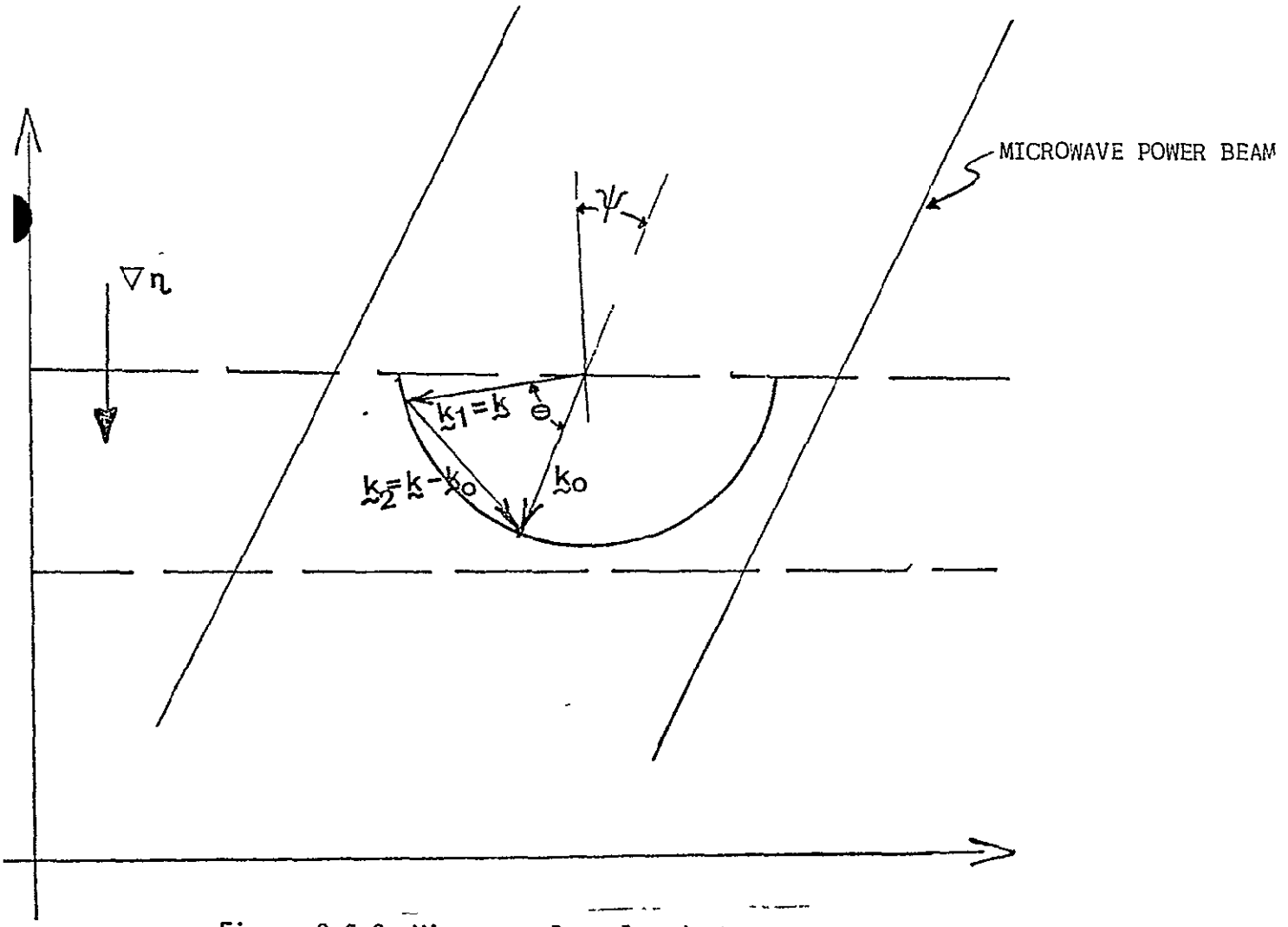

Figure 2.6.2 Microwave Beam Incident upon the magnetospheric plasma

where the resonance conditions are $\omega_0 = \omega_1 + \omega_2 = \omega + (\omega_0 - \omega)$ and $\underset{\sim}{k} = \underset{\sim}{k}_1 + \underset{\sim}{k}_2 = \underset{\sim}{k} + (\underset{\sim}{k}_0 - \underset{\sim}{k})$ which is satisfied for all $\underset{\sim}{k}$ lying upon a sphere of radius $|\underset{\sim}{k}_0|$ and origin at the foot of $\underset{\sim}{k}_0$ as shown above.

The magnetosphere is radially stratified as indicated by ∇n and thus the resonance conditions will generally be satisfied at only one point in space. As one moves away from that point the spatial variation of the magnetospheric plasma causes the energy transfer between the pump wave and the scattered waves to become nonresonant and hence to decrease. Thus the plasma and beam have a finite region of strong interaction. If now the instability which is excited is convective, then it will propagate out of the region of strong interaction and thus its growth will be substantially reduced.

The effects of convective instability and mismatch of the resonance conditions have been treated in some detail by Rosenbluth and by Liu et al.[33] We note here that each effect is characterized by a scale length

1) the convective scale length

$$Lc = (V_1 V_2)^{1/2}/\gamma_0$$

where

$V_1 = \frac{\partial \omega_1}{\partial k_1}$; $V_2 = \frac{\partial \omega_2}{\partial k_2}$ are the group velocities of waves 1 and 2 and γ_0 is the homogeneous plasma growth rate of the instability

2) the mismatch scale length

$$Lm = (k')^{-1/2}$$

where $k' = \frac{\partial \Delta k}{\partial x}$ with $\Delta k = k_0 - k_1 - k_2$ the WKB shift in wave number which develops as one moves away from that point in the plasma where $k_0 = k_1 + k_2$.

Analysis shows that waves will be amplified by a factor of e^{λ} where $\lambda = \left(\frac{Lm}{Lc}\right)^2$. Thus for instability one requires $\lambda > 1$, i.e., the wave must grow convectively more rapidly than it mismatches. It would appear (see Table 2.1) that mismatch rather effectively quenches the backscattered instabilities.

MODE	STABILITY CONDITION	RESULT FOR MAGNETOSPHERE
Stimulated Brillouin Scattering	$L < \left(\frac{Ve}{vo}\right)^2 \left(\frac{Wo}{Wp}\right)^2 \frac{8}{Ko} \sim 10^8 - 10^9$ Km	Stable
Stimulated Raman Scattering	$L < \left(\frac{c}{Vo}\right)^2 \frac{2}{Ko} \sim 4 \times 10^5$ Km	Stable
Stimulated Bernstein Scattering	$L < \left(\frac{c}{Vo}\right)^2 \frac{1}{2Ko} \sim 10^5$ Km	Stable

Table 2.6.1

Critical Scale Lengths for Quenching of Parametric Instabilities in the Magnetosphere..

Appendix B - Basic Equations

In this appendix we develop the basic equations describing Stimulated Raman Scattering (SRS). Similar derivations, differing mostly in the inclusion of more plasma phenomena into the low frequency equations are used to describe a vast array of parametric interactions between a high frequency transverse electromagnetic wave and a plasma. The presentation is meant only to be illustrative of the basic ideas and is in no way a complete treatment of even SRS.

1.1 The scattering process

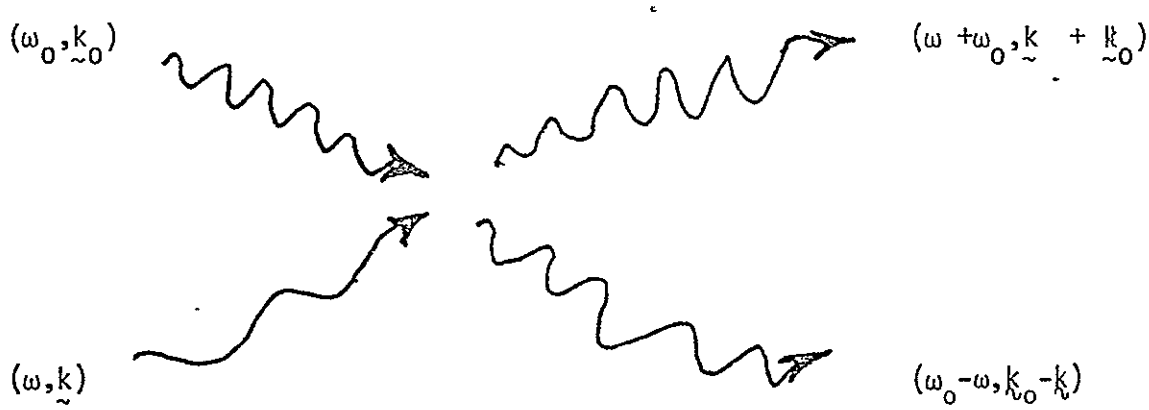

The high frequency wave $(\omega_0, \underset{\sim}{k}_0)$ scatters off of a low frequency wave $(\omega, \underset{\sim}{k})$ and produces two sideband modes $(\omega+, \underset{\sim}{k}+) = (\omega + \omega_0, \underset{\sim}{k} + \underset{\sim}{k}_0)$ and $(\omega-, \underset{\sim}{k}-) = (\omega_0 - \omega, \underset{\sim}{k}_0 - \underset{\sim}{k})$.

Typically one of the sideband modes will be much larger than the other thus the process reduces to the three wave resonant interaction which involves only the $(\omega-, \underset{\sim}{k}-)$ sideband.

1.2 Eqns for the high frequency transverse modes:

$$\nabla \times \underset{\sim}{E} = -\frac{1}{c}\frac{\partial \underset{\sim}{B}}{\partial t} \tag{1}$$

$$\nabla \times \underset{\sim}{B} = \frac{4\pi}{c}\underset{\sim}{J} + \frac{1}{c}\frac{\partial \underset{\sim}{E}}{\partial t} \tag{2}$$

thus

$$\frac{\partial^2 E}{\partial t^2} + c^2 \nabla \times (\nabla \times \underset{\sim}{E}) = -4\pi \frac{\partial \underset{\sim}{J}}{\partial t} \tag{3}$$

only the electrons respond at high frequencies

so

$$\underset{\sim}{J} = -ne\underset{\sim}{v}\ , \quad \frac{\partial \underset{\sim}{J}}{\partial t} = -e\frac{\partial n\underset{\sim}{v}}{\partial t} = -\frac{ne^2}{m}\underset{\sim}{E} \tag{4}$$

therefore

$$\frac{\partial^2 \underset{\sim}{E}}{\partial t^2} + c^2 \nabla \times (\nabla \times \underset{\sim}{E}) = \frac{4\pi ne^2}{m}\underset{\sim}{E} \tag{5}$$

or in final form

$$\frac{\partial^2 \underset{\sim}{E}}{\partial t^2} + c^2 \nabla \times (\nabla \times \underset{\sim}{E}) = \omega_{po}^{\ 2}\ \frac{n}{n_o}\ \underset{\sim}{E} \tag{6}$$

where $\omega_{po}^{\ 2} = \dfrac{4\pi n_o e^2}{m}$ is the plasma frequency

1.3 Equations for the low frequency longitudinal modes

A. The pondermotive force

An average low frequency force, called the pondermotive force, is exerted upon a plasma by a spatially inhomogeneous high frequency field. A simple derivation of the force which results is given in Chen[39]. The pondermotive force is

$$\underset{\sim}{F} = -\frac{e^2 n}{m\omega_o^2}\nabla \frac{1}{2}\langle \underset{\sim}{E} \cdot \underset{\sim}{E}\rangle \tag{7}$$

where the < > denotes an average over the phase of the high frequency field. The physical basis for this force is in the fact that as the particle oscillates back and forth in a spatially inhomogeneous field it will see an average force which tends to push it into regions of weaker field.

B. The low frequency equations

Most generally we simply add the pondermotive force to the full equations for the low frequency motion of a plasma.

A simple example is the electron plasma, for which

$$\frac{\partial n}{\partial t} + \nabla \cdot n \, \underset{\sim}{v} = 0 \tag{8}$$

$$\frac{\partial n \underset{\sim}{v}}{\partial t} = - \frac{ne}{m} \underset{\sim}{E}_{\ell} - \frac{ne^2}{m^2 \omega_o^2} \nabla \frac{1}{2} < \underset{\sim}{E} \cdot \underset{\sim}{E} > \tag{9}$$

$$\nabla \cdot \underset{\sim}{E}_{\ell} = - 4\pi ne \tag{10}$$

Combining these equations there results

$$\frac{\partial^2 \delta n}{\partial t^2} + \left(\omega_{po}\right)^2 \left(\frac{\delta n}{n_o}\right) = \frac{1}{4\pi m} \nabla \cdot \left(\frac{\omega po}{\omega o}\right)^2 \left(\frac{n}{n_o}\right) \nabla \; \frac{1}{2} < \underset{\sim}{E} \cdot \underset{\sim}{E} > \tag{11}$$

where δn is the electron density perturbation $\delta n = n - n_o$.

1.4 Solutions - the example of Stimulated Raman Scattering

Equations (6) and (11) form a basic coupled system describing the scattering processes outlined in section 1.1. Enough physics has been included in the low frequency equation to describe the process called Stimulated Raman Scattering (SRS) in the limit of weak damping.

We wish to study the stability of linearized perturbations about an electromagnetic pump at $(\omega_o, \underset{\sim}{k}_o)$. Thus we substitute into

equations (6) and (11) the basic ansatz for the high frequency field.

$$\underset{\sim}{E} = \underset{\sim}{E}_o \cos(\underset{\sim}{k}_o \cdot \underset{\sim}{X} - \omega_o t) \quad \leftarrow \quad \text{pump}$$

$$+ \delta \underset{\sim}{E}_+ \cos(\underset{\sim}{k}_+ \cdot \underset{\sim}{X} - \omega_+ t) \quad \leftarrow \quad \text{upper sideband}$$

$$+ \delta \underset{\sim}{E}_- \cos(\underset{\sim}{k}_- \cdot \underset{\sim}{X} - \omega_- t) \quad \leftarrow \quad \text{lower sideband}$$

$$n = n_o$$

$$+ \delta n \cos(\underset{\sim}{k} \cdot x - \omega t) \quad \leftarrow \quad \text{plasma oscillation}$$

where $\underset{\sim}{k}_\pm = \underset{\sim}{k}_o \pm \underset{\sim}{k}$, $\omega\pm = \omega_o \pm \omega$

From equation (6) we obtain

$$\omega_o^2 = c^2 k_o^2 + \omega_{po}^2, \text{ the pump dispersion relation}$$

and

$$\left\{ \left[k_\pm^2 - \frac{1}{c^2}(\omega_\pm^2 - \omega_{po}^2) \right] \underset{\sim}{I} - \underset{\sim}{k}_\pm \underset{\sim}{k}_\pm \right\} \cdot \delta \underset{\sim}{E}_\pm = -\frac{1}{2}\left(\frac{\omega_{po}^2}{c^2}\right)\left(\frac{\delta n}{n_o}\right) \underset{\sim}{E}_o$$

which may be inverted to obtain

$$\delta \underset{\sim}{E}_\pm = -\frac{1}{2}\omega_{po}^2 \frac{\delta n}{n_o} \underset{\sim}{M}_\pm \cdot \underset{\sim}{E}_o \tag{12}$$

where

$$\underset{\sim}{M}_\pm = \frac{\underset{\sim}{e}_\pm \underset{\sim}{e}_\pm - \underset{\sim}{I}}{D_\pm} - \frac{\underset{\sim}{e}_\pm \underset{\sim}{e}_\pm}{\omega_\pm^2 - \omega_{po}^2} \tag{13}$$

with the unit vectors

$$\underset{\sim}{e}_\pm = \frac{\underset{\sim}{k}_\pm}{|\underset{\sim}{k}_\pm|}$$

and $D_\pm = \omega_\pm^2 - c^2 K_\pm^2 - \omega_{po}^2$

From equation (11) we obtain

$$(\omega^2 - \omega_{po}^2)\ \delta n = \frac{k^2}{8\pi m}\left(\frac{\omega_{po}}{\omega_o}\right)^2 (\underset{\sim}{E}_o \cdot \delta \underset{\sim}{E}_+ + \underset{\sim}{E}_o \cdot \delta \underset{\sim}{E}_-)$$

Inserting (12) we obtain

$$(\omega^2 - \omega_{po}^2)\ \delta n = -\frac{k^2 \omega_{po}^2}{\pi 16\ m}\left(\frac{\omega_{po}}{\omega_o}\right)^2 \left(\frac{\delta n}{n_o}\right)\left(\underset{\sim}{E}_o\ \underset{\approx}{M}_+ \cdot \underset{\sim}{E}_o + \underset{\sim}{E}_o \cdot \underset{\approx}{M}_- \cdot \underset{\sim}{E}_o\right) \quad (14)$$

For Stimulated Raman Scattering (SRS) the backscattered wave is dominant, thus

$$D_- = \omega_-^2 - c^2 k_-^2 - \omega_{po}^2 \simeq 0$$

In this instance the right hand side of equation (14) will be dominated by that term in $\underset{\sim}{M}_-$ in which has D_- as its denominator. Equation (14) then reduces to

$$(\omega^2 - \omega_{po}^2)\ (\omega_-^2 - c^2 k_-^2 - \omega_{po}^2) = \frac{1}{4} k^2 v_o^2\ \omega_{po}^2 \quad (15)$$

where $v_o = \left(\frac{eEo}{m\omega o}\right)$ is the quiver velocity of an electron in the field of the pump. This dispersion relation has unstable solutions describing the growth of SRS. The growth rate obtained from (15) is

$$\gamma = \frac{1}{\sqrt{2}} k_o v_o\ (\frac{\omega p}{\omega o})^{1/2}, \text{ SRS growth rate.} \quad (16)$$

If in setting up the low frequency plasma response we allow for ion dynamics then a similar analysis will lead to the dispersion relation

$$(\omega^2 - k^2 c_s^2)\ (\omega_-^2 - c^2 k_-^2 - \omega_{po}^2) = \frac{1}{4} k^2 v_o^2\ \omega_{pi}^2 \quad (17)$$

where $c_s = (\frac{Te}{mi})^{1/2}$ is the ion acoustic speed

$$\gamma = \frac{1}{\sqrt{2}}(k_o v_o) \frac{\omega_{pi}}{(\omega_o \omega_s)^{1/2}} \quad \text{, SBS growth rate} \tag{18}$$

where $\omega_s = kc_s$ is the ion acoustic mode frequency.

Quite similar results are obtained for the much more general case of a Vlasov plasma with a uniform magnetic field background. For such a plasma the electrons are described by

$$\frac{\partial f}{\partial t} + \underline{v} \cdot \nabla f + \left(- \frac{e}{m} \underset{\sim}{E} + \frac{1}{m} \underset{\sim}{F} - \frac{e}{mc} \underset{\sim}{V} \times \underset{\sim}{B} \right) \cdot \frac{\partial f}{\partial \underset{\sim}{v}} = 0 \tag{19}$$

where $\underset{\sim}{F}$ is given by equation (7).

Using this Vlasov equation one finds a general dispersion relation of the form [15]

$$\frac{1}{X_e(k,\omega)} + \frac{1}{X_i(k,\omega) + 1}$$

$$= k^2 \left(\frac{|k_- \times v_o|^2}{k_-^2 D_-} - \frac{|k_- \cdot v_o|^2}{k_-^2 \omega_-^2 \varepsilon_-} + \frac{|k_+ \times v_o|^2}{k_+^2 D_+} - \frac{|k_+ \cdot v_o|^2}{k_+^2 \omega_+^2 \varepsilon_+} \right), \tag{20}$$

where

$X_{e,i}$ are the susceptibility and ε is the electron dielectric polarizability.

B. Phase Distortion and the Microwave Transmission System

A low density magnetized plasma is characterized by a frequency dependent index of refraction N given by

$$N^2 = 1 - X \left[1 - \frac{Y_T^2}{2(1-x)} \pm \left(\frac{Y_T^4}{4(1-x)^2} + Y_L^2 \right)^{\frac{1}{2}} \right]^{-1}$$

where

$$X = \left(\frac{\omega_p}{\omega}\right)^2$$

$$Y = \left(\frac{\Omega_e}{\omega}\right)^2, \quad Y_T = Y\sin\phi, \; Y_L = Y\cos\phi$$

and

$$\omega_p = (4\pi n_o e^2/m_e)^{\frac{1}{2}}, \text{ plasma frequency}$$

$$\Omega e = (eB/m_e c), \text{ cyclotron frequency}$$

$$\cos\phi = \hat{k}\cdot\hat{B}$$

For the magneto-ionospheric plasma $Y_{max} \simeq 2.5 \times 10^{-4}$ and $X_{max} \simeq 1.4 \times 10^{-7}$ for an SPS transmitting at a frequency $f_o = 3.3 \times 10^9$ Hz. Thus a useful approximation is

$$N = 1 - \frac{1}{2} X$$

and for most purposes the magnetic field corrections can be neglected. (Exceptions are polarization effects, e.g., Faraday rotation).

In the approximation of geometric optics waves propagate through a spatially inhomogeneous medium along a trajectory given by

$$\frac{d}{ds} N \frac{d\underset{\sim}{r}}{ds} = \nabla N$$

where s is the distance along the ray. Along this path the wave phase (apart from a common factor ωt) will vary as

$$\phi = \frac{\omega}{c} \int_0^s ds N(s)$$

where the integral is understood to be along the ray trajectory $\underset{\sim}{r}(s)$.

The difference in phase caused by the presence of the plasma is

$$\Delta\phi = \phi - \phi_{\text{free space}}$$

$$= \frac{\omega}{c}\int_0^s ds\ (N-1)$$

$$= -\left(\frac{\omega}{c}\right)\left(\frac{2\pi e^2}{m_e\omega^2}\right)\int_0^s ds\ \ n$$

The quantity $\int_0^{s_0} ds\ n$ is called the total electron content and is ordinarily measured by Faraday rotation techniques.

For an SPS

$$\Delta\phi = -\ 9.2 \times 10^{-14}\int_0^s ds\ n$$

Typical values for the total electron content and $\Delta\phi$ are shown in Figure 2.6.3, which is taken from Lanzerotti, et al. We note that typically the phase shifts are fractional but may exceed 2π during mid-afternoon. Phase shifts are also enhanced by the enhanced total electron content associated with storms. The effect of this phase shift is to cause the wavefront incident upon the rectenna to be distorted in a irregular fashion as is shown in Figure 2.6.1.

A selfphasing antenna system has been proposed as a means of restoring the wavefront phase distortion which is caused by the intervening plasma. In the operation of the selfphasing antenna, which is illustrated in Figures 2.6.1 and 2.6.4, it is assumed that the propagation medium is reciprocal; that is, its properties do not depend upon the direction of propagation. Also, it is further assumed that the medium does not change

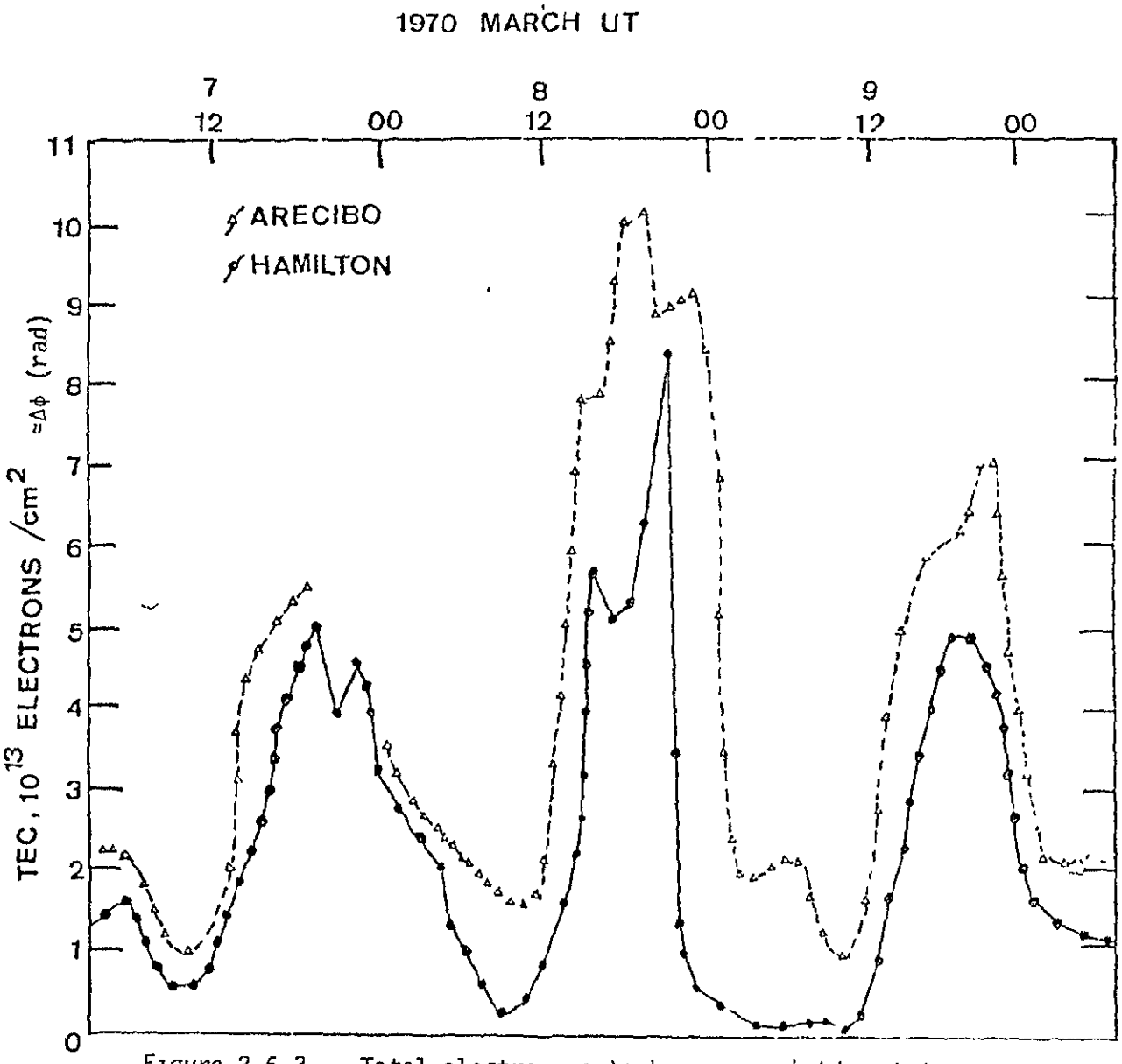

Figure 2.6.3. Total electron content as measured by stations at Hamilton, Massachusetts and Arecibo, Puerto Rico. The resulting phase shift in an SPS microwave beam is indicated (Lanzerotti, et al., 1975)

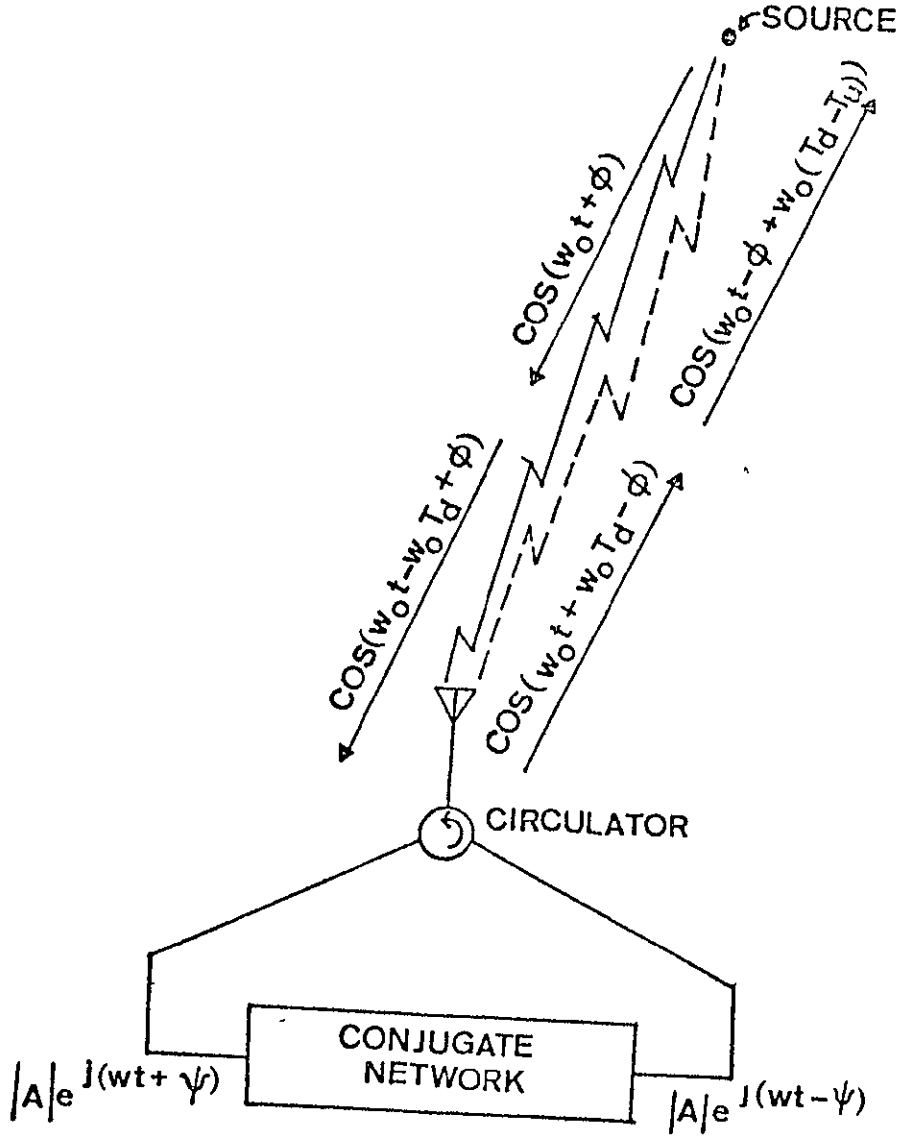

Figure 2.6.4. One element, or subaperture, of the selfphasing array

character over the system response time, which can be no less than the round trip transit time through the critical part of the propagation path.

For an SPS in GSO the round trip transit time is approximately 0.3 seconds. Thus any significant change in the total electron content occurring on such time scales could cause the antenna system to lose its phase coherence. To illustrate this consider the four relevant signals at the ith subapperture

1) source signal = $A_0\cos(\omega_0 t + \phi)$
2) signal received = $A_1\cos[\omega_0(t-T_d) + \phi]$
3) signal radiated = $A_2\cos[\omega_0(t+T_d) - \phi]$
4) signal returned to source = $A_3\cos[\omega_0 t - \phi + \omega_0(T_d-T_u)]$

where T_d = transit time on downlink

T_u = transit time on uplink

For a time stationary, reciprocal medium where both uplink and downlink propagate over the same path $T_d = T_u$ and hence the signal radiated by the selfphasing subaperature is independent of the transit time. Note though that if the medium changes on a time comparable to the round trip transit time, $T_r = T_u + T_d = 0.3$ secs for an SPS at GSO, that T_u will not equal T_d and the phase of the radiated signal will be dependent upon $\Delta T = T_d - T_u$ and hence upon the properties of the intervening medium.

During magnetic storms, ecllipses and other infrequent but recurring phenomena the total electron content may exhibit changes with characteristic periods of 0.3 seconds. Wave phenomena may also perturb the intervening medium with periods of 0.3 seconds. For instance, the PC1 micropulsations characterized by periods in this range. A model should be constructed which will allow the simulation of these effects and the impact of medium time variation studied with this model.

BIBLIOGRAPHY

A. PARAMETRIC INSTABILITY

1. Chen, F.F., "Physical Mechanisms for Laser-Plasma Parametric Instabilities," in Laser Interaction and Related Plasma Phenomena, edited by H. Schwarz and H. Hora, (Plenum Press, New York, 1974), p. 291.

2. Comisar, C G., "Theory of Stimulated Raman Effect in Plasmas," Phys. Rev., Vol. 141, 200 (1966).

3. Bloembergen, N. and Y.R. Shen, "Optical Nonlinearities of a Plasma," Phys. Rev., Vol. 141, p. 298 (1966).

4. Goldman, M V. and D.F. Dubois, "Stimulated Incoherent Scattering of Light from Plasmas," Phys. Fluids, Vol. 8, p. 1404 (1965).

5. Gorbunov, L.M., "Perturbation of a Medium by a Field of a Strong Electromagnetic Wave," Sov. Phys. JETP, Vol. 28, p. 1220 (1969).

6. Gorburov, L.M. and V.P. Silin, "Stability of a Magnetized Plasma in a Strong High Frequency Field," Sov. Phys. Tech Phys., Vol. 14, p. 1 (1969).

7. Perkins, F.W , C. Oberman, and E.J. Valeo (1974), Parametric instabilities and ionospheric modification, J. Geophys. Res., 79, p. 1478-1496.

8. Fejer, J.A., and K.N. Graham (1974), Electron acceleration by parametrically excited Langmuir waves, Radio Science, 9, p. 1081-1084.

9. Wienstock, J. (1974), Enhanced airglow, alectron acceleration, and parametric instabilities, Radio Science, 8, p. 1085-1087.

10. Perkins, F.W. and E.J. Valeo (1974), Thermal Self-Focusing of Electromagnetic Waves in Plasmas, Phys. Rev. Lett., 32, p. 1234-1237.

11. Utlaut, W F. (1970), An ionospheric modification experiment using very high power radio waves, J. Geophys. Res., 75, p. 6402-6405.

12. Gordon, W.E., H.C. Carlson, and R.L. Showen (1971), Ionospheric heating at Arecibo: First tests, J. Geophys. Res., 76, p. 7808-7813.

13. Utlaut, W.F. and E.J. Violette (1974), A Summary of vertical incidence radio observations of ionospheric modification, Radio Science, 9, p. 895-903.

14. Rosenbluth, M.N. and R.Z Sagdeev, "Summary of Activities of the Trieste Working Group on the Interaction Between Plasmas and Intense Laser and Electron Beams," Comments Plasma Phys. Controlled Fusion, Vol. 2, p. 3 (1973).

15. Drake, J.F., P.K. Kaw, Y.C. Lee, G. Schmidt, C.S. Liu, and Marshall N. Rosenbluth, "Parametric Instabilities of Electromagnetic Waves in Plasmas," Phys. Fluids, Vol. 17, p. 778 (1974).

16. Liu, C.S., M N. Rosenbluth, and R.B. White, "Raman and Brillouin Scattering of Electromagnetic Waves," Phys. Fluids, 17, p. 1211 (1974).

17. Forslund, D.W., J.M. Kindel, and E.L. Lindman, "Theory of Stimulated Scattering Processes in Laser-irradiated Plasmas," Phys. Fluids, Vol. 18, p. 1002 (1975).

18. Nishikawa, K., and C.S. Liu, "General Formalism of Parametric Excitation," Advances in Plasma Physics, V. 6, p. 3 (1975).

19. Liu, C.J. and P.K. Kaw, "Parametric Instabilities in Homogeneous Unmagnetized Plasmas," Advances in Plasma Physics, V. 6, p. 83 (1975).

20. Liu, C.S., "Parametric Instabilities in an Inhomogeneous Unmagnetized Plasma," Advances in Plasma Physics, V. 6, p. 121 (1975).

21. Valeo, E.J. and C. R. Oberman, "Model of Parametric Excitation by an Imperfect Pump," Phys. Rev. Letters, Vol. 30, p. 1035 (1973).

22. Thomson, J.J., "Finite-Bandwidth Effects on the Parametric Instability in an Inhomogeneous Plasma," Nucl. Fusion, 15, p. 237 (1975).

23. Chiao, R.Y., C.H. Townes, and B. Stoicheff, "Stimulated Brillouin Scattering and Coherent Generation of Intense Hypersonic Waves," Phys. Rev. Lett., Vol. 12, p. 592 (1964).

24. Kroll, N.M., "Excitation of Hypersonic Vibrations," J. Appl. Phys., Vol. 36, p. 34 (1965).

25. Batra, I.P., R.H. Enns, and D. Pohl, "Stimulated Thermal Scattering of Light," Phys. Stat. Solids, Vol. 28, p. 11 (1971).

26. Bloembergen, N., Nonlinear Optics, (Benjamin, New York, N.Y.) 1965.

27. Massey, R., K. Berggren, and Z.A. Pietrzyk, "Observation of Stimulated Brillouin Backscattering from an Underdense Plasma," Phys. Rev. Letters, Vol. 36, p. 963 (1976).

28. Turechock, John J. and Francis, F. Chen, "Detection of Brillouin Backscattering in Underdense Plasma," Phys. Rev. Letters, Vol. 36, p. 720 (1976).

29. Hooke, W.M. and S. Bernabei, "Observation of a Parametric Instability near the Lower Hybrid Resonance Frequency," Phys. Rev. Letts., Vol. 29, p. 1208 (1972).

30. Berger, R.L. and F.W. Perkins, "Thresholds of Parametric Instabilities near the Lower-hybrid Frequency," Phys. Fluids, Vol. 19, p. 406 (1976).

31. Kulsrud, Russel M., "Statistical Acceleration of Relativistic Particles in an Assembly of Spherical Electromagnetic Waves," The Astrophysical Journal, V. 198, p. 709 (1975).

32. Langdon, A Bruce, "Filamentation and Subsequent Decay of Laser Light in Plasmas," Phys. Rev. Letters, Vol. 34, p. 934 (1975).

33. Liu, C.S., M.N Rosenbluth, and R.B. White, "Parametric Scattering Instabilities in Inhomogeneous Plasmas," Phys. Rev. Lett., Vol. 31, p. 697 (1973).

34. Klein, H H., Wallace M Manheimer, and Edwart Ott, "Effect of Side-scatter Instabilities on the Propagation of an Intense Laser Beam in an Inhomogeneous Plasma," Phys. Rev. Lett., Vol. 31, p. 1187

35. Mostrom, M.A., D.R. Nicholson and A.N. Kaufman, Lawrence Berkeley Laboratory Report No. 2032 (1973).

36. Rosenbluth, Marshall N., "Parametric Instabilities in Inhomogeneous Media," Phys. Rev. Letters, Vol. 29, p. 565 (1972).

37. Rosenbluth, M.N., R.B. White, and C.S. Liu, "Temporal Evolution of a Three-Wave Parametric Instability," Phys. Rev. Lett., Vol. 31, p. 1190 (1973).

38. Sagdeev, R.Z. and A.A. Galeev, Nonlinear Plasma Theory, edited by T.M. O'Neil and D. Book, (Benjamin, New York, 1969), p. 16.

39. Chen, F.F., "Introduction to Plasma Physics", (Plenum Press, New York, 1974), p. 256.

B. PHASE DISTORTION AND THE MICROWAVE TRANSMISSION SYSTEM

1. Thrane, E.V., "Radio Wave Propagation" in Cosmical Geophysics, Edited by A. Egeland, O Holter and A. Omhdt, Chap. 19, p. 267 (1973) Universitetsforlaget.

2. Lanzerotti, L J., L.L. Cogger and M. Mendillo, "Latitude Dependence of Total Ionospheric Electron Content", J. Geophys. Res. V 80, No. 10, p. 1287 (1975).

3. Skolnik, M.I. and D.D. King, "Self Phasing Array Antennas", IEEE Transactions on Antennas and Propagation, Vol. AP-12, p. 142 (1965).

4. Jörgensen, T. Stockflet, "Micropulsations Whistlers and VLF Emissions", in Cosmical Geophysics, Edited by A. Egeland, O. Holter and A. Omhdt, Chap. 21, p. 301 (1973) Universitetsforlaget.